Lithium-ion batteries – Current state of the art and anticipated developments

Michel Armand [a], Peter Axmann [b], Dominic Bresser [c,d,*], Mark Copley [e], Kristina Edström [f,g], Christian Ekberg [h], Dominique Guyomard [i], Bernard Lestriez [i], Petr Novák [k], Martina Petranikova [h], Willy Porcher [l], Sigita Trabesinger [k], Margret Wohlfahrt-Mehrens [b,c], Heng Zhang [a]

[a] *Centre for Cooperative Research on Alternative Energies (CIC EnergiGUNE), Basque Research and Technology Alliance (BRTA), Alava Technology Park, Albert Einstein 48, 01510, Vitoria-Gasteiz, Spain*
[b] *Zentrum für Sonnenenergie- und Wasserstoff-Forschung Baden-Württemberg (ZSW), Helmholtzstrasse 8, 89081, Ulm, Germany*
[c] *Helmholtz Institute Ulm (HIU), Helmholtzstrasse 11, 89081, Ulm, Germany*
[d] *Karlsruhe Institute of Technology (KIT), P.O. Box 3640, 76021, Karlsruhe, Germany*
[e] *WMG, University of Warwick, Coventry, CV4 7AL, United Kingdom*
[f] *Department of Chemistry-Ångström Laboratory, Uppsala University, Box 538, SE-751 21, Uppsala, Sweden*
[g] *ALISTORE-European Research Institute CNRS FR 3104, Hub de l'Energie, 15 Rue Baudelocque, 80039, Amiens Cedex, France*
[h] *Nuclear Chemistry and Industrial Material Recycling, Department of Chemistry and Chemical Engineering, Chalmers University of Technology, Gothenburg, 41296, Sweden*
[i] *Université de Nantes, CNRS, Institut des Matériaux Jean Rouxel, IMN, F-44000 Nantes, France*
[k] *Electrochemistry Laboratory, Paul Scherrer Institute, CH-5232 Villigen PSI, Switzerland*
[l] *Université Grenoble Alpes, CEA-Liten, 17 Avenue des Martyrs, F-38054 Grenoble, France*

GRAPHICAL ABSTRACT

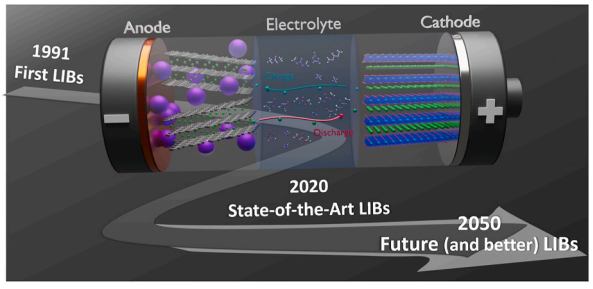

ARTICLE INFO

Keywords:
Anode
Cathode
Electrolyte
Processing
Recycling
Lithium-ion battery

ABSTRACT

Lithium-ion batteries are the state-of-the-art electrochemical energy storage technology for mobile electronic devices and electric vehicles. Accordingly, they have attracted a continuously increasing interest in academia and industry, which has led to a steady improvement in energy and power density, while the costs have decreased at even faster pace. Important questions, though, are, to which extent and how (fast) the performance can be further improved, and how the envisioned goal of truly sustainable energy storage can be realized.

* Corresponding author. Helmholtz Institute Ulm (HIU), Helmholtzstrasse 11, 89081 Ulm, Germany
E-mail address: dominic.bresser@kit.edu (D. Bresser).

Herein, we combine a comprehensive review of important findings and developments in this field that have enabled their tremendous success with an overview of very recent trends concerning the active materials for the negative and positive electrode as well as the electrolyte. Moreover, we critically discuss current and anticipated electrode fabrication processes, as well as an essential prerequisite for "greener" batteries – the recycling. In each of these chapters, we eventually summarize important remaining challenges and propose potential directions for further improvement. Finally, we conclude this article with a brief summary of the performance metrics of commercial lithium-ion cells and a few thoughts towards the future development of this technology including several key performance indicators for the mid-term to long-term future.

1. Introduction

Efficient energy storage is considered key for the successful and entire transition to renewable energy sources and electrochemical energy storage technologies are and will be playing an important role for achieving this desirable goal – especially for mobile devices and the transportation sector, but also stationary storage [1–6]. While generally all applications call for high energy and power density, low cost, safety, and ideally high sustainability, the relative importance of these characteristics varies significantly depending on the specific needs [6]. A rather small battery to power, e.g., a mobile phone does not necessarily need to be very cheap, as the corresponding costs add little to the overall cost of such a device, but in the case of electric vehicles, for instance, the much larger size of the battery renders cost an important factor. Nonetheless, lithium-ion batteries are nowadays the technology of choice for essentially every application – despite the extensive research efforts invested on and potential advantages of other technologies, such as sodium-ion batteries [7–9] or redox-flow batteries [10,11], for particular applications. This great success is based on their very high energy and power density, long cycle life, relatively high safety, and the continuously decreasing cost [12–17]. In fact, part of this success story is also that the term "lithium-ion battery" (just like for other battery technologies as well) is not defining specific battery cell components, but rather referring to the general charge storage mechanism, involving lithium ions that are shuttling back and forth between the negative and positive electrode, which are serving as host matrices for these cations (see Fig. 1 for a schematic illustration involving state-of-the-art cell components). Accordingly, the choice of the electrochemically active and inactive materials eventually determines the performance metrics and general properties of the cell, rendering lithium-ion batteries a very versatile technology. While electrochemically inactive components, such as the current collector [18], binder [19–21], separator [22–24], or the conductive additives, ensuring sufficient electronic wiring within the electrode [25–27], are of great importance as well in this regard, we will focus herein on the critical discussion of a selected set of electrode active materials (*Chapter 2/3*) and electrolytes (*Chapter 4*) – specifically those which are already used in commercial cells or are anticipated to be employed in near future. Moreover, we highlight the impact of the electrode coating process (*Chapter 5*) and, in light of the continuously increasing importance of sustainability, we will discuss the available and foreseen recycling technologies (*Chapter 6*), before summarizing the present and anticipated performance metrics (*Chapter 7*), and finally concluding this perspective article (*Chapter 8*).

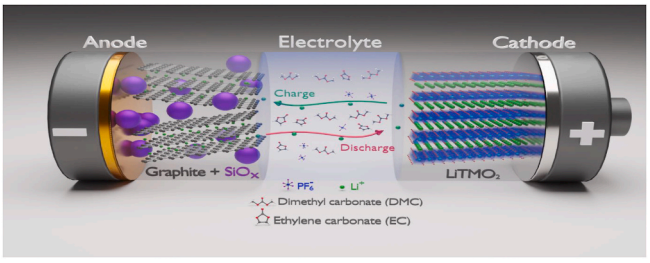

Fig. 1. Schematic illustration of the state-of-the-art lithium-ion battery chemistry with a composite of graphite and SiO_x as active material for the negative electrode (note that SiO_x is not present in all commercial cells), a (layered) lithium transition metal oxide ($LiTMO_2$; TM Ni, Mn, Co, and potentially other metals) as active material for the positive electrode, and a liquid electrolyte based on organic carbonates as solvents and $LiPF_6$ as conducting salt; the electrolyte commonly comprises moreover a set of additives and potentially also additional solvents and lithium salts.

2. Electrode active materials – the negative electrode

2.1. Intercalation/insertion-type materials – graphite and $Li_4Ti_5O_{12}$

2.1.1. Graphite – the industrially dominating anode material[1]

The breakthrough of the lithium-ion battery technology was triggered by the substitution of lithium metal as an anode active material by carbonaceous compounds, nowadays mostly graphite [29]. Several comprehensive reviews partly or entirely focusing on graphite are available [28,30–34]. The theoretical specific capacity[2] of graphite is 372 mAh g^{-1} when LiC_6 is formed. The intercalation of lithium proceeds via the prismatic surfaces between 0.25 V and 0 V vs. Li^+/Li (almost 3 V vs. the normal hydrogen electrode, NHE) and increases the interlayer distance by ca. 10% [35]. At the basal planes, the intercalation can only occur at defect sites [36]. The potential plateaus, observed during intercalation, correspond to two-phase regions of co-existing single phases [37], where there is no driving force for equilibration, and therefore inhomogeneities in local concentration of lithium stay stable, both at the electrode and graphite particle level. Only a few classes of aprotic electrolytes kinetically stabilize (i.e., passivate) the graphite surface, covering it with electrolyte reduction products [38–40] (see also *Chapter 4*). The passivation film (commonly referred to as solid electrolyte interphase, SEI) kinetically protects the electrolyte from further reduction [38,41]. Good SEI films are electronically insulating and should act as a "sieve", permeable only for Li^+ cations, but impermeable to other electrolyte components [42]. The composition and morphology of SEI layers depends on the kind of the electrolyte and in particular the lithium salt [43–46]. Electrochemical parameters, like the current density during the first reduction ("formation") and the temperature during the formation, influence the SEI quality. The SEI films are typically non-homogeneous and composed of (at least) two interpenetrating components [32,47]. At the surface of the electrode, there is a rather thin and more compact film of mostly inorganic decomposition products. Further towards the electrolyte, there is a thicker, possibly porous, and electrolyte-permeable film of organic decomposition products. The SEI films are typically rough; their average thickness increases from about 0.02 μm for freshly formed SEI up to about 0.1 μm for films on strongly aged electrodes [48–50]. In some electrolytes, the SEI films are partially soluble. The protective SEI films can be damaged, when there is, e.g., an excursion of the potential to >1.5 V vs. Li^+/Li. In a given

[1] Parts of the text are from the review chapter of Novák et al. cited herein as reference [28].

[2] The correct term according to the IUPAC nomenclature is "specific charge". However, the term most often used in current technical documents is "specific capacity" which is therefore used throughout this manuscript as well.

electrolyte solution, there is a similarity in the mechanism of SEI formation on carbon and metallic lithium [42,51–55]. As received, carbonaceous materials are covered by surface oxide groups [56], influencing the reactivity towards the electrolyte. There is a competition among many parallel and follow-up reduction reactions of surface groups, electrolyte salts, electrolyte solvents, electrolyte additives (if present), and impurities. The reaction products, precipitating on the surface of the electrode, introduce additional effects, governed by unknown parameters, which are difficult to identify and measure such as the local ohmic resistance. The diffusion and migration rates of numerous species in the electrolyte, the SEI layer, and the electrode must be considered as well [57]. Finally, it must be considered that the reactions of some electrolyte additives (e.g., vinylene carbonate, VC) are initiated electrochemically, but then the reaction proceeds chemically, i.e., without significant charge consumption, and the reaction products are forming layers on the electrode surface [58]. The SEI typically contains LiF, Li_2O, Li_2CO_3, organic semicarbonates, oligomers, and polymers [43]. The reduction of the solvents forms also gases (ethylene, propylene, hydrogen, CO_2, etc.). Occasionally, the reduction of traces of water, oxygen, and/or solvents used during the manufacturing of the electrodes must be considered [59]. Typically, 20 to 40 full charge/discharge cycles are needed to complete the formation of the SEI layer [60]. The SEI formation is a strictly surface-related process. There is a linear dependence of the irreversible charge consumption on the BET specific surface area (SSA) of graphite [49,61] and a similar dependence on the double-layer capacity of graphite electrodes [61]. Thus, from the SSA of a particular graphite type, the irreversible charge consumption in a lithium-ion cell can be directly estimated. Additionally, there is a small irreversible charge due to the reduction of the binder [62] and due to impurities in the electrolyte. In some electrolytes, the graphite structure exfoliates, which can be suppressed if ethylene carbonate is used as a major electrolyte component [63–68] and/or by the use of suitable electrolyte additives such as VC [68–71]. The chemistry of the surface groups and the extent of surface defects are then important for a good SEI formation, both parameters being related [72]. The cumulated surface area of these defects corresponds to the “active surface area” (ASA), an intrinsic characteristic of carbons [73–75]. The elimination of surface defects hinders the SEI formation and favours the exfoliation of graphite. The increase in ASA results in faster electrolyte decomposition and subsequent graphite surface passivation [76]. The distribution of the local electric potential inside the porous electrode [77,78] and, as a consequence, the distribution of the local current densities at every single graphite particle is also important [79]. There is a rather reversible expansion/contraction of graphite, leading to pronounced mechanical fatigue of carbon electrodes upon prolonged cycling [80–85]. Moreover, the SEI periodically swells and shrinks [86]. The carbon particles can therefore break-up and create new surface as well as cracks in the SEI layer. Thus, a new SEI layer is formed on continuously-created “defect” areas, a process consuming both lithium and charge. Therefore, during the lifetime of the cell, the average thickness of the SEI increases (the consequence of which is cell capacity fading), accompanied by an increase of the interfacial resistance (the consequence of which is power fading).

Finally, carbonaceous conductivity enhancers [87], used in small amounts (below 1-2%) to control the electronic and thermal conductivity in most of the commercial carbon negative electrodes, must be mentioned. In contrast to carbon black, graphite additives in the negative electrode have a double function — they act as conductivity enhancers and at the same time as electrochemically active electrode materials.

2.1.2. $Li_4Ti_5O_{12}$ - the safer alternative for high-power batteries

Despite the reliable and well-acquainted performance of graphite, the expanding field of rechargeable battery applications reveals shortcomings of carbon-based anodes. The first and foremost being the question of lithium plating, caused by a thermodynamic potential shift at low temperatures, due to the low working potential of graphite (ca. 0.1 V vs. Li^+/Li) and overpotentials at high currents [88], due to the nowadays required ever-higher charging speeds [89]. The plating of metallic lithium is a safety issue and, therefore, the use of an electrochemical redox couple with a lithiation potential higher than the one of graphite [90], is of definite interest.

Titanium oxides and, especially, lithium titanate ($Li_4Ti_5O_{12}$, LTO) have substantially higher working potentials – in case of LTO it is ca. 1.55 V vs. Li^+/Li – for the Ti^{3+}/Ti^{4+} redox couple, and are appealing alternatives to overcome the safety issues [91]. However, the improved safety comes with significantly lower energy density due to its halved specific capacity of 175 mAh g^{-1}, as compared to graphite, and the reduced voltage window of the battery cell by ~1.5 V. Nonetheless, LTO offers several advantageous characteristics in addition to the improved safety. It is a “zero strain” Li^+ host [92], as its unit cell volume changes only by 0.2% upon lithiation and de-lithiation. Therefore, it is an inherently structurally stable material with excellently reversible Li^+ de-/insertion [93–95]. It also features an extremely flat potential plateau on both charge and discharge, characteristic for a two-phase reaction mechanism [96]. LTO, having a 3D structure, is expected to have excellent rate performance. However, it is characterized by a rather low intrinsic electronic conductivity ($<10^{-13}$ S cm^{-1}) and low Li^+ diffusion coefficient, and therefore performs poorly at high rates [97,98]. Large part of the research work over the years was dedicated to an improvement of the electronic conductivity as a main cause for poor rate capability. Doping with various atoms [99,100], nanosizing [94,95], nanostructuring [101,102], and applying various coatings [97,101,103,104] have been the main strategies at hand. The synthetic routes, incorporating aforementioned conductivity-improving strategies, led to LTO materials capable of extremely high rates and unprecedented cycling stability, making LTO highly relevant for the mass production of batteries. At the same time, the research on LTO has been marked by on-going discussion about its surface reactivity towards the electrolyte and the question whether an SEI is formed on the LTO surface, since its working potential is well within the electrochemical stability window of common liquid electrolytes. As it is well-known, the SEI formation is accompanied by gas formation, and in case of graphite, electrolyte decomposition products form a protective layer, ceasing further electrolyte decomposition. However, it has been recently shown that in the first cycle between 2.6 V and 1.7 V vs. Li^+/Li water is reduced and the thus formed hydroxide ions initiate the autocatalytic hydrolysis of EC, even at very low water contents of <10 ppm [105]. In the case of LTO, the reactivity and gassing during cycling have also been attributed to water residues in the electrolyte and electrode [106] and to a significant exaggeration of electrolyte decomposition at elevated temperatures, while in dry electrolytes at room temperature the gassing has been minimal [107]. Keeping in mind that the water-initiated electrolyte decomposition is happening at potentials above the de-/lithiation potential of LTO, an SEI caused by electrolyte decomposition can be formed, indeed. The main gaseous species evolved are H_2, C_2H_4, and CO_2, all of which are characteristic to solvent reduction and SEI formation. In fact, the formation of an SEI on LTO has been demonstrated [98], but the question remained whether it is formed on LTO or other electrode components, such as the conductive additive. This has been clarified recently by using X-ray photoemission electron microscopy (XPEEM), characterized by high lateral resolution down to the nanometer scale and high surface sensitivity. The XPEEM analysis showed that electrolyte decomposition is specifically detected on LTO particles and the carbon black conductive additive remains SEI-free [108]. The combination of these operando and post mortem studies have confirmed the LTO surface reactivity towards the electrolyte, especially at elevated temperatures, suggesting that the SEI formed is less stable on LTO than on graphite and that, due to its solubility at elevated temperatures, electrolyte decomposition can proceed even after the formation of the initial SEI.

2.1.3. Perspectives for graphite and $Li_4Ti_5O_{12}$

Both graphite and LTO are nowadays established commercial materials. Graphite anodes are the industrial standard for lithium-ion batteries, and it is anticipated that only minor improvements can be expected in the future. Similar fate awaits LTO anodes, as they occupy a niche market, where extreme safety is of utmost importance, such as medical devices and public transportation. The use of LTO-comprising batteries might increase with the development of electrolytes which are stable at high voltages, thus allowing for the use of high-voltage cathodes, as in such case energy densities, competitive to the current graphite-based batteries might be reached – with the valuable add-on of avoiding lithium plating. While the successful realization of solid-state electrolytes might bring comparable safety features, LTO will presumably remain to be the anode material of choice for highly safe lithium-ion batteries – at least in a short-to mid-term perspective. Similarly, graphite is anticipated to remain the anode material of choice for commercial lithium-ion batteries. Despite only minor improvements possible for pure graphite negative electrodes in the future, the next step involves pairing graphite with high-capacity active materials with a similar de-/lithiation potential, such as silicon, tin, or phosphorous.

With regard to the use of graphite as conductive additive, which is also needed for LTO electrodes, the future will presumably be nanostructured carbons, such as graphene, carbon nanotubes and carbon nanofibers, which promise an improved thermal and electronic conductivity, especially when high power will be the decisive factor.

2.2. Alloying-type materials – silicon and silicon oxide (SiO_x

2.2.1. Recent development and achievements

Alloying-type anodes generally offer much higher specific capacities than carbonaceous anodes. Among the elements, metals and metalloids electrochemically forming alloys with lithium silicon is the most promising towards real applications thanks to the highest gravimetric[3] and volumetric capacity [109]. For this reason, Si anodes have been widely studied and reviewed, see for instance Ref. [110–121] and the references therein. Si is a very promising candidate to replace graphite for the following reasons: (1) It is abundant, eco-friendly, and non-toxic, (2) it offers extremely high gravimetric and volumetric capacities (3579 mAh g^{-1} and 2194 mAh cm^{-3}, respectively, at room temperature (RT)), and (3) it displays an appropriate average voltage of ca. 0.4 V vs. Li^+/Li. However, Si suffers from poor cyclability due to the large volume change (280% during full-capacity cycling at RT), leading to subsequent mechanical and chemical degradation. Mechanical degradation occurs as pulverization of silicon particles, loss of electronic contact between the Si particles and the electrode conductive network, and delamination from the current collector. Chemical degradation takes place along with the irreversible consumption of the electrolyte and active lithium due to the continuous growth of an unstable SEI, which lowers the coulombic efficiency (CE). Research on RT Si anodes started in the mid-90's with the basic understanding of Li reaction mechanism and the study of Si thin films, Si-metal alloys, and Si/C composites. To tackle the volume change issue and increase cycle life, various nano-sizing strategies were first developed leading to Si 0D nanoparticles, 1D nanowires, nanotubes, nanofibers, nanorods, and 2D thin films and nanosheets. A new step forward was achieved with coupling void-engineering, and metal or carbon composite strategies, that led to various 3D nanoporous structures (e.g., yolk-shell [122], pomegranate [123], hollow silicon [124], watermelon [125], raspberry [126]) with high capacity – commonly more than twice that of graphite was retained for more than 100 cycles in half-cells. A large surface area, however, results in decreased CEs (due to the increased SEI formation) and the low tap density lowers the volumetric energy density. Thus, recent developments focused towards microscale materials assembled from nanostructured subunits. The co-utilization of graphite and Si (or SiO_x) in blends and composites provides the best volumetric performance while retaining good cyclability. SiO_x materials consist of Si and SiO_2 nano-domains and silicon sub-oxides at their interfaces [127]. The presence of oxygen allows a trade-off between volume expansion and initial CE (ICE) [128]. The good cyclability is attributed to silicate which prevents the Si domains from sintering [129]. Moreover, SiO_x does not undergo a phase transition to a c-$Li_{15}Si_4$-like structure [129,130]. Nevertheless, the low ICE limits the use of SiO_x to about 5 wt% in combination with graphite. Rather than simply blending graphite with silicon, constructing micrometer-sized hierarchical structures of silicon/graphite/carbon (Si/G/C) composites is a more efficient way of tailoring the morphology, surface and robustness [30] – also with respect to the overall electronic conductivity within the electrode.

Together with the work on the active material itself, great progress has been achieved also for another highly important electrode component for maintaining the structural integrity – the binder.

As a matter of fact, the binder is essential to contain the volume expansion of the electrode, maintain the contact with the current collector, and minimize the degradation of the liquid electrolyte by forming a protective "artificial" SEI layer, see for instance Refs. [19,20,131–133] and references therein. Numerous studies have established the key characteristics of their chemical composition, such as the presence of functional groups capable of interacting specifically with the silicon surface, and of their molecular structure. In this regard, three-dimensional branched polymers seem to be superior to linear polymers and physical crosslinking via labile bonds such as hydrogen and ionic bonds, which would confer self-healing properties, seems to be superior to chemical crosslinking. Some promising results were obtained on multifunctional conductive polymers. Besides these developments, a lot of research has been conducted in order to better understand the SEI formation, morphology, and composition on Si with the aim of designing a stable and robust surface film. The SEI is a thin film with a complex and heterogeneous sub-structure with an inner layer that is commonly more inorganic and a relatively soft and more electrical resistive organic outer layer. The Si native oxide layer influences the reactivity with the electrolyte. Fluoroethylene carbonate (FEC) and CO_2 are very efficient SEI-forming electrolyte additives for Si and/or Si-based composite anodes. However, both additives are consumed upon cycling and their complete consumption coincides with a significant Li trapping. Isocyanates nitrogen containing additives, apart from serving as SEI-building precursors, can also scavenge H_2O and HF impurities from the electrolyte solution, thus, minimizing their deleterious effect in the battery system. Ionic (salt-type) and silane additives offer the opportunity to modify the conductivity and mechanical properties of the SEI [134]. Prelithiation is often proposed to solve the issue of the too low ICE [135,136]. This strategy is also a way to introduce a lithium reservoir into the anode and achieve very long cyclability [137].

As a result, the technological improvement and enhanced understanding have led to the first commercially available Si-based anodes in 2015 with 730 Wh L^{-1} (e.g., the INR18650-MJ1 from LG Chem [138] or the NCR18650BF & G from Panasonic [139]), compared to 690 Wh L^{-1} for pure graphite anodes, with material suppliers such as Hitachi, Shin-Etsu, or BTR.

2.2.2. Remaining challenges and future research directions

Over the last 20 years several inherent issues encountered by Si anodes have been tackled. Innovative advances on the material design have been fruitfully pursued with substantial efforts at the electrode design & processing level to increase the proportion of active silicon in the cell. However, most studies use low areal Si loadings (<1 mg cm^{-2}) and/or low electrode densities (<0.5 g cm^{-3}), resulting in a lower volumetric energy density than obtained for graphite. Additionally, most lab-scale processing protocols are difficult to scale-up. In fact, for thick and dense electrodes, the lithium-ion transport is limited, while

[3] Note that the terms "gravimetric" and "specific" are equally used herein – both referring to the mass (i.e., kg^{-1}) rather than the volume (i.e., L^{-1}).

mechanical damages such as cracking and delamination of the active material from the current collector are more pronounced [114]. Calendering, commonly used to increase the electrode density and volumetric capacity, unfortunately destroys some porous/hollow Si/C composites due to their poor mechanical strength and/or breaks the binder network [140]. Furthermore, the synthesis of complex porous/hollow structures requires expensive multi-step processes that hinder further development. Last but not least, many Si anode studies still lack from evaluation in full-cells.

Globally, for the optimization of the volumetric energy density, the initial electrode density and thickness and their control upon cycling are important factors to be addressed [114]. It is still poorly understood, how stress develops in the porous structure during cycling and how materials, electrodes, cells, and ultimately the whole battery pack can be rationally designed to mitigate the effects of the volume changes occurring [141]. Obrovac [113] concludes that it is of utmost importance to minimize or eliminate the volume expansion to limit any stress in the cell and to stick to the use of thin separators and current collectors, and to keep the ratio of inactive components low. Indeed, to maintain high safety the separator should not experience any significant stress and any swelling should be accommodated at the electrode level. The initial electrode and active material porosity needs to be adjusted to allow for an acceptable electrode deformation during charging [142]. Accordingly, we propose to discuss the total volumetric capacity $Q_{v,tot}$ as follows:

$$Q_{v,tot} = Q_{spe} \times \omega_{AM} \times \rho_{an} \times \Delta L \times ICE$$

Q_{spe} is the specific capacity, ω_{AM} is the active material (AM) weight ratio, ρ_{an} is the initial anode density, and ΔL is the swelling at 100% SOC (i.e., in the fully lithiated state for the anode). Practically, for typical graphite in commercial cells, we have calculated a total volumetric capacity of 550 Ah L^{-1} ($360 \times 0.98 \times 1.65 \times 1.095 \times 0.94$). A continuous improvement is observed at the anode level (in Ah L^{-1}) when increasing the capacity of the graphite/Si composite anode (Fig. 2a), contrary to what has been published earlier and finally retracted [143]. The improvement at the cell level (in Wh L^{-1}) is "much less", since the anode volume stands for only a third of the total cell volume. Hence, any improvement cannot exceed this third. Note that the cell improvement levels off at about 1500 mAh g^{-1}. Nonetheless, this calculation highlights that further improvement at the cell level can be realized also by further advances concerning the anode.

In this regard, future developments should be oriented towards the design of Si-based cells, readily useable in practical applications, with high volumetric capacity, long cycle life, high rate capability, non-expensive materials, and low-cost scalable synthesis and processing methods. This means that the Si anodes should have high areal (>3 mAh cm^{-2}) and volumetric capacity (see Fig. 2a), good mechanical strength for calendaring, a stable SEI, low electrode swelling upon cycling, high intrinsic conductivity, as well as fabrication simplicity and low cost. We anticipate that, like this, energy densities of 800–1000 Wh L^{-1} can be reached (see also Fig. 2b) with anodes based on, e.g., Si/G/C composites, Li_ySiO_x-C [128], porous silicon materials, and innovative 3D nanostructures. For instance, the recently published TiO_2-coated Si with a self-healing SEI and densified electrodes (1.4 g cm^{-3}) or microscroll-structured electrodes with a reversible volumetric capacity of 720 Ah L^{-1} might be promising research directions for the future [144,145]. Other promising research directions are the use of self-healing binders [146–148], new electrolytes (e.g., with high lithium salt concentrations or new ionic liquids) [149], or new electrolyte additives with higher dipole moment [150]. Also pre-lithiation strategies are a suitable approach to address the remaining challenges, keeping in mind, however, that they should be easily scalable. Moreover, many complimentary material design strategies might be combined at different levels, ranging from the electrochemically active and non-active components to the whole electrode and, finally, to the complete lithium-ion cell. In fact, the full-cell development will, thus, require also the exploration of an optimal anode/cathode compatibility, optimized electrolytes, and enhanced separators.

At least as important, future developments should also target an improved basic understanding of the reaction and aging mechanisms occurring and, for this purpose, the development of advanced *in situ/operando* characterization techniques [151]. Electrochemical dilatometry, for example, is a suitable non-destructive technique for measuring the electrode and cell swelling as a function of the applied pressure [114,152]. Tomographic imaging techniques in 3D of the electrode architecture are very valuable for understanding the cracking and delamination mechanisms [153–156]. The data obtained by these measurements and the digitization of the electrode architectures can feed numerical simulations for elucidating the mechanical behaviour of the electrode at its different scales. Similarly, the development of molecular simulations along with *in situ* surface characterization techniques are essential to better understand the SEI formation and design a robust one [117,157].

There is also a strong need for standardization and more systematic studies. As reaction mechanisms and battery performance are greatly affected by numerous variables, the comparison of published data is very challenging. The credibility of any cycle life comparison is therefore questionable. For example, comparing different binders requires much more careful studies than is generally done. The optimal composition of the electrode slurry and of the dry electrode may vary from one binder to another [158] and with the loading of the electrode as well as its densification. There is almost no exhaustive study of this set of factors, since such tedious studies are commonly not valued, as novelty is preferred by journal editors and the number of publications by evaluators. Nonetheless, standardization and in-depth studies are necessary for progressing towards reliable and low-cost high energy density batteries in the context of the acceleration of global warming.

3. Electrode active materials – the positive electrode

3.1. Lithium transition metal phosphates

3.1.1. The state of the art – $LiFePO_4$

Lithium transition metal phosphates with an olivine structure were first introduced as cathode materials for lithium-ion cells over twenty years ago [159]. Since then, a wide variety of transition metals and combinations have been evaluated, including iron, manganese, vanadium, cobalt, and nickel [160]. The reversible de-/lithiation mechanism involves the transition between different crystalline phases, e.g., between $LiFePO_4$ (LFP) and $FePO_4$. This has important implications for the design of the active material particles and electrode structure, and in understanding the electrode reaction mechanisms [161,162]. A severe challenge is the rather poor electronic conductivity [163]. To overcome this, the active material particles are surface coated with carbon, rather than just using one or more conductive carbons as an electrode additive [164,165]. Despite this lower electronic conductivity, phosphate materials are mostly used in high power applications like hybrid electric vehicles thanks to the important progress in active material design. Nowadays, there are numerous synthetic methods to produce $LiFePO_4$, usually in a carbon-coated form [166]. These divide into solid-state and solution-based techniques. The former include traditional solid-state synthesis, mechano-chemical activation, carbo-thermal reduction, and micro-wave heating. The latter include hydrothermal synthesis, sol-gel synthesis, spray pyrolysis, co-precipitation, and micro emulsion drying. Typically, the solution based routes use less energy, and produce a better product (higher capacity, smaller and more uniform particle size, high purity, more homogeneous carbon coating). Carbon coating is achieved through various precursors, e.g., pyrolysis of sucrose. Performance at high rates is improved by using small particles, and low concentrations of metal ion dopants. The maximum theoretical specific capacity of LFP is 170 mAh g^{-1}. At an average discharge voltage of 3.45 V, this gives a theoretical specific energy of 586 Wh kg^{-1}. A variety of

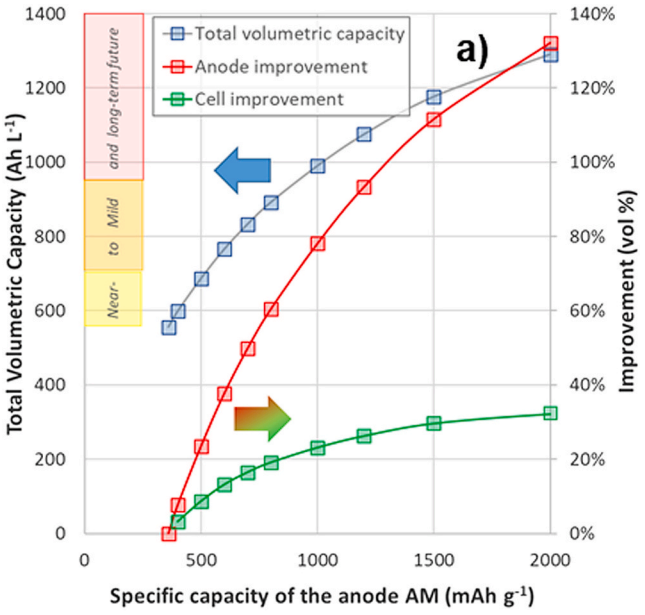

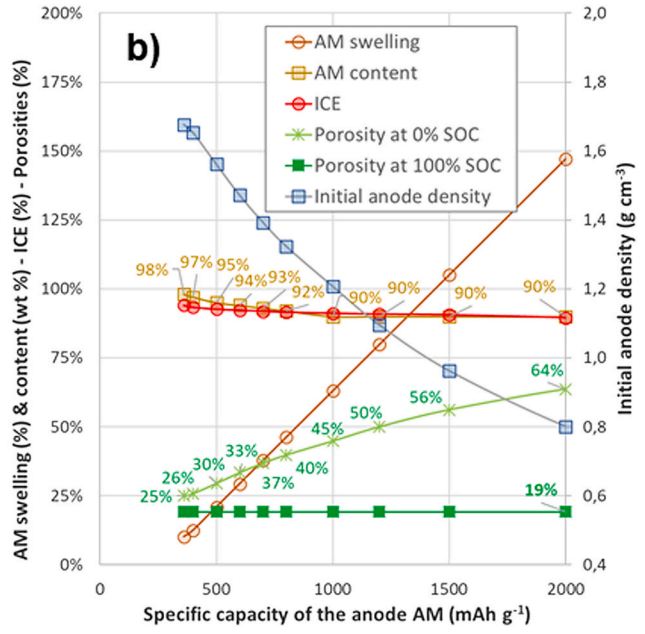

(caption on next column)

Fig. 2. (a) Total volumetric capacity as a function of the specific capacity of the anode active material (AM) and the resulting improvement at the anode and cell level (in vol%). (b) Hypothetical calculation of the total volumetric capacity: For the specific capacity, a composite of graphite and silicon is assumed, considering a specific capacity of 372 and 3579 mAh g^{-1}, respectively. The AM swelling is then calculated assuming a linear variation (following the approximation for graphite [430]) and a maximum swelling of 10.1% and 280.1% for graphite and silicon, respectively. Note that for a lower effective specific capacity of silicon and/or graphite, the swelling will not follow a proportional factor. Then, at the anode level, a commercially relevant AM content of >90 wt % and an ICE of 90% have been used for the calculation. The thickness of the anode is considered constant upon lithiation and the porosity at 100% SOC is always the same as the one calculated for the pure graphite anode to maintain an efficient lithium transport. However, the initial porosity is adjusted to buffer the swelling. Note that the porosity takes into account the whole anode including the AM itself. The initial anode density considers an inactive materials density of 1.7 g cm^{-3}. The improvement at the cell level (in Wh L^{-1}) is calculated considering 700 Ah L^{-1} for the reversible volumetric capacity of the cathode and a total of 67% active material in the cell. This means, for instance for a 21700 cell, an areal capacity of more than 3 mAh cm^{-2} for both the anode and the cathode and thicknesses of 16 μm for the separator, and 10 μm and 15 μm for the copper and aluminium current collector, respectively. (For interpretation of the references to colour in this figure legend, the reader is referred to the Web version of this article.)

experimental conditions was evaluated using a solution-based synthesis that also includes mechanical activation by ball milling, and subsequent heat treatment at 450–700 °C [167]. For the material milled with medium energy, the particle size increased with heat treatment temperature from 73 nm at 450 °C to 181 nm at 700 °C. Adding carbon during the mechanical milling step reduced the particle size and the electrode resistance, and thus increased the achievable capacity. Two different surfactants were used in a solution-based synthesis of LFP [168]; a cationic surfactant cetyl trimethylammonium bromide (CTAB), and an anionic surfactant sodium dodecylbenesulphonate (SDBS). With no surfactant, there was a bimodal particle size distribution, with peaks at 10 μm and 100 μm. With SDBS the peaks were at 4 and 8 μm, and with CTAB just at 3 μm. The surfactants produced some improvements in rate performance and capacity retention during cycling, and a remarkable difference in the alternating current impedance spectra. The CTAB surfactant was also used in an LFP synthesis based on a $Fe_{1.5}P$ precursor, containing trace amounts of impurities like manganese and titanium [169]. The LFP prepared with the highest CTAB content had a capacity higher than the theoretical maximum, due to the presence of other phases in the material. A mixed protective/reducing gas (5% hydrogen in argon) was used during the calcination stage of an LFP material at 700 °C [170]. The gas formed Fe_2P on the surface of the particles, improving the electronic conduction pathway between them. The best rate performance was obtained with intermediate gas flow levels. A Fe_3P phase was detected on the surface of LFP prepared with a sucrose precursor, calcined at temperatures above 710 °C [171]. This phase is assumed to increase the electronic conductivity, but to interfere with lithium diffusion. A solid-state synthetic route for LFP used an induction furnace at 1100 °C to melt the precursors [172]. After solidification and grinding, the sub-micron sized particles were spray-dried with lactose and PVA (poly vinyl alcohol), before calcination at 700 °C. The best cycle life was obtained with an LFP: lactose: PVA ratio of 90 : 10: 1. Another less common carbon precursor was a polymerized hydroquinone-formaldehyde resin, which was intended to create an improved interconnected carbon structure [173]. The discharge capacity at 20C was increased over a control sample using glucose. General comparisons of cycle life and rate performance, however, are difficult, because of the influence of electrode formulations and loading, test protocols, and other experimental conditions. For example, Table 1 compares the ratios of the discharge capacities at 2C and 0.2C for the LFP papers listed above, where this information was provided (capacities shown with an asterisk* are for 0.1C rather than 0.2C). The range of

Table 1
Overview for several very recent studies on LFP-based positive electrodes with varying synthesis methods, carbon coating procedures, and electrode compositions and the reported discharge capacity at 0.2C (*0.1C) and 2C; **reference [174] employed a carbon-coated aluminium current collector instead of blank aluminium foil.

Electrode (wt%)Active: Binder: Carbon	Discharge capacity (mAh g $^{-1}$)		2C: 0.2CRatio (%)	Reference
	0.2C	2C		
80 : 5: 15	156	139	88.9	[167]
75 : 10: 15	151	132	87.3	[168]
80 : 10: 10	172*	118	68.7	[169]
80 : 10: 10	154	133	86.3	[170]
84 : 07: 09	160	152	95.2	[172]
80 : 10: 10	169*	145	86.0	[173]
95.5 : 4.5 : 0**	150	142	95.0	[174]

electrode formulations is evident, without even considering the particle size distribution, carbon coating content, coat weight and electrolyte formulation. The material, out of those presented in Table 1, with the best rate performance was spray dried with lactose and PVA, before calcination. Remarkable, though, is also the work reported by Busson et al. [174], who did not include any conductive carbon, but used a carbon-coated aluminium current collector instead of blank aluminium foil. The high capacity achieved at 2C highlights that the carbon coating might ensure sufficient electronic wiring and that the contact resistance between the electrode composite and the current collector is playing a decisive role for the rate capability.

Commercial lithium-ion cells containing LFP cathodes are produced by a range of different manufacturers (see Table S1 for a few examples), for various applications, and in a wide range of sizes and hence capacities. The Chinese electric bus market, for instance, is currently dominated by LFP-based lithium-ion cells, though for buses outside China, the split between LFP and layered lithium transition metal cathodes (see also the following chapter) is roughly 50:50. Many cells with a $Li_4Ti_5O_{12}$ (LTO) anode also use a high rate LFP cathode, since the charge rate limitation in standard LFP cells is actually the graphite anode (see also Section 2.12).

3.1.2. *Increasing the energy density by going beyond $LiFePO_4$*

Despite the commercial success of LFP cathodes, the resulting lithium-ion cells struggle to achieve the energy density of the layered lithium transition metal oxide materials (especially so-called Ni-rich oxides, which will be discussed in the subsequent chapter) due to their lower operating voltage (3.45 V), capacity (170 mAh g $^{-1}$), and crystalline density (3.6 g cm $^{-3}$; see also Table 2 and Fig. 3). One way to increase the energy density is to increase the operating voltage, by replacing some or all of the iron with other metals. The operating voltage for $LiMnPO_4$ (LMP) is 4.1 V [175], with $LiCoPO_4$ (LCP) at 4.75 V and $LiNiPO_4$ (LNP) at 5.1 V [176]. This gives theoretical gravimetric energy densities of 701, 783, and 851 Wh kg $^{-1}$, respectively, compared to 586 Wh kg $^{-1}$ for LFP (all values referring to the cathode active material only with reference to a theoretical lithium counter electrode). Nonetheless, the last two voltages for LCP and especially LNP are beyond the electrochemical stability of conventional electrolytes based on cyclic and linear organic carbonates, thus, compromising electrochemical tests and requiring specifically designed electrolyte compositions [177]. Additionally, LCP, which is characterized by a rather complicated polymorphic structure [178,179], is generally considered critical with respect to the criticality of cobalt [9,180]). To reduce the cost of the material, some of the cobalt can be replaced with nickel. A range of materials in the $LiNi_xCo_{1-x}PO_4$ family were synthesized, but the highest capacity was still observed for pure LCP [176]. In the case of LMP, with a more suitable de-/lithiation potential with regard to the electrochemical stability of common electrolytes, moreover, the electronic conductivity is even lower than that of LFP. To address this issue, the synthesis of (nanoparticulate) LMP has been optimized and carbon coatings have been applied, e.g., by pyrolising glucose [175]. Another approach to enhance the performance of phosphate-type cathodes has been the

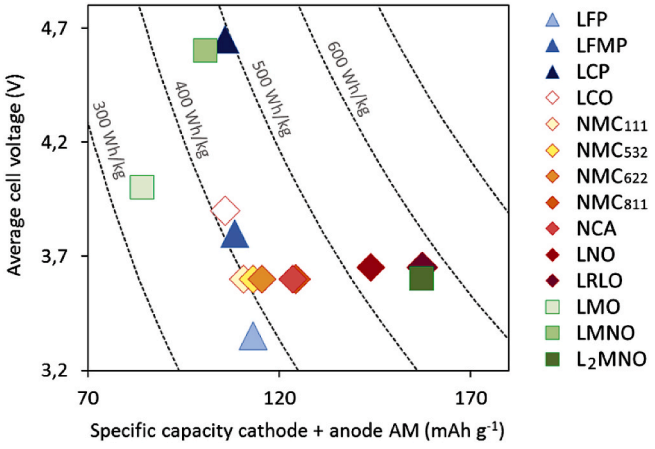

Fig. 3. Average cell voltage, specific capacity, and specific energy for different cathode active material/graphite combinations, calculated for a cathode/anode balancing of 1.0 and a specific capacity of 360 mAh g^{-1} for graphite (considering solely the mass of the two active materials) in accordance with Table 2.

Table 2
Overview of the herein discussed lithium-ion cathode materials, their stoichiometry, structure, space group (SG), specific capacity, and average de-/lithiation potential; the specific energy is calculated for such cathode when combined with a graphite anode, assuming a specific capacity of 360 mAh g^{-1} and an average potential of 0.1 V vs. Li^+/Li for graphite with a cathode/anode balancing of 1.0.

Code	Stoichiometry	Structure type	SG	Practical specific capacity (mAh g $^{-1}$)	Average potential (V vs. Li^+/Li)	Specific energy active material combination (Wh kg $^{-1}$)
LFP	$LiFePO_4$	phospho olivine	*Pnma*	165	3.45	379
LFMP	$LiMn_{0.7}Fe_{0.3}PO_4$	phospho olivine	*Pnma*	155	3.90	412
LCP	$LiCoPO_4$	phospho olivine	*Pnma*	150	4.75	492
LCO	$LiCoO_2$	layered oxide	R-3m	150	3.90	402
NMC_{111}	$LiNi_{0.33}Mn_{0.33}Co_{0.33}O_2$	layered oxide	R-3m	160	3.70	399
NMC_{532}	$LiNi_{0.5}Mn_{0.3}Co_{0.2}O_2$	layered oxide	R-3m	165	3.70	407
NMC_{622}	$LiNi_{0.6}Mn_{0.2}Co_{0.2}O_2$	layered oxide	R-3m	170	3.70	416
NCA	$LiNi_{0.8}Co_{0.15}Al_{0.05}O_2$	layered oxide	R-3m	188	3.70	445
NMC_{811}	$LiNi_{0.8}Mn_{0.1}Co_{0.1}O_2$	layered oxide	R-3m	190	3.70	448
LNO	$LiNiO_2$	layered oxide	R-3m	240	3.75	526
LRLO	$Li[Li_{0.2}Ni_{0.2}Mn_{0.6-x}M_x]O_2$	layered oxide	C/m	280	3.75	575
LMO	$LiMn_2O_4$	spinel	Fd-3m	110	4.10	337
LMNO	$LiNi_{0.5}Mn_{1.5}O_4$	spinel	$P4_332$	140	4.70	464
L_2MNO	$Li_2Ni_{0.5}Mn_{1.5}O_4$	spinel (tetragonal)	$I4_1/amd$	280	3.70	567

combination of different transition metals – for instance, the partial replacement of Fe by Mn, i.e., $LiFe_{1-x}Mn_xPO_4$ (LFMP). These materials operate at a higher average voltage than LFP (basically along two plateaus – one for Fe and one for Mn), and have higher electronic conductivity than pure LMP. The various synthetic routes developed for LFP have also been used to make LFMP materials, with different Fe: Mn ratios. These include inter alia a hydrothermal reaction at 200 °C [181], melting at 1000–1100 °C [182], carbo-thermal reduction [183], and solid state ball milling [184]. The materials were then carbon coated using various precursors. It is difficult to make direct comparisons of these materials, due to the different amounts of carbon coating, and the proportion of conductive carbon used in the electrode formulations. However, within each method observations included that the iron content should be at least 20% [181], and an increased pore volume in the material was beneficial [183]. To improve the rate performance of LFMP, for instance, vanadium was added as a third transition metal, in a hydrothermal synthesis route that also incorporated graphene oxide [185]. Analysis showed that the product was a mixture of orthorhombic $LiFe_{0.5}Mn_{0.5}PO_4$ and monoclinic $Li_3V_2(PO_4)_3$. The material achieved more than 50% of its C/5 capacity at 50C, and 1000 cycles at 10C and 20C.

3.2. Lithium transition metal oxides

Several lithium transition metal oxide chemistries find application as cathode materials in lithium-ion batteries. Their function follows the host/guest principle, providing stable MO_2 host structures with nickel, manganese, and cobalt as common redox-active centres, and lithium as mobile guest. The roadmap for electric mobility [15,186] mentions especially three material classes for the realization of high-energy lithium-ion batteries: "common" layered lithium transition metal oxides (especially with a high Ni content), presently dominating the lithium-ion battery market, and, for the near-to mid-term future, high-voltage spinel oxides and lithium-rich layered oxides. An overview of the main characteristics of the cathode materials discussed herein (including the earlier discussed phosphates) is provided in Table 2, including also a calculation of the achievable specific energy when coupled with a graphite anode (see also Fig. 3).

3.2.1. "Common" layered transition metal oxides – from $LiCoO_2$ to Ni-rich $LiNi_{1-x-y}Mn_xCo_yO_2$

The first lithium-ion cathode material, commercialized in 1991 by Sony, was $LiCoO_2$ (LCO) [187].

LMO ($LiMn_2O_4$) [188,189] was introduced a few years later, followed by $LiNi_{1-x-y}Al_xCo_yO_2$ (NCA) [190] and $LiNi_{1-x-y}Mn_xCo_yO_2$ (NMC) [191–193]. While LCO still dominates the market for portable electronic devices, LMO is of lower relevance today and mainly used as additive in cathode blends. Differently, the introduction of NCA led to an outstanding increase in specific energy and longer lifetime compared to LCO, while the introduction of NMC significantly improved lifetime and safety, but at the cost of lower energy density.

The theoretical specific capacity of LCO is 274 mAh g^{-1}; however, practical utilization is limited to about 50%, due to structural instability at higher states of delithiation. Thermal instability in the charged state, raw materials cost, and limited availability of cobalt [9,180] limit the application to small cells. $LiNiO_2$ (LNO) [194,195], having a similar theoretical energy as LCO, is attractive due to lower raw material cost and the greater availability of nickel. Nonetheless, contrary to cobalt, nickel and lithium easily exchange lattice positions, which significantly affects performance and renders the precise control of the synthesis and material quality very challenging. In fact, despite more than 20 years of research, pure LNO could not yet be commercialized. The breakthrough was the approach of substituting part of the Ni in LNO by Co [196,197], Mn [198], and/or Al [199]. Co as substituent reduces the Li/Ni disorder, becoming fully effective for $x > 0.2$ [200,201], and as Co is electrochemically active, there is no capacity loss. Due to similarity in structure and ionic size, LNO and LCO form a full solid-solution series $LiNi_{1-x}Co_xO_2$. The additional substituents Mn and Al can form layered phases with LNO up to a substitution degree of $x = 0.5$. They stabilize the lattice, but reduce the achievable capacity, since they are not redox active in the commonly applied voltage range. The careful adjustment of the composition succeeded in balancing energy density, stability, safety, and cost with respect to the targeted application, which eventually led to the commercial success of NCM and NCA. As a result, these two materials are nowadays dominating the lithium-ion battery market, and further increase is anticipated, especially for NMC. Both derive from the isostructural endmembers LNO and LCO. Their structure can be described as an ordered rock-salt structure with lithium and the transition metals occupying alternate (111)-planes in a cubic close-packed arrangement of oxygen ions, crystallizing in the space group R-3m. The term NMC comprises a wide range of compositional variations, indicated by a short code, which combines the initial letters of the transition metals with a three-digit number for their stoichiometric ratio, as exemplified for NMC_{111} ($LiNi_{0.33}Mn_{0.33}Co_{0.33}O_2$) and NMC_{622} ($LiNi_{0.6}Mn_{0.2}Co_{0.2}O_2$). NMC_{111} as the first commercially used cathode material from this family offers highly stable cycling, combined with reasonably high safety and moderate specific capacity. After having been well established for a long time, however, it now progressively loses market shares, as NMC compounds with a higher Ni content provide two major benefits: (i) A reduced Co content and (ii) significantly (NMC_{532}, NMC_{622}) to substantially (NMC_{811}) higher energy densities – all of them being commercially available now and applied in cells. Nonetheless, the "simple" stoichiometric shift from NMC_{111} to Ni-rich materials has a strong impact on their implementation, since key steps of the value chain are affected, starting with the synthesis and further processing, and ending with the cycle life and safety of the final cell [202,203]. With an increasing nickel content, the synthesis becomes more challenging, as the tendency to form lithium off-stoichiometric phases during the thermal treatment, following the general reaction path of $LiNiO_2 \rightarrow 1/(1+z)\ Li_{1-z}Ni_{1+z}O_2 + z/(1+z)\ Li_2O + z/(2+2x)\ O_2$, becomes prominent [204]. From the structural point of view, the off-stoichiometry is described as $[Li_{1-z}Ni^{2+}_z]_{3a}[Ni^{2+}_zNi^{3+}_{1-z}]_{3b}[O_2]_{6c}$, with divalent nickel on the lithium positions. These interlayer nickel ions, when oxidized during initial charge, contract the interlayer distance, thereby kinetically hindering the electrochemical re-occupation of the directly neighboured vacant lithium positions [205,206]. The consequence is a high irreversible first-cycle capacity loss, the extent of which depends on z. Annealing at moderate temperatures under oxygen atmosphere, using LiOH as lithium source, effectively shifts the equilibrium in the direction of the stoichiometric phases for Ni-rich materials. Once synthesized successfully, however, aging due to storage under ambient air occurs. It follows, according to general acceptance, the same pathway to $Li_{1-z}Ni_{1+z}O_2$ and Li_2O [207], accompanied by the formation of Li_2CO_3 and LiOH [208,209] at the surface together with the slow segregation of Li_2O. These lithium-based surfaces species can cause gelation of the slurry during electrode preparation due to an increased alkalinity of the powder (specifically, LiOH). Additionally, upon cycling they promote gas evolution (specifically, Li_2CO_3) and lead to an increased charge-transfer resistance, which eventually results in rapid capacity fading [209–212]. Washing steps as counter measure to remove these surface impurities are still under controversial discussion [212–214].

Generally, the increase in specific capacity and, hence, energy density come at the cost of cycle life and thermal stability. The root cause is the thermodynamic instability of the delithiated phase, increasing with the ratio of tetravalent nickel. The layered structure becomes unstable with respect to oxygen release to form a progressively growing, dense NiO-like rock-salt reconstruction layer at the surface of the particles [215,216]. This is considered a main reason for the impedance increase and capacity loss during cycling. On top of the reconstruction layer, solid species such as LiF, Li_xPF_y, $Li_xPF_yO_z$, Li_2CO_3, and polycarbonates form a cathode electrolyte interphase (CEI), further contributing to

impedance increase [39]. The onset temperature for the exothermal reaction of the delithiated material with the electrolyte, i.e., one trigger for a thermal runaway, is significantly lowered for an increasing nickel content, rendering these materials less safe.

Simultaneously, prominent mechanical degradation may occur upon cycling, which is related to the phase transitions occurring at high degrees of delithiation and accelerates the aging of Ni-rich NMC. While these do not occur for NMC_{111}, they become increasingly pronounced for a rising nickel content – just like for LNO, which follows a series of first-order transitions between three hexagonal (H) phases and one monoclinic (M) phase [217]: H1→M→H2→H3. Each transition is characterized by an individual plateau in the de-/lithiation potential curve. Particularly, the H2→H3 transition involves a strong anisotropic change in lattice parameters, inducing severe crack formation at the (secondary) particle level [218–221]. This leads to the formation of fresh surfaces, at which new rock-salt phases are formed and electrolyte is decomposed – even more pronounced than at the initial surface [221].

Nevertheless, the target is an even higher nickel content, and promising mitigation strategies follow five main concepts:

(i) Doping and element substitution to enhance the thermodynamic stability of the lattice: The introduction of cobalt [196,197,200,201] and magnesium [222,223], for instance, reduces the presence of anti-site nickel on lithium positions. In the latter case, magnesium replaces lithium up to a substitution degree of 10%, acting as a pillar. The thermal stability in the delithiated state increases when introducing manganese [198], aluminium [199,224], or titanium [225], with aluminium and magnesium suppressing phase transitions, thus, reducing mechanical degradation. High-valence metal cations, such as tungsten [226], molybdenum [227], and zirconium [228] significantly stabilize cycle life and thermal stability even for pure LNO at levels of only 1%, with tungsten being the most effective.

(ii) The application of thin surface coatings to stabilize the interface between the electrolyte and the active material, reduce electrolyte decomposition, and stabilize the surface against oxygen release and reconstruction; suited chemistries act also as HF-scavenger [229].

(iii) The realization of core-shell [230] or gradient [231] active material particles, combining a high capacity core with highly stable surface composition, allowing for an improved cycle life and thermal stability – even at very high capacity levels.

(iv) The tailored design of the grain boundaries, e.g., by infiltrating low-melting oxides into the grain structure of the polycrystalline particles, thus, effectively suppressing crack formation without (significantly) affecting the achievable capacity [232,233].

(v) The synthesis of single-crystalline particles, which show exceptional cycle life and efficiency compared to polycrystalline secondary particles, with nearly no gassing even at elevated temperatures [234–238].

However, the strong focus on Ni-rich chemistries may drive nickel into supply risks. Forecasts on the future lithium-ion battery demand show, in fact, that a significant increase in nickel supply is needed, which is not covered by the existing mines. Accordingly, new mining projects and recycling strategies are inevitable, while ideally also new, low nickel content chemistries will be explored.

3.2.2. *High-voltage spinel oxides and Li-rich layered transition metal oxides*

Two cathode material candidates with less nickel are the high-voltage spinel ($LiMn_{2-x}Ni_xO_4$ (with $x \leq 0.5$), LMNO) and Li-rich layered oxides (LRLO). Both are based on the abundant manganese as main element and can be produced free from cobalt. Different from NMC, however, they operate at least partly beyond the stability window of today's standard electrolytes, and strong emphasis in research and development lies on stabilising the electrolyte/electrode interface to enable long-term stable cycling. Therefore, their market entrance is expected earliest in the next few years.

a) High-voltage spinel oxides

The class of high-voltage spinel is based on $Li[Mn^{3+}Mn^{4+}]O_4$, with Mn^{3+}/Mn^{4+} being oxidized/reduced at 4.1 V vs. Li^+/Li. The partial substitution of manganese with redox-active elements M can introduce an additional redox step, the contribution of which increases with x in $Li[Mn_{2-x}M_x]O_4$. Suited elements are Ni^{2+}/Ni^{4+} (4.7 V), Cu^{2+}/Cu^{3+} (4.9 V), Cr^{3+}/Cr^{4+} (4.8 V), Fe^{3+}/Fe^{4+} (4.9 V), and Co^{3+}/Co^{4+} (5.0–5.1 V; all values are given vs. Li^+/Li) [239–242]. The substitution of manganese is limited to a maximum of $x = 0.5$ and $x = 1.0$ for divalent and trivalent substituents, respectively. Among those, only $LiNi_{0.5}Mn_{1.5}O_4$ (LMNO) and $LiCo_{1.0}Mn_{1.0}O_4$ can enable a single full-length high-voltage plateau, while only $LiNi_{0.5}Mn_{1.5}O_4$ fulfils the future requirements on availability and cost given the earlier mentioned drawbacks of cobalt.

LMNO is highly sensitive to the synthesis conditions [243], losing oxygen at annealing temperatures >700 °C, thereby forming oxygen deficient phases $LiNi_xMn_{1.5-x}O_{4-\delta}$ and finally segregating NiO or $Li_{z-}Ni_{1-z}O$ from the structure. The oxygen stoichiometry δ and nickel content x control the potential characteristics [244]: Following the general formula $Li^+[Ni^{2+}{}_xMn^{3+}{}_{1-2x+2\delta}Mn^{4+}{}_{1+x-2\delta}]O_{4-\delta}$, the contributions of Mn^{3+}/Mn^{4+} (4.1 V) and Ni^{2+}/Ni^{4+} (4.7 V) account for $(1\text{-}2x+2\delta)$ and $(2x\text{-}2\delta)$ electrons per formula unit, respectively. A single high-voltage step is obtained for $x = 0.5$ and an ideal oxygen stoichiometry of $\delta = 0$. In this phase, an ordering of the transition metal sub-lattice occurs, lowering symmetry from Fd-3m to $P4_332$ and showing superlattice reflections in the diffractograms. A potentially beneficial effect of a slight oxygen-deficiency on the rate capability and performance is discussed controversially. Structurally stable, LMNO does not release oxygen within its operation window [245]. The main challenge is the instability of the electrolyte at such potentials, with the decomposition products contributing to the aging at the active material and cell level. This makes the careful design of the LMNO/electrolyte interface crucial. Promising strategies are (i) the crystal facet design [246–249], with the (111)-facets having the highest stability, (ii) the design of particles with low surface area [250], and (iii) the application of protective surface coatings to minimize side reactions [249,251–254]. LMNO is able to utilize remaining Mn^{4+} as additional redox-centre working at 2.7 V to form $Li_{2.0}Ni_{0.5}Mn_{1.5}O_4$ (L_2MNO) [255,256]. This significantly contributes to the achievable energy density. Application concepts include making use of both potential plateaus to maximise energy or using the excess lithium x in L_{1+x}MNO to compensate for the initial capacity loss, especially in combination with silicon-comprising anodes [257].

b) Li-rich layered transition metal oxides

The second class of potential future cathode material candidates are Li-rich layered oxides (LRLO) [258–260]. They have the general formula $Li[Li_xM_{1-x}]O_2$ with excess lithium ions x on transition metal positions (M = Ni, Co, Mn, etc.), forming a partially ordered honeycomb structure, indicated by superlattice reflections in the X-ray diffractograms. The general notation x $Li_2MnO_3\cdot$ $1\text{-}x$ $LiMO_2$ describes the system as a structural combination of Li_2MnO_3 and stoichiometric layered oxides [261], which may form a solid solution or a composite of the respective nano-domains – depending on the eventual chemical composition and synthesis conditions. These materials can reach high specific capacities of up to 300 mAh g ^{1}, greatly exceeding the theoretical contribution of their transition metals. This is explained by a reversible contribution of anionic redox reactions in the crystal structure, according to $2O^{2} \rightarrow O_2^{n} + (4\text{-}n)$ e , with $n = 1$–3 [262–264]. The pristine structure needs to be activated first, though, to make the anion redox contribution accessible. The activation occurs during the initial charge process at high operating voltages (>4.4 V vs. Li^+/Li), leading to the formation of oxygen vacancies near the surface [265], structural replacement of the

transition metals [266], release of oxygen [267], and the formation of different lithium oxygen compounds.

However, despite the promising high specific energies, several issues need to be solved to bring LRLO into commercial cells: (i) Due to the structural rearrangements and oxygen release, the materials show a high first-cycle capacity loss. (ii) The materials have slow kinetics attributed to the contribution of the anion redox activity, which, so far, limits fast charging. (iii) The pronounced voltage hysteresis lowers the round trip efficiency, irreversibly transforming electrical energy into heat, which is then released in the cell. (iv) Side-reactions with the electrolyte due to the required high cut-off voltage and (v) a severe voltage fading during cycling, attributed to the progressive formation of spinel-like phases, are main aging phenomena to be understood and solved.

Remarkably, for future high-energy cells with, e.g., a silicon-based anode, the use of the high irreversible first cycle loss of LRLO is, in fact, discussed as a promising strategy to compensate the irreversible first cycle loss of the anode. Nonetheless, the main challenge is the improvement of the long-term stable cycling in full-cells. The complexity of the structure and the related phase transitions leave, indeed, wide space for material improvement in the future, e.g., by introducing suitable dopants or larger concentrations of other elements [268,269], the application of surface coatings on the material level [270,271], as well as electrolyte development and the realization of protective coatings at the electrode level.

4. Electrolytes

4.1. Liquid electrolytes

4.1.1. Well established solvents, salts, and additives

Present lithium-ion batteries employ a liquid organic solution as Li-ion conducting electrolyte, comprising lithium hexafluorophosphate ($LiPF_6$) as conducting salt and a mixture of linear (e.g., dimethyl carbonate (DMC), ethyl methyl carbonate (EMC), and diethyl carbonate (DEC)) and cyclic (e.g., ethylene carbonate (EC)) carbonates as solvents, and fluoroethylene carbonate (FEC) or vinylene carbonate (VC) as additive(s) (see also Fig. 4). The electrolyte formulations are coined on the basis of several considerations: (i) $LiPF_6$ possesses low dissociation energy and good solubility in carbonate solutions, affording superior ionic conductivity (up to 10^{-2} S cm^{-1} at room temperature), due to the weakly coordinating, highly fluorinated anion [272]; (ii) the perfluorinated PF_6 anion is stable towards oxidation, thus allowing the use of >4 V positive electrodes [273]; (iii) the Al current collector used for the positive electrode is not corroded at high potentials (>4 V vs. Li^+/Li) due to the formation of a stable passivation layer [274]; and (iv) the electrochemical reduction of the "magic" solvent EC together with FEC or VC as additives on the graphite electrode yields a high-quality SEI, which ensures the reversible intercalation of the Li^+ cations for hundreds (and even thousands) of cycles [275]. However, there are two major drawbacks of $LiPF_6$-based liquid electrolytes: (i) $LiPF_6$ undergoes thermal decomposition at a relatively low temperature (ca. 105 °C [276]), and trace amounts of moisture substantially accelerate the degradation of the electrolyte, thus of the battery, especially at elevated temperature (e.g., 60 °C) [277]; (ii) the organic carbonate solvents are highly flammable, raising critical concerns regarding the safety of LIBs under abuse conditions [278]. Hence, as the positive/negative electrodes are strong oxidants/reductants, $LiPF_6$-based lithium-ion batteries may encounter severe thermal runaway causing fire and toxic gases emissions [279]. In search for a suitable replacement of $LiPF_6$, numerous anions have been conceived and prepared in the past 30 years, including phosphates, imides, borates, Hückel-type salts, and many others. Among them, lithium bis(trifluoromethanesulfonyl)imide (LiTFSI) has gained the most attention from both academia and industry. LiTFSI was proposed as electrolyte salt in 1983 [280] and later commercialized by 3 M and Rhodia (later acquired by Solvay). Nowadays, hundreds of tons of LiTFSI have been produced and are used as co-salt for lithium-ion batteries, as well as electrolyte salt for post-lithium-ion batteries such as Li-S batteries. LiTFSI is thermally stable up to 380 °C [281], readily soluble in most donor solvents, and the resulting solution shows decent ionic conductivities (e.g., σ (25 °C) = 7.6×10^{-3} S cm^{-1} for 1 M LiTFSI-EC/EMC (30:70, v/v) vs. σ (25 °C) = 9.3×10^{-3} S cm^{-1} for 1 M $LiPF_6$-EC/EMC (30:70, v/v) [282]). However, the practical application of LiTFSI as sole conducting salt is hindered by the anodic dissolution of the aluminium current collector in LiTFSI-based carbonate electrolytes [274,283]. Another alternative to LiTFSI, its successor, lithium bis(fluorosulfonyl)imide (LiFSI, Fig. 4) which was also discovered by Armand and co-workers in 1995 [284], and has emerged as an auspicious lithium salt for lithium-ion batteries due to a higher ionic conductivity and better stability against the Al current collector compared to LiTFSI [282]. Consequently, LiFSI is being commercialized by Suzhou Fluolyte and Nippon Shokubai, and added to $LiPF_6$-based electrolytes to improve the rate capability of lithium-ion batteries while maintaining the Al passivation. Meanwhile, the unique SEI-forming properties of fluorosulfonyl group (FSO_2-) on various electrode materials have raised

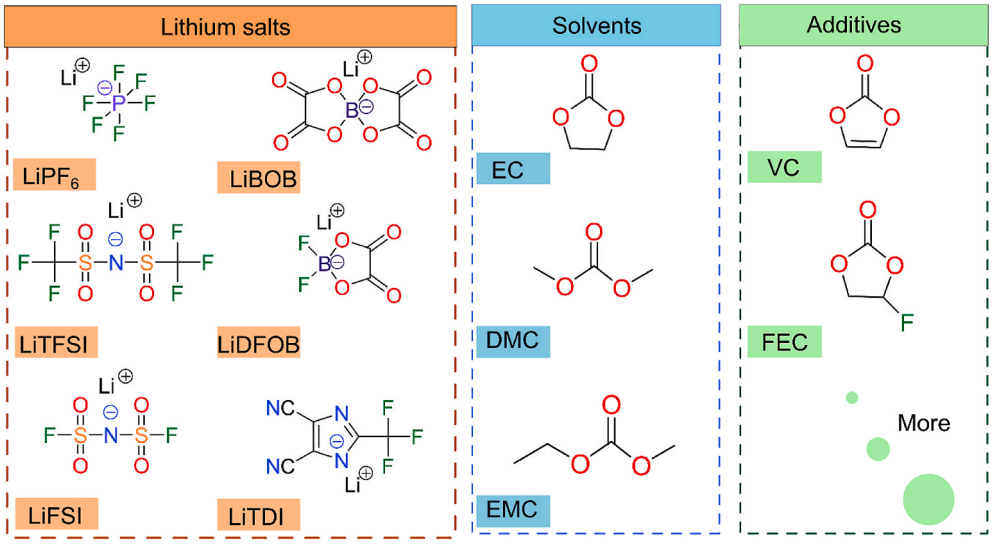

Fig. 4. Chemical structures of lithium salts (left), solvents (middle), and additives (right) which are widely used in state-of-the-art lithium-ion batteries and discussed herein.

great interest for investigating LiFSI-based liquid and polymer electrolytes [285–287].

Another class of lithium salts that has attracted considerable attention in view of their film-forming ability on electrode/electrolyte interphases [288] are borate salts such as lithium bis(oxalato)borate (LiBOB) [289,290] and lithium difluoro(oxalato)borate (LiDFOB) [291] (Fig. 4). However, the C_2O_4 moieties tend to oxidize at high voltage resulting in gassing. Hückel-type salts (e.g., lithium 2-trifluoromethyl-4, 5-dicyanoimidazole (LiTDI), Fig. 4) initially proposed in 1995 [292] have been spotlighted recently [293,294]. For example, an optimal amount of LiTDI effectively suppresses the degradation of $LiPF_6$-based electrolytes and stabilizes the SEI layer on graphite, which could markedly improve the performance of LIBs [294].

On the other side, to improve the safety of the liquid electrolytes, the replacement of carbonate solvents with non-flammable ionic liquids (ILs) and the incorporation of flame-retardant additives (e.g., organic phosphorus compounds) have been intensively investigated [278,295, 296]. IL-based electrolytes are inherently safer, but their ionic conductivities are somewhat lower than those of carbonate-based ones, which results in relatively poorer rate-capability at room temperature [297]. Taking into account the (at present) significantly higher cost of ILs, such electrolytes have not been commercially used in LIBs yet. The FSI anion is singled out for the high conductivity, i.e., the low viscosity it imparts to ILs, especially at high concentrations ($\geq$2.5 M) of the Li salt [298, 299]. Alternatively, flame-retardant additives could sufficiently block the combustion process, but commonly at the expense of cyclability. Recently, new additives such as 2(2,2,3,3,3-pentafluoro-propoxy)-4-(trifluoromethyl)-1,3,2-dioxaphospholane (PFPOEPi-1CF3) have been reported to have a positive impact on the cell performance by contributing to the formation of a robust SEI layer on graphite for >1200 cycles [300]. A localized high-concentration electrolyte (LCE) containing LiFSI and a ternary solvent, i.e., triethyl phosphate (TEP), EC, and bis(2,2, 2-trifluoroethyl) ether (BTFE), also allowed for the stable cycling of graphite||NMC_{811} cells [301]. Hence, using electrolyte additives or co-solvents tends to be an economical and effective approach.

4.1.2. *Anticipated future directions*

The progress on the discovery of novel lithium salts has been sluggish since 2000s, due to (i) the arduous efforts required to develop battery-grade moisture-sensitive compounds and (ii) the multi-directional and stringent requirements for an "ideal" lithium salt. Nonetheless, Zhou and co-workers [302–304], for instance, reported a series of fluorosulfonimide salts (Li[N(SO_2F)(SO_2R_F)], $R_F = n$-C_mF_{2m+1}) and their use as electrolytes for LIBs. An improved capacity retention was observed for graphite||$LiCoO_2$ and graphite||$LiMn_2O_4$ cells at elevated temperature when replacing $LiPF_6$ with Li[N(SO_2F)($SO_2C_4F_9$)] (LiFNFSI). Later, the same group [305,306] introduced a super-delocalized imide anion, ($[CF_3SO(=NSO_2CF_3)_2]^-$, sTFSI$^-$), where the charge is spread on five oxygen and two nitrogen atoms, with three CF_3 electron withdrawing groups. The LisTFSI-based electrolyte showed high conformity with the Al current collector, and decent ionic conductivity. Preliminary tests using graphite||$LiCoO_2$ cells demonstrated the suitability of LisTFSI as electrolyte salt for lithium-ion batteries; however, the main difficulty lies in the development of a scalable synthesis.

Differing from the arduous design of new lithium salts, a vast majority of research activities is dedicated to the combination of commercial salts with new electrolyte additives, in hope of enhancing the interfacial stability between the electrodes and the electrolyte [307, 308]. This is largely ascribed to the unique nature of such additives: "small dose, big impact". Besides conventional additives enlisting FEC and VC, numerous new additives have been developed. For instance, lithium difluorophosphate ($LiPO_2F_2$) was found to improve the cycling performance of graphite||NMC cells, due to its participation in forming a stable interphase on both electrodes [309–311]. The combination of $LiPO_2F_2$ with conventional additives such as FEC or VC was reported to further suppress parasitic reactions at the electrode/electrolyte interphase and, thus, expand the lifespan of lithium-ion cells [312]. In another example, introducing a few percent of propane sultone into $LiPF_6$-based carbonate electrolytes effectively suppressed the co-intercalation of PC in graphite as well as the deposition of Li metal on the graphite anode [313,314]. Interesting to note is that imide-based salts such as LiTFSI and LiFSI are also used as additives or co-salt (e. g., at 30 mol%) to reduce the interfacial resistance [315], as well as to improve the storage properties [316], by virtue of the formation of a thin LiF-based SEI layer on graphite [317].

To attain a higher energy density than the graphite||$LiCoO_2$ cells, the use of high-voltage cathodes, which operate at a potential higher than 4.5 V vs. Li^+/Li (e.g., LMNO), is investigated. Accordingly, the electrochemical stability window of the electrolyte needs to be further expanded by replacing ordinary carbonates that are readily oxidized at $\geq$4.5 V vs. Li/$^+$Li. Fluorinated carbonates are assessed as solvents for 5-V lithium-ion batteries. Zhang et al. [318] reported that electrolytes composed of fluorinated cyclic or linear carbonates possess superior anodic stability, enabling a good capacity retention for graphite||LMNO cells.

An additional challenge for future lithium-ion electrolytes – together with the implementation of high-voltage cathodes – is the paradigm shift from graphite to silicon/graphite (Si/Gr) composite anodes. In a recent work, Xu and co-workers [319] adopted the aforementioned LCE comprising 1.2 M LiFSI-TEP/BTFE for Si/Gr||NMC cells, observing remarkable improvement in capacity retention and rate-capability compared to conventional carbonate electrolytes.

Finally, the demand for fast-charging LIBs has also incentivized the search of highly Li-ion conductive electrolytes, as recently reviewed by Logan and Dahn [320]. This in turn asks for the ingenious design of new electrolyte compositions based on new lithium salts with low anion mobility, low viscosity solvents, and Li-ion conductive SEI-forming additives. Hence, considerable improvement of liquid electrolytes is still critical for accessing high-performance batteries, though there has been ca. 30 years of practical usage of the $LiPF_6$-based carbonate electrolytes in commercial lithium-ion batteries.

4.2. *Gel polymer electrolytes – the early days, recent developments, and future perspective*

Dating back to the early stage, Wright and co-workers [321] discovered ionic conduction in plastic materials (a.k.a., solid polymer electrolytes, SPEs) in 1973. Subsequently, Armand et al. [322] proposed the use of such polymeric ionic conductors as electrolytes for safe rechargeable batteries in 1978. However, when in a fully dry state, the ionic conductivity of such SPEs ($\leq 10^{-4}$ S cm^{-1}) is significantly lower than that of traditional liquid electrolytes (ca. 10^{-2} S cm^{-1}) at room temperature, limiting the operational temperature of cells comprising SPEs to temperatures above 60 °C [323]. To compromise between safety and performance, gel polymer electrolytes (GPEs) comprising a certain portion of liquid components have been widely investigated on account of their reduced risk of leakage compared to the carbonate- or ether-based liquid electrolytes, and higher ionic conductivities compared to SPEs [324]. The research activities on GPEs were initiated by Feuillade and Perche [325] in 1975, who tested the electrochemical properties of Li||CuS cells with various kinds of GPEs. Among all the kinds of polymer matrices, polyvinylidene difluoride (PVdF) and its derivatives such as poly(vinylidene fluoride-*co*-hexafluoropropylene) (PVdF-HFP) are the most popular skeletons for fabricating GPEs [324]. In 1995, Gozdz et al. [326–328], working at Bell Communications, disclosed a scalable route, the "Bellcore process", which could be carried out under a "non-controlled environment" via a three-step procedure. This procedure, however, is relatively complex: (i) the preparation of a polymer membrane with plasticizers but free of any Li salt; (ii) the extraction of the plasticizer with a low-boiling point solvent (such as diethyl ether or methanol) leaving a porous membrane; and (iii) refilling the polymer membrane with a liquid electrolyte into the voids, thus,

obtaining a GPE in LIBs. Nevertheless, if EC is a gelling agent for PVdF, its mixture with linear carbonates is not and only a partial swelling takes place. Most importantly, the volatile and flammable linear carbonates cause again safety concerns. High-boiling point carbonates, such as PC [329], or electrolyte additives, such as TEP [330], are proven to form a real gel and also increase the thermal stability while decreasing the flammability of the resulting GPEs. Yet, the compatibility between the graphite anode and GPEs needs to be further improved.

In addition to the use of flame-retardant additives, the replacement of linear carbonates with less volatile ILs and a polymer is deemed as a solution to enhance the safety of LIBs with a quasi-solid electrolyte [331–333]. Nonetheless, since the advantage of IL-based GPEs lies in their better compatibility with the high-capacity lithium-metal anode, most of the research efforts are dedicated to lithium-metal batteries instead of lithium-ion batteries. Besides, self-healing polymers are receiving increasing attention for flexible batteries [334,335], and various types of self-healing GPEs are available through dynamic non-covalent bonds (e.g., hydrogen bonding [336]) and dynamic covalent bonds (e.g., in boronic esters [337]).

In sum, the electrolyte is the battery component with the greatest complexity, but also where there is the greatest latitude for improvement. Undoubtedly, remarkable progress will be seen in this domain in the years to come.

5. Electrode processing

5.1. The general principle and recent developments towards higher energy densities

The essential principles to produce composite electrodes have remained unchanged since the original lithium-ion cells in 1991 [338] and the main steps are schematically depicted in Fig. 5. The active material, a polymer binder, and conductive carbon are mixed together in a solvent, to produce an ink. This is coated onto a thin aluminium or copper foil (respectively, for the cathode and anode), and the solvent is evaporated in a controlled drying process. Finally, the coating is calendared to the required thickness, before cutting or slitting to the size required for cell assembly. While the overall process is the same, there continue to be changes and improvements. There have also been significant advances in the theoretical understanding of these processes, and the ability to model them [339]. For the positive electrode, PVdF remains the binder of choice, due to its oxidation resistance. There are a very few solvents for PVdF, and in practice this means *N*-methyl-2--pyrrolidone (NMP). This is an unpleasant (teratogenic) chemical [340], which requires a solvent recovery system in industrial operation [20, 341]. There are obvious benefits to using aqueous or solvent-free coating systems, which are discussed in later sections. In terms of electrode formulations, these are usually expressed as the active material: binder: conductive carbon weight ratio. There is often a large difference between research papers (e.g., 80:10:10) and industrial electrode formulations (e.g., 96:2:2).

Mixing processes should produce a homogenous ink, which is stable against both agglomeration and sedimentation [342]. The solid content is selected to give an ink viscosity compatible with the coating equipment, i.e., not too viscous or too runny. It is necessary to optimize the energy input into the mixing process. Too little energy will not achieve complete dispersion. However, too much energy can damage the active material and shred the polymer chains. Historically, the mixing sequence was usually “wet”. The PVdF binder would be pre-dissolved in NMP, and the conductive carbon bead milled in NMP, to achieve full dispersion. The active material would then be wetted with NMP, and the three liquids would be stirred together, to produce the ink. More recently, “dry” mixing sequences and equipment have been introduced [343]. The three solids are added in powder form, and mixed thoroughly, before being dosed with the NMP solvent. The total mixing time can be reduced, and better coatings can be achieved, e.g., with an improved distribution of the conductive carbon.

The coating processes used in lithium-ion cathode preparation are based on standard equipment used in other coating industries [344]. Slot-die coating is the most widely used technique in industrial lithium-ion cell manufacture [345]. In the research laboratory, draw down coatings with a “doctor blade” are commonly used. “Comma bar” systems are convenient in prototyping, often combined with a reverse roller transfer system. Having applied a uniform coating at the required coat weight, the drying stages are an equally important part of the process [346,347]. Lithium-ion battery factories use long drying ovens, with zones set to different temperatures. If drying is too fast, then there is increased binder migration towards the surface [348], and the electrodes may even crack. However, the coating must be dry by the time it emerges from the oven. Typically, coating speeds of 30 ± 5 m min ^{1} are used in commercial lithium-ion cell production, compared to around 1 m min ^{1} in R&D laboratories. Speeds of up to 100 m min ^{1} have been achieved, even with pattern coatings [349]. Clearly, this requires an increased rate of drying, to keep the length of the coating equipment down to a manageable size.

Calendering is the final stage of electrode processing [350]. For a given coat weight and electrode formulation, the coating thickness, porosity and average density are all inter-related. However, different pore structures can lead to the same overall porosity value, and will have an influence on electrode performance.

One route to higher energy densities is to increase the thickness of the electrode coatings, provided electronic and ionic conduction pathways can be maintained [351]. Binder migration during solvent drying is also an increased problem with ultra-high loadings. Tests on 500 g m ^{2} cathodes (rated at 8 mAh cm ^{2}) showed clear micro-structural differences with drying temperature, which could be correlated with electrochemical performance [351].

There are two approaches to electrode preparation that eliminate the use of solvents; electrostatic spray coating and extrusion (the general process for the latter is displayed schematically in Fig. 6). In the former, fluidized dry particles become charged, and are then deposited onto an earthed metal foil. The coated foil is then passed through a hot roller, to thermally activate the binder, and control the coating thickness [352]. Cycling performance was comparable to conventional wet slurry

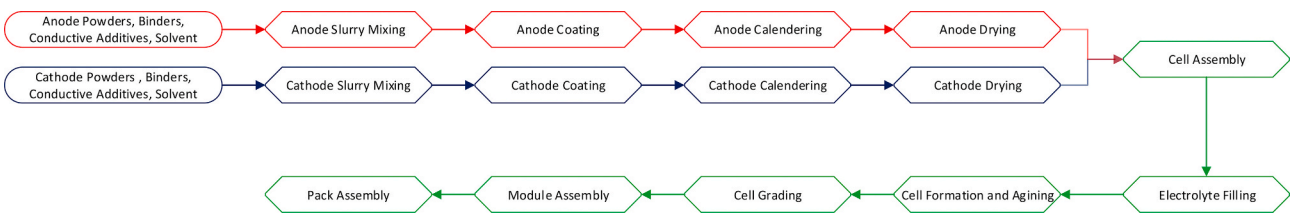

Fig. 5. Schematic showing the processing steps for converting battery materials into battery packs, starting from the initial slurry mixing, electrode coating, calendering, and drying (in red and blue for the anode and cathode, respectively), over the cell assembly and electrolyte filling until the eventual module and pack assembly (in green). (For interpretation of the references to colour in this figure legend, the reader is referred to the Web version of this article.)

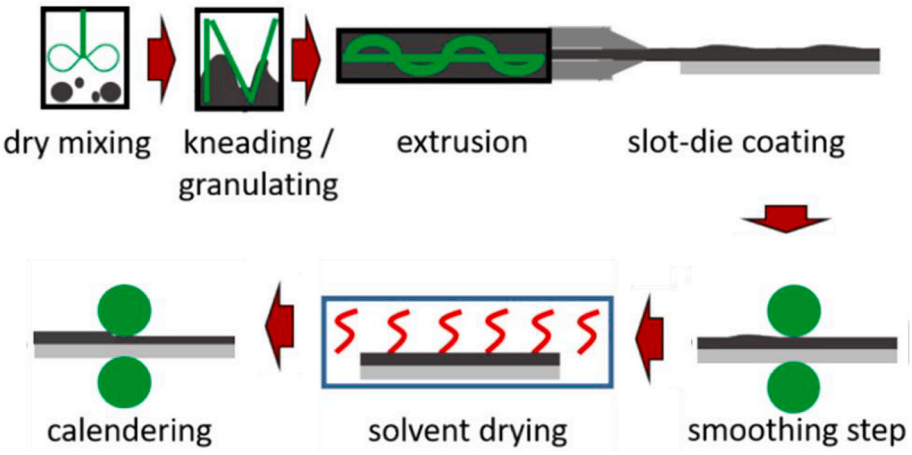

Fig. 6. Schematic illustration of a developed extrusion-based manufacturing process for thick Li-ion cathodes, starting from the dry mixing and kneading, followed by extrusion and slot-die coating as well as the smoothing step, drying, and eventual calendering (Reprinted from Ref. [431] with permission from Elsevier).

coatings, with PVdF as binder and either LCO or NMC as active materials. Coating adhesion was better with the electrostatic spray process, for higher roller temperatures and slower feed rates. A similar approach was used to prepare NMC_{111} electrodes, though the foils were heated after coating, and then calendered at room temperature [353]. The dry coated electrodes had improved capacity retention on cycling than wet slurry coated control electrodes, though the capacity at 10C was reduced. Electrostatic spraying has also been applied to graphite anodes [354]. Three binders were evaluated; PVdF, a fluorinated ethylene propylene co-polymer, and THV tri-polymer (tetrafluoro ethylene, hexafluoro propylene, and vinylidene fluoride). A two stage mixing process was adopted, to fully disperse the carbon black component.

Extrusion has been used to make coatings with a variety of active materials, including NMC_{111}, LFP, and LTO [355]. The binder was HNBR (hydrogenated nitrile butadiene rubber), and polypropylene carbonate (PPC) was used as a polymer processing aid. After dry mixing at 90 °C, a 0.4 mm film was thinned and then rolled onto a carbon-coated aluminium foil. A porous electrode structure was achieved by thermally decomposing the PPC at 230 °C. The electrochemical performance was comparable to electrodes produced by conventional slurry coating. A similar approach has been used to prepare graphite anodes and NCA cathodes [356], both with HNBR binders. Again PPC was used as both a polymer processing aid and a porogen (pore generator). For both electrodes, the rate performance was okay up to 2C, and the NCA capacity was okay up to a coating thickness of 150 μm. Similar equipment based on a twin screw system is also being used for continuous rather than batch mixing with liquid solvents, followed by standard coating.[4]

There are a range of 3D printing techniques that could be applied to lithium-ion cell manufacture [357]. The challenge is achieving the throughput necessary to match existing coating techniques. At present, the most promising use of 3D printing is in the production of lithium micro-batteries.

Laser cutting has been proposed as an alternative to the standard mechanical cutting approach used to prepare electrodes for stacked cells. However, lasers can also be used to create patterns in coated electrodes, to improve electrolyte wetting and rate performance [358, 359]. Very high speed femto-lasers are required. The patterning can be an array of holes, parallel trenches, or a grid pattern.

In sum, great progress has been achieved in developing new coating technologies and it appears likely that one or the other will be adopted by industry in the near-to mid-term future for realizing (ideally) less costly and more sustainable methods for the fabrication of lithium-ion batteries with enhanced energy density, while maintaining suitable power performance and cycle life.

5.2. *Water-based electrode coating – current status, remaining challenges, and potential solutions*

Aqueous processing using a blend of sodium carboxymethyl cellulose (NaCMC) and styrene butadiene rubber (SBR) binders is the standard for graphite anodes, but conventionally the manufacturing process of cathodes still involves PVdF as binder dissolved in NMP (see also the previous chapter). However, according to REACH regulations, the utilization of NMP must now be carefully controlled or ideally fully prevented [20]. Even though numerous works have shown the feasibility of aqueous processing with CMC, SBR, or polyacrylates ($PAAH_{1-x}Li_x$) as binders, for both anodes (e.g., LTO) and cathodes (e.g., LFP, LMO, and NMC cathodes [20], the industrial implementation of cathode aqueous processing still remains marginally divulged.[5] However, eliminating the use of NMP, associated with the absence of solvent recovery, by using water instead results in a substantial reduction on capital and operating costs of the electrode manufacturing process [346,360], and in turn of the overall battery. Moreover, during the recycling process, materials' recovery becomes possible easily by dissolution compared to the standard pyrolysis with PVdF (see also the forthcoming chapter on recycling). Aqueous binders which are more sustainable than PVdF allow for a better anode SEI and cathode CEI, more homogeneous electrode microstructure, better electrode wettability by the liquid electrolyte, while still retaining better mechanical strength due to lower swelling, and thus better cyclability, and even better safety (less heat generated) than PVdF [20].

The main issue for aqueous processing is the active material reactivity with water. For NMC or NCA materials, it alters the particles surface by the formation of LiOH and Li_2CO_3 species [361,362]. Besides, lithium leaching occurs along with Li^+/H^+ cation exchange which leads to capacity loss [207,361] and triggers the formation of a resistive rock-salt phase on the particle outer surface [362–364]. The surface compounds formed may lead to side reactions with the electrolyte, thus lowering the capacity retention upon cycling [361]. Moreover, the strong alkalinity of aqueous slurries (up to a pH of 12) causes corrosion

[4] https://www.buhlergroup.com/content/buhlergroup/global/en/industries/batteries/Continuous-electrode-slurry-production.html.

[5] https://www.leclanche.com/our-technologies/cells/.

of the aluminium current collector, accompanied by H_2 release, which increases the electrical resistance at the electrode/collector interface and generates macro-porosity in the electrode [365,366].

The aluminium current collector corrosion can be solved by carbon coating [367]. Also the addition of an acid to the aqueous slurry in order to lower the pH is a straightforward method to avoid corrosion [363, 368]. While some works report negative effects on lithium leaching, slurry rheology, or electrode conductivity and adhesion, when using mild organic acids [369], the use of phosphoric acid does not only avoid aluminium corrosion, but also spontaneously reacts at the lithium transition metal oxide surface, resulting in a thin metal phosphate surface layer [366,368]. Such coating protects against the reaction with the electrolyte and leads to better cycle life than NMP-processed cathode materials such as LMNO [366], NMC_{532} [370], and even LRLO [371]. The application of protective surface coatings on the active material itself is an alternative interesting route [20,372].

Generally, despite significant progress in recent years, the aqueous processing of battery electrodes is still a rather unexplored field. However, numerous studies report satisfactory electrochemical performance for full cells even with NMC_{811} [373] or for 15–60 Ah prototypes [374].[6] This technology is not an easy task and requires additional research; for example, to obtain thick electrodes achieving satisfactory electrochemical performance [375,376]. However, this route opens up new opportunities, such as the use of low-cost and high-throughput manufacturing processes from the paper industry [377]. In the context of the creation of Gigafactories in Europe, would it not be wise to switch to the more sustainable aqueous route?

6. Recycling

6.1. Critical discussion of the state of the art in industry

The rising importance of electric mobility will significantly increase the demand for raw materials and the need for sustainable recycling technologies. An increased volume of battery production will notably affect the environment due to raw material processing and generation of secondary streams [378]. Currently in the European Union, only 50 wt% of lithium-ion batteries is required to be recycled based on the directive 2006/66/EC [379]. However, a future battery directive is expected to set much higher limits focused on particular battery components. Such a change will be challenging for many battery recyclers today, which use technologies with low recovery and selectivity. Due to these expected demands, a higher efficiency in the recycling of Li-ion batteries is necessary to decrease the impact of the fast-developing battery industry on our environment. The commonly used pyrometallurgical processes cannot provide sustainable recycling, even if some of them already integrate hydrometallurgical steps to produce a high purity metal salt, since some components such as aluminium, manganese, and lithium are not recovered. Pyrometallurgical approaches are used by recycling companies such as Umicore (Belgium), with a capacity 7000 t year ^{1} or Nickelhütte (Germany) with the same capacity [380]. In such pyrometallurgical processing, both NiMH batteries and Li-ion batteries are smelted together [381,382]. Components such as lithium, manganese, or aluminium are not recovered as they end up in the by-product – slag [383]. Cobalt, copper, iron, and nickel are recovered as an alloy, further processed by hydrometallurgical methods in order to produce separate products. The main advantage of such an approach is the elimination of the need for mechanical pre-treatment.

For other recycling approaches, mechanical pre-treatment and separation is one of the most crucial steps [384]. Mechanical pre-treatment is either applied by a company specified only on this step, while all recovered components are further distributed to other recyclers and metal producers, or separated components are processed within the same company. The first practice is applied at Akkuser (Finland) or Batrec (Switzerland). Both companies perform mechanical pre-treatment followed by mechanical separation of black mass (mixture of cathode and anode active material) from current collectors (Al and Cu foils) and other battery components (printed circuit boards, casing, cables, etc.). The latter are then sold to specialised recyclers or metal producers [380].

More modern processing of spent lithium-ion batteries uses a combination of methods to achieve much higher yields. Such combinations may comprise thermal pre-treatment (below melting point of the major metals), followed by a hydrometallurgical processing. The thermal pretreatment is mainly used to remove organic components and elemental carbon that could interfere with the subsequent hydrochemical processing [385]. Such an approach is already used by several companies such as Accurec (Germany), Redux (Germany), Fecupral (Slovakia; the company performs the thermal pre-treatment only), etc. Currently there are two types of thermal pre-treatment used in industry: incineration (in the presence of oxygen) and pyrolysis (in the absence of oxygen). However, some negative effects on the posterior processing have been identified after using incineration [386]. Mixed oxide formation ($CoMn_2O_4$ and $NiMn_2O_4$) at higher temperatures cause lower leachability of valuable metals. On the other hand, in the case of pyrolysis some positive effects, such as improved leachability due to cathode material decomposing and due to organic components removal, have been reported [381] and, thus, pyrolysis became the more preferable option for industrial processing. In order to simplify the recycling process by, e.g., eliminating issues of discharging and mechanical separation, pyrolysis is applied. Other potential down sides of thermal pretreatment are, for instance, the formation of HF and other organic compounds as a consequence of organic components decomposition. The remedy for this issue is the inclusion of more or less complex off-gas treatment [385].

The last step in metal recovery is hydrometallurgical processing based on the leaching of active material with preferable mineral acids, followed by metal separation using solvent extraction and precipitation. Presently, hydrometallurgical processing is mostly used in China (Brunp, Soundon New Energy, GEM, Huayou Cobalt, Ganpower, etc.) and South Korea, where the majority of batteries is produced nowadays and, thus, the infrastructure is well developed for the production waste and obsolete batteries [387]. In Europe, hydrometallurgical processes are used in Sweden, where the battery producer Northvolt integrates a hydrometallurgical recycling process in the loop to secure the raw materials supply chain and to decrease the environmental impact of the battery production. Hydrometallurgical processing is also used in companies such as Accurec (Germany), Recupyl (France), Fortum (Finland), etc. The main advantage of hydrometallurgy is the possibility to produce new battery precursors from the waste with sufficient purity [388].

Despite the large demand for the chemical reagents, hydrometallurgy allows the use of many solvents for several years and re-utilization of several by-products within the same technology, thus minimizing the overall secondary waste generation [389]. Accordingly, with future battery legislation and demands for higher material recovery rates, hydrometallurgy is one of the most promising approaches to meet the requirements, but also to create a path to circular economy in the battery market.

6.2. Anticipated future developments

Extensive research has been performed in the material recovery of different battery components, applying mechanical separation as well as pyrometallurgical and hydrometallurgical methods. Nevertheless, due the industrial development, combined methods using thermal pretreatment followed by hydrometallurgical processing represent the future trend in lithium-ion batteries recycling [380,390]. However, incineration has been mostly defined as less suitable if performed at higher temperature (>900 °C), and thus the pyrolysis of battery waste

[6] https://www.leclanche.com/our-technologies/cells/.

has been studied to a larger extent. Pyrolysis is usually performed as a dynamic process under a constant gas flow or in vacuum. Vacuum pyrolysis has been used to process cathode materials or black mass and also to remove the binder [391,392]. The advantage of vacuum pyrolysis is the formation of a well-defined environment and efficient reduction of the oxides. Dynamic pyrolysis has been performed to achieve the decomposition of organic components and carbothermic reduction [381,393]. The waste of Li-ion batteries (comprising NMC or LFP) was usually pyrolysed in a nitrogen atmosphere within a temperature range from 400 to 700 °C. It was concluded that present carbon and carbon monoxide reduced the metal oxides of the active materials to Co^0, CoO, Ni^0, NiO, Mn^0, and Mn_3O_4, and lithium forms Li_2CO_3. The most optimal temperature was 600 °C. The reduction reactions transformed the metal compounds to more soluble chemical forms. Thermally treated materials are then processed hydrometallurgically.

In the hydrometallurgical step, the most common inorganic acids used for the leaching are HCl, H_2SO_4, and HNO_3 [394]. It was concluded that hydrochloric acid usually performs the best among these acids [395,396]; however, sulphuric acid is more preferable due to economic reasons. Zhang et al. [397] found that a leaching efficiency of more than 99% for cobalt and lithium can be achieved using 4 M HCl at a temperature of 80 °C during 1 h. Many researchers [398–400] performed leaching with sulphuric acid and different reduction agents. The presence of, e.g., hydrogen peroxide allows a lower acid concentration in the leaching media for the same concentration of lithium and cobalt in the leaching liquor [401]. This is due to the reduction of Co^{3+} to Co^{2+} which can be readily dissolved [402]. If sulphuric acid is used, the optimal concentration of the acidic leaching media varies between 2 M and 4 M and the optimal concentration of hydrogen peroxide oscillates from 1 to 6 vol%. Leaching temperatures around 60–80 °C and a leaching time of 1h are the optimal conditions for cobalt and lithium leaching [397,398].

A more modern approach is the use of organic acids such as citric, ascorbic, malic, oxalic, or aspartic acid together with H_2O_2 as reducing agent. Relatively high leaching efficiency has been reported for the majority of the organic acid used [403–406]. Organic acids are considered to be a more environmentally friendly alternative to the inorganic acids; nonetheless, due to economic reasons their application in industry is more challenging.

Future metal purification and separation is based on the use of solvent extraction. More traditional extractants such as bis(2,4,4-trimethylpentyl)phosphinic acid (Cyanex®272), di-(2-ethylhexyl) phosphoric acid (D2EHPA), 2-ethylhexyl phosphonic acid mono-2-ethylhexyl ester (PC-88A), or hydroxy-oxime derivative (Acorga M5640) have been used for metal recovery in batteries recycling [388,407–409]. Several technologies based on the use of solvent extraction have been developed to separate cobalt, nickel, copper, and manganese [388,410–412]. Very recently, a novel extractant (Cyanex®936) has been developed by Solvay to purify lithium from sodium, which has been until now mostly performed by precipitation. Innovation in this field will decrease the environmental burden of precipitation methods for lithium production.

Solvent extraction allows very efficient separation of cobalt, manganese, and nickel, which is otherwise challenging, if precipitation techniques are used [413,414]. In solvent extraction, the obtained purity of the metal salts is sufficiently high, so that the recycled metals can be re-utilized for the battery production. Solvent extraction is, for example, used in the industrial recycling at Umicore (Belgium), Northvolt (Sweden), Nickelhütte (Germany), and Accurec (Germany).

7. Performance metrics in academia and industry and expected progress

Following the available literature, a set of theoretically achievable and estimated, or already realized practical specific capacities and energy densities have been provided in the previous chapters, especially those dealing with the active materials for the negative and positive electrode, frequently though based on the mass or volume of the active materials only. This kind of "simplification" is intended to allow for a rather facile comparison with earlier studies, but neglects important parameters, such as the amount of electrolyte in the cell, the electrode composition, the density, porosity, and tortuosity of the electrode coating, and the presence of inactive components, including the current collectors, the separator, and the cell casing (cylindrical, prismatic hard-case or pouch – all with their specific advantages and drawbacks concerning packing density, costs, and safety [415–418]). In fact, taking all these (mostly not yet known) parameters into account would result in listing essentially incomparable and therefore irrelevant and meaningless data from most lab-scale studies, rendering them hardly comparable with each other, and certainly not comparable with the values to be obtained in industrial lithium-ion cells. Nonetheless, they have to be kept in mind in order to achieve meaningful progress towards further improved performance metrics — at least when it comes to the evaluation of the results in light of the envisioned application. Accordingly, it is of utmost importance to report comprehensive data sets, particularly for studies that are (or claim to be) immediately relevant for commercial cells [419]. In fact, compared to other emerging battery technologies, lithium-ion batteries have the great advantage of being commercialized already, allowing for at least a rough estimation of what might be possible at the cell level when reporting the performance of new cell components in lab-scale devices. This is nicely highlighted by comparing the specific energy values given in Table 2, which are based on the active material mass loading only, while considering practically achievable specific capacities, and the values reported for commercial cells, summarized in Table S1 and Fig. 7. For instance, Table 2 provides a specific energy of 379 Wh kg^{-1} for graphite||LFP (based on the active materials only), while commercial cells frequently offer only about 110 Wh kg^{-1} (Table S1), i.e., less than one third. It should be noted, though, that LFP-based lithium-ion cells are commonly more designed for high-power applications and, therefore, frequently provide lower energy densities. As a matter of fact, the difference is less pronounced for graphite||NMC, for which a specific energy of around 400–450 Wh kg^{-1} is indicated in Table 2 (based on the active materials only), while specific energies of around 240 Wh kg^{-1} and about 680 Wh L^{-1} have been commercially realized already in 21700 cylindrical cells [418,420], i.e., more than half of the value provided in Table 2. Generally, this quick comparison illustrates that a factor of roughly 2–3 has to be taken into account, when estimating realistic energy density values based on lab-scale results, as also reported earlier [421,422], even though the

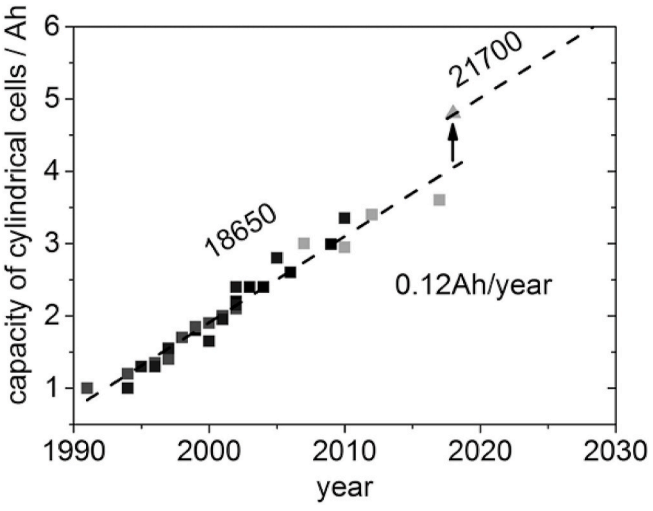

Fig. 7. Evolution of the cell capacity in cylindrical 18650 and 21700 cells since the first commercialization of lithium-ion batteries by Sony in 1991 until today. The presented data have been extracted from Ref. [432,433] and the manufacturers' data sheets.

steady, essentially linear increase in cell capacity depicted in Fig. 7 suggests that this factor might decrease in future; simultaneously providing hope for continuous performance improvements. Finally, it is important to keep in mind that complete battery systems will always have lower gravimetric and volumetric energy densities and higher cost when compared to the data for single industrial cells.

In this regard, it has to be kept in mind as well that, in the past, research has mainly focused on materials and the improvement of the cell chemistry. The steady increase in cell performance (Fig. 7), however, has been achieved also by optimizing the electrode and cell design as well as the manufacturing processes, e.g., by saving inactive materials, elevating the electrode loadings, increasing the coating areas, as well as a higher utilization of the cell volume due to optimized stacking and winding processes. Future development requires model-based electrode designs for higher loading electrodes with an optimized microstructure in order to increase the areal capacity and to decrease simultaneously the costs for cell manufacturing [360,423]. Modelling can help to better understand the performance of electrodes and can significantly contribute to the optimization of the electrode and manufacturing processes [424–429].

Altogether, the extensive availability of performance metrics in literature allows us to set up key performance indicators (KPIs) for the mid-to long-term research and development targets (Table 3). We may note that these KPIs are based on several assumptions, as also specified in Table 3, and especially the estimation of the targeted cost will be substantially affected by the availability of the raw materials needed, political decisions regarding, for instance, subsidies, as well as several other factors like economies of scale and market competition, which are, however, beyond the scope of this manuscript.

8. Conclusive summary and perspective

Lithium-ion batteries are considered to remain the battery technology of choice for the near-to mid-term future and it is anticipated that significant to substantial further improvement is possible. With respect to the negative electrode, this will be based particularly on an increasing contribution of silicon (or understoichiometric silicon oxide) in composites with carbonaceous materials, especially graphite, and advances towards optimized electrode architectures, while alternatives like lithium titanate will presumably still play a role – at least for specific niche applications where high safety and power are of primary importance. For the positive electrode, further improvement is expected by increasing the nickel content in common layered lithium transition metal oxides, while also addressing the resulting safety and stability issues – e.g., by the development of suitable coatings or dopants. Overcoming the remaining challenges for Li-rich transition metal oxides as well as high-voltage spinel oxides and transition metal phosphates will also allow for enhanced performances – though the eventual success of such materials also depends on the realization of safer electrolyte systems (salts, solvents, and additives) with an extended electrochemical stability towards elevated potentials. In fact, very recently also solid-state electrolytes, being either organic (i.e., polymers), inorganic, or hybrid, have been studied for lithium-ion battery applications, even though the focus here is so far clearly on the use with lithium-metal anodes. It might very well be, however, that also for lithium-ion batteries the incorporation of solid or hybrid electrolyte systems might enable a great push forward regarding performance, cycle life, and safety. Not least for this reason, an essential field of research will be the understanding of the reactions occurring at the different interfaces in the battery cell and, based on this, the careful design of tailored interfaces (and interphases) and electrolyte additives.

Taking into account that substantial improvement in the past has been achieved by optimizing the cell and electrode design, as well as reducing the content of electrochemically inactive components, it appears highly likely that also advanced electrode preparation procedures will contribute to further advances in energy and power density as well as safety and cost. With regard to the latter, the use of water rather than NMP and bio-derived polymer binders will certainly add to this development when the remaining challenges can be overcome.

Speaking of which, the continuously rising importance of lithium-ion

Table 3
Key performance indicators for lithium-ion battery research and development efforts in the mid- and long-term future, estimated based on the work and studies discussed herein.

		Current (2020)	2030	2050
Performance targets for automotive applications unless indicated otherwise				
1	**Gravimetric energy density (Wh kg^{-1})**			
	Pack level	90–180	190–230	>250
	Cell level	160–260[a]	275–320	>350
2	**Volumetric energy density (Wh L^{-1})**			
	Pack level	250–400	450–550	>600
	Cell level	450–730	750–900	>1000
3	**Typical gravimetric power density (continuous discharge from 100% - 20% SOC; W kg^{-1})**			
	Cell level	340–500[7]	800–1100	>1200
4	**Typical volumetric power density (continuous discharge from 100% - 20% SOC; W L^{-1})**			
	Cell level	ca. 1000	ca. 2000	>3000
5	**Typical fast charging time (min)**			
	Fast charging time for BE (20%–80% SOC, 25 °C)	15–30	10–15	<10
6	**Battery lifetime**			
	Cycle life for BEV to 80% end-of-life capacity (cycles; ca. 25 °C ambient temperature)	ca. 1000	up to 2000	2500–5000
	Cycle life for stationary to 80% end-of-life capacity (cycles; 40–50 °C)[b]	5000	10,000	>10,000
	Calendar life (years; 80% energy)	ca. 10	10–15	15–20
7	**Safety**			
	Hazard levels (according to EUCAR [435] and SAE J2464 [436])	≤4	≤3	≤3
Cost targets				
1	Cell level (€ kWh^{-1})	60–100	40–60	<50
	Battery pack level (€ kWh^{-1})[c]	90–140	65–110	40–70
Recycling targets[d]				
1	Battery collection/take back rate		>50%	>90%
2	Recycling efficiency (by average weight)	15%[e]	>40%[f]	>90%
3	Economy of recycling[g]		ca. 150%	ca. 50%

[a] Strongly depending on whether the focus is on energy or power density, as well as the cycle life required. Here, we focus especially on economically viable battery cells with a relatively high energy density rather than cells which are outlined for (extremely) high power – see also Andre et al. [434], for instance, differentiating between different automobile applications (hybrid (HEV) vs. plug-in hybrid (PHEV) vs. full electric vehicles (BEV)).

[b] Average values – highly dependent on the cycling conditions (e.g., depth of discharge and dis-/charge rate) and the cell chemistry.

[c] The given values are partially based on the numbers reported by Marinaro et al. [15] and the studies referred to therein as well as information from industry about their cost targets.

[d] We may note that there are large differences – depending on the technologies and processes used and the legal regulations in different countries – and the given values are an attempt to provide an average across European countries. In fact, the comprehensive recycling of lithium-ion batteries is not really limited by suitable technologies available already, but rather by economic considerations.

[e] The recycling efficiency varies substantially for the different components and elements in a Li-ion cell. For instance, lithium is presently hardly recycled, while cobalt is recycled with an efficiency of around 80%.

[f] By 2030, it should be possible to recycle about 99% of the metals – at least from the technological point. The actual recycling rate, however, will essentially depend on the given legislation and economical aspects.

[g] In comparison to the price of the non-recycled materials and components (i.e., “first-time use”).

batteries has to come along with substantial improvements concerning their sustainability – starting from the electrochemically active and inactive materials, their synthesis and further processing, the electrode coating and cell assembly, up to the extension of the cycle life, e.g., extended by second-life applications. Moreover, there is an urgent need for efficient recycling technologies – for instance, by realizing an (economically efficient) direct recovery of the various components, which enables their re-use in new lithium-ion batteries. However, it has to be kept in mind that even a recycling rate of 100% after the battery's end of life will cover only a minor part of the total need of raw materials, given that the overall deliveries will continue to increase at the current rate.

We may finally note that we have focused herein on those materials, components, and processes that are already of commercial relevance or anticipated to be of commercial relevance (very) soon. There are other in-/active material candidates and processes, which are presently investigated, and might become important in the mid-to long-term future. Additionally, there will likely be materials and processes that are not yet known today. Accordingly, this review is not considered to be exhaustive and we would like to encourage scientists and engineers working in this field to remain curious and open-minded towards new developments and ideas – just like at the very beginning of lithium battery research. New approaches and techniques, from DFT calculations to artificial intelligence, could be additional triggers of the progress.

CRediT authorship contribution statement

K.E. has conceived the general idea for this manuscript. All authors jointly conceived the general outline of this article. D.B. wrote the abstract and introduction, and prepared the first draft of the joint manuscript based on the input from all authors. S.T. and P.N. wrote the chapter on graphite and LTO negative electrodes. D.G., W.P., and B.L. wrote the chapters on silicon-based anodes and the aqueous electrode processing. M.C. wrote the chapters on lithium transition metal phosphate cathodes and electrode coating technologies. P.A. wrote the chapter on lithium transition metal oxides. M.A. and H.Z. wrote the chapter on electrolytes. M.P. and C.E. wrote the chapter on recycling. D. B., S.T., P.N., and M.W.-M. wrote the chapter on the performance metrics and all authors jointly developed Table 3. D.B. and S.T. wrote the conclusive summary and perspective. All authors jointly discussed and revised the final manuscript.

Declaration of competing interest

The authors declare that they have no known competing financial interests or personal relationships that could have appeared to influence the work reported in this paper.

Acknowledgements

P.A., M.W., and D.B. would like to acknowledge financial support from the German Federal Ministry of Education and Research (BMBF) within the ExcellBattUlm project (03XP0257A & 03XP0257D). D.B. acknowledges moreover financial support from the Helmholtz Association. D.B. and all authors would like to thank Mr. Tobias Eisenmann for providing Fig. 1 and the Graphical Abstract. M.A. and H.Z. are grateful for the financial support from the Basque Government by ELKARTEK-2016. D.G. and B.L. gratefully thank the support from the Institut des Matériaux Jean Rouxel (IMN), the Centre de la Recherche Scientifique (CNRS), and the University of Nantes, France. W.P. acknowledges the support from the French Atomic and Alternative Energies Commission (CEA), France. K.E. acknowledges the European Union's Horizon 2020 research and innovation programme BATTERY 2030+ under grant agreement 854472 and Batteries Europe.

References

[1] M. Armand, J.-M. Tarascon, Building better batteries, Nature 451 (2008) 652–657, https://doi.org/10.1038/451652a.
[2] B. Dunn, H. Kamath, J.-M. Tarascon, Electrical energy storage for the grid: a battery of choices, Science 334 (2011) 928–935.
[3] B. Scrosati, J. Garche, Lithium batteries: status, prospects and future, J. Power Sources 195 (2010) 2419–2430.
[4] S. Chu, A. Majumdar, Opportunities and challenges for a sustainable energy future, Nature 488 (2012) 294–303, https://doi.org/10.1038/nature11475.
[5] Z.P. Cano, D. Banham, S. Ye, A. Hintennach, J. Lu, M. Fowler, Z. Chen, Batteries and fuel cells for emerging electric vehicle markets, Nat. Energy. 3 (2018) 279–289, https://doi.org/10.1038/s41560-018-0108-1.
[6] D. Bresser, A. Moretti, A. Varzi, S. Passerini, The role of batteries for the successful transition to renewable energy sources, in: Encyclopedia of Electrochemistry: Batteries, first ed., Wiley-VCH, Weinheim, Germany, 2020, pp. 3–11.
[7] N. Yabuuchi, K. Kubota, M. Dahbi, S. Komaba, Research development on sodium-ion batteries, Chem. Rev. 114 (2014) 11636–11682, https://doi.org/10.1021/cr500192f.
[8] J.-Y. Hwang, S.-T. Myung, Y.-K. Sun, Sodium-ion batteries: present and future, Chem. Soc. Rev. 46 (2017) 3529–3614, https://doi.org/10.1039/C6CS00776G.
[9] C. Vaalma, D. Buchholz, M. Weil, S. Passerini, A cost and resource analysis of sodium-ion batteries, Nat. Rev. Mater. 3 (2018), 18013.
[10] W. Wang, Q. Luo, B. Li, X. Wei, L. Li, Z. Yang, Recent progress in redox flow battery research and development, Adv. Funct. Mater. 23 (2013) 970–986, https://doi.org/10.1002/adfm.201200694.
[11] P. Leung, X. Li, C. Ponce de León, L. Berlouis, C.T.J. Low, F.C. Walsh, Progress in redox flow batteries, remaining challenges and their applications in energy storage, RSC Adv. 2 (2012) 10125–10156, https://doi.org/10.1039/C2RA21342G.
[12] S. Tobishima, K. Takei, Y. Sakurai, J. Yamaki, Lithium ion cell safety, J. Power Sources 90 (2000) 188–195, https://doi.org/10.1016/S0378-7753(00)00409-2.
[13] B. Nykvist, M. Nilsson, Rapidly falling costs of battery packs for electric vehicles, Nat. Clim. Change 5 (2015) 329–332.
[14] J. Janek, W.G. Zeier, A solid future for battery development, Nat. Energy 1 (2016), 16141.
[15] M. Marinaro, D. Bresser, E. Beyer, P. Faguy, K. Hosoi, H. Li, J. Sakovica, K. Amine, M. Wohlfahrt-Mehrens, S. Passerini, Bringing forward the development of battery cells for automotive applications: perspective of R&D activities in China, Japan, the EU and the USA, J. Power Sources 459 (2020) 228073, https://doi.org/10.1016/j.jpowsour.2020.228073.
[16] T. Tsujikawa, K. Yabuta, M. Arakawa, K. Hayashi, Safety of large-capacity lithium-ion battery and evaluation of battery system for telecommunications, J. Power Sources 244 (2013) 11–16, https://doi.org/10.1016/j.jpowsour.2013.01.155.
[17] R. Wagner, N. Preschitschek, S. Passerini, J. Leker, M. Winter, Current research trends and prospects among the various materials and designs used in lithium-based batteries, J. Appl. Electrochem. 43 (2013) 481–496, https://doi.org/10.1007/s10800-013-0533-6.
[18] S.-T. Myung, Y. Hitoshi, Y.-K. Sun, Electrochemical behavior and passivation of current collectors in lithium-ion batteries, J. Mater. Chem. 21 (2011) 9891–9911.
[19] S.-L. Chou, Y. Pan, J.-Z. Wang, H.-K. Liu, S.-X. Dou, Small things make a big difference: binder effects on the performance of Li and Na batteries, Phys. Chem. Chem. Phys. 16 (2014) 20347–20359, https://doi.org/10.1039/C4CP02475C.
[20] D. Bresser, D. Buchholz, A. Moretti, A. Varzi, S. Passerini, Alternative binders for sustainable electrochemical energy storage – the transition to aqueous electrode processing and bio-derived polymers, Energy Environ. Sci. 11 (2018) 3096–3127, https://doi.org/10.1039/C8EE00640G.
[21] B. Lestriez, Functions of polymers in composite electrodes of lithium ion batteries, C. R. Chimie. 13 (2010) 1341–1350, https://doi.org/10.1016/j.crci.2010.01.018.
[22] P. Arora, Z.-M. Zhang, Battery separators, Chem. Rev. 104 (2004) 4419–4462.
[23] H. Lee, M. Yanilmaz, O. Toprakci, K. Fu, X. Zhang, A review of recent developments in membrane separators for rechargeable lithium-ion batteries, Energy Environ. Sci. 7 (2014) 3857–3886, https://doi.org/10.1039/C4EE01432D.
[24] J. Nunes-Pereira, C.M. Costa, S. Lanceros-Méndez, Polymer composites and blends for battery separators: state of the art, challenges and future trends, J. Power Sources 281 (2015) 378–398, https://doi.org/10.1016/j.jpowsour.2015.02.010.
[25] S. Ahn, Y. Kim, K.J. Kim, T.H. Kim, H. Lee, M.H. Kim, Development of high capacity, high rate lithium ion batteries utilizing metal fiber conductive additives, J. Power Sources 81–82 (1999) 896–901, https://doi.org/10.1016/S0378-7753(99)00133-0.
[26] M.E. Spahr, D. Goers, A. Leone, S. Stallone, E. Grivei, Development of carbon conductive additives for advanced lithium ion batteries, J. Power Sources 196 (2011) 3404–3413, https://doi.org/10.1016/j.jpowsour.2010.07.002.
[27] R. Raccichini, A. Varzi, S. Passerini, B. Scrosati, The role of graphene for electrochemical energy storage, Nat. Mater. 14 (2015) 271–279.

[28] P. Novák, D. Goers, M.E. Spahr, Carbon materials in lithium-ion batteries, in: Carbons for Electrochemical Energy Storage and Conversion Systems, first ed., CRC Press, Taylor & Francis Group, Boca Raton, London, New York, 2010, pp. 263–328.
[29] Y. Nishi, The development of lithium ion secondary batteries, Chem. Rec. 1 (2001) 406–413, https://doi.org/10.1002/tcr.1024.
[30] J. Asenbauer, T. Eisenmann, M. Kuenzel, A. Kazzazi, Z. Chen, D. Bresser, The success story of graphite as a lithium-ion anode material – fundamentals, remaining challenges, and recent developments including silicon (oxide) composites, Sustainable Energy Fuels, 2020, https://doi.org/10.1039/D0SE00175A.
[31] S. Flandrois, B. Simon, Carbon materials for lithium-ion rechargeable batteries, Carbon 37 (1999) 165–180.
[32] M. Winter, J.O. Besenhard, M.E. Spahr, P. Novák, Insertion electrode materials for rechargeable lithium batteries, Adv. Mater. 10 (1998) 725–763.
[33] R. Yazami, Chapter 2. Electrode materials based on carbon and graphite intercalation compounds in liquid and polymeric electrolytes, in: Lithium Batteries: New Materials, Developments, and Perspectives, Elsevier, Amsterdam, Netherlands, 1994, pp. 49–91.
[34] N. Imanishi, Y. Takeda, O. Yamamoto, Development of the carbon anode in lithium ion batteries, in: Lithium Ion Batteries - Fundamentals and Performance, Wiley, New York, U.S.A., 1998, pp. 98–126.
[35] D. Billaud, E. McRae, A. Hérold, Synthesis and electrical resistivity of lithium-pyrographite intercalation compounds (stages I, II and III), Mater. Res. Bull. 14 (1979) 857–864, https://doi.org/10.1016/0025-5408(79)90149-1.
[36] T. Tran, K. Kinoshita, Lithium intercalation/deintercalation behavior of basal and edge planes of highly oriented pyrolytic graphite and graphite powder, J. Electroanal. Chem. 386 (1995) 221–224, https://doi.org/10.1016/0022-0728(95)03907-X.
[37] M. Heß, P. Novák, Shrinking annuli mechanism and stage-dependent rate capability of thin-layer graphite electrodes for lithium-ion batteries, Electrochim. Acta 106 (2013) 149–158, https://doi.org/10.1016/j.electacta.2013.05.056.
[38] K. Xu, Nonaqueous liquid electrolytes for lithium-based rechargeable batteries, Chem. Rev. 104 (2004) 4303–4418, https://doi.org/10.1021/cr030203g.
[39] K. Edström, T. Gustafsson, J.O. Thomas, The cathode–electrolyte interface in the Li-ion battery, Electrochim. Acta 50 (2004) 397–403, https://doi.org/10.1016/j.electacta.2004.03.049.
[40] A. Würsig, H. Buqa, M. Holzapfel, F. Krumeich, P. Novák, Film formation at positive electrodes in lithium-ion batteries, Electrochem. Solid State Lett. 8 (2005) A34, https://doi.org/10.1149/1.1836114.
[41] E. Peled, The electrochemical behavior of alkali and alkaline earth metals in nonaqueous battery systems—the solid electrolyte interphase model, J. Electrochem. Soc. 126 (1979) 2047–2051.
[42] P.B. Balbuena, Y. Wang, Lithium-ion Batteries: Solid-Electrolyte Interphase, first ed., Imperial College Press, London, UK, 2004.
[43] P. Verma, P. Maire, P. Novák, A review of the features and analyses of the solid electrolyte interphase in Li-ion batteries, Electrochim. Acta 55 (2010) 6332–6341, https://doi.org/10.1016/j.electacta.2010.05.072.
[44] A.M. Andersson, K. Edström, Chemical composition and morphology of the elevated temperature SEI on graphite, J. Electrochem. Soc. 148 (2001) A1100, https://doi.org/10.1149/1.1397771.
[45] A.M. Andersson, M. Herstedt, A.G. Bishop, K. Edström, The influence of lithium salt on the interfacial reactions controlling the thermal stability of graphite anodes, Electrochim. Acta 47 (2002) 1885–1898, https://doi.org/10.1016/S0013-4686(02)00044-0.
[46] K. Edström, M. Herstedt, D.P. Abraham, A new look at the solid electrolyte interphase on graphite anodes in Li-ion batteries, J. Power Sources 153 (2006) 380–384, https://doi.org/10.1016/j.jpowsour.2005.05.062.
[47] E. Peled, Advanced model for solid electrolyte interphase electrodes in liquid and polymer electrolytes, J. Electrochem. Soc. 144 (1997) L208, https://doi.org/10.1149/1.1837858.
[48] D. Alliata, R. Kötz, P. Novák, H. Siegenthaler, Electrochemical SPM investigation of the solid electrolyte interphase film formed on Hopg electrodes, Electrochem. Commun. 2 (2000) 436–440, https://doi.org/10.1016/S1388-2481(00)00056-4.
[49] P. Novák, F. Joho, M. Lanz, B. Rykart, J.-C. Panitz, D. Alliata, R. Kötz, O. Haas, The complex electrochemistry of graphite electrodes in lithium-ion batteries, J. Power Sources 97–98 (2001) 39–46, https://doi.org/10.1016/S0378-7753(01)00586-9.
[50] R. Kostecki, B. Schnyder, D. Alliata, X. Song, K. Kinoshita, R. Kötz, Surface studies of carbon films from pyrolyzed photoresist, Thin Solid Films 396 (2001) 36–43, https://doi.org/10.1016/S0040-6090(01)01185-3.
[51] D. Aurbach, B. Markovsky, A. Shechter, Y. Ein-Eli, H. Cohen, A comparative study of synthetic graphite and Li electrodes in electrolyte solutions based on ethylene carbonate-dimethyl carbonate mixtures, J. Electrochem. Soc. 143 (1996) 3809–3820, https://doi.org/10.1149/1.1837300.
[52] D. Rahner, The role of anions, solvent molecules and solvated electrons in layer formation processes on anode materials for rechargeable lithium batteries, J. Power Sources 81–82 (1999) 358–361, https://doi.org/10.1016/S0378-7753(98)00218-3.
[53] O.(Youngman) Chusid, E. Ein Ely, D. Aurbach, M. Babai, Y. Carmeli, Electrochemical and spectroscopic studies of carbon electrodes in lithium battery electrolyte systems, J. Power Sources 43 (1993) 47–64, https://doi.org/10.1016/0378-7753(93)80101-T.
[54] W. van Schalkwijk, B. Scrosati, Advances in Lithium-Ion Batteries, first ed., Springer, Boston, Mass., U.S.A., 2002.
[55] D. Aurbach, I. Weissmann, Nonaqueous Electrochemistry, first ed., Marcel Dekker, New York, U.S.A., 1999.
[56] M. Kikuchi, Y. Ikezawa, T. Takamura, Surface modification of pitch-based carbon fibre for the improvement of electrochemical lithium intercalation, J. Electroanal. Chem. 396 (1995) 451–455, https://doi.org/10.1016/0022-0728(95)04082-Y.
[57] D. Aurbach, Common electroanalytical behavior of Li intercalation processes into graphite and transition metal oxides, J. Electrochem. Soc. 145 (1998) 3024, https://doi.org/10.1149/1.1838758.
[58] D. Aurbach, K. Gamolsky, B. Markovsky, Y. Gofer, M. Schmidt, U. Heider, On the use of vinylene carbonate (VC) as an additive to electrolyte solutions for Li-ion batteries, Electrochim. Acta 47 (2002) 1423–1439, https://doi.org/10.1016/S0013-4686(01)00858-1.
[59] F. Joho, B. Rykart, R. Imhof, P. Novák, M.E. Spahr, A. Monnier, Key factors for the cycling stability of graphite intercalation electrodes for lithium-ion batteries, J. Power Sources 81–82 (1999) 243–247, https://doi.org/10.1016/S0378-7753(99)00195-0.
[60] J. Vetter, P. Novák, Novel alkyl methyl carbonate solvents for lithium-ion batteries, J. Power Sources 119–121 (2003) 338–342, https://doi.org/10.1016/S0378-7753(03)00151-4.
[61] F. Joho, B. Rykart, A. Blome, P. Novák, H. Wilhelm, M.E. Spahr, Relation between surface properties, pore structure and first-cycle charge loss of graphite as negative electrode in lithium-ion batteries, J. Power Sources 97–98 (2001) 78–82, https://doi.org/10.1016/S0378-7753(01)00595-X.
[62] G. Li, R. Xue, L. Chen, The influence of polytetrafluorethylene reduction on the capacity loss of the carbon anode for lithium ion batteries, Solid State Ionics 90 (1996) 221–225, https://doi.org/10.1016/S0167-2738(96)00367-0.
[63] M.E. Spahr, H. Wilhelm, T. Palladino, N. Dupont-Pavlovsky, D. Goers, F. Joho, P. Novák, The role of graphite surface group chemistry on graphite exfoliation during electrochemical lithium insertion, J. Power Sources 119–121 (2003) 543–549, https://doi.org/10.1016/S0378-7753(03)00284-2.
[64] H. Buqa, D. Goers, M.E. Spahr, P. Novák, The influence of graphite surface modification on the exfoliation during electrochemical lithium insertion, J. Solid State Electrochem. 8 (2003) 79–80, https://doi.org/10.1007/s10008-003-0409-5.
[65] S.-K. Jeong, M. Inaba, Y. Iriyama, T. Abe, Z. Ogumi, Electrochemical intercalation of lithium ion within graphite from propylene carbonate solutions, Electrochem. Solid State Lett. 6 (2003) A13, https://doi.org/10.1149/1.1526781.
[66] T. Abe, N. Kawabata, Y. Mizutani, M. Inaba, Z. Ogumi, Correlation between cointercalation of solvents and electrochemical intercalation of lithium into graphite in propylene carbonate solution, J. Electrochem. Soc. 150 (2003) A257, https://doi.org/10.1149/1.1541004.
[67] M. Inaba, Z. Siroma, A. Funabiki, Z. Ogumi, T. Abe, Y. Mizutani, M. Asano, Electrochemical scanning tunneling microscopy observation of highly oriented pyrolytic graphite surface reactions in an ethylene carbonate-based electrolyte solution, Langmuir 12 (1996) 1535–1540, https://doi.org/10.1021/la950848e.
[68] B. Simon, S. Flandrois, A. Fevrier-bouvier, P. Biensan, Hexagonal vs rhombohedral graphite: the effect of crystal structure on electrochemical intercalation of lithium ions, molecular crystals and liquid crystals science and technology, Section A. Molecular Crystals and Liquid Crystals 310 (1998) 333–340, https://doi.org/10.1080/10587259808045358.
[69] M. Holzapfel, C. Jost, A. Prodi-Schwab, F. Krumeich, A. Würsig, H. Buqa, P. Novák, Stabilisation of lithiated graphite in an electrolyte based on ionic liquids: an electrochemical and scanning electron microscopy study, Carbon 43 (2005) 1488–1498, https://doi.org/10.1016/j.carbon.2005.01.030.
[70] J.S. Gnanaraj, R.W. Thompson, J.F. DiCarlo, K.M. Abraham, The role of carbonate solvents on lithium intercalation into graphite, J. Electrochem. Soc. 154 (2007) A185, https://doi.org/10.1149/1.2424419.
[71] D. Aurbach, B. Markovsky, I. Weissman, E. Levi, Y. Ein-Eli, On the correlation between surface chemistry and performance of graphite negative electrodes for Li ion batteries, Electrochim. Acta 45 (1999) 67–86, https://doi.org/10.1016/S0013-4686(99)00194-2.
[72] M.E. Spahr, H. Wilhelm, F. Joho, J.-C. Panitz, J. Wambach, P. Novák, N. Dupont-Pavlovsky, Purely hexagonal graphite and the influence of surface modifications on its electrochemical lithium insertion properties, J. Electrochem. Soc. 149 (2002) A960, https://doi.org/10.1149/1.1486238.
[73] W.P. Hoffman, F.J. Vastola, P.L. Walker, Chemisorption of alkanes and alkenes on carbon active sites, Carbon 22 (1984) 585–594, https://doi.org/10.1016/0008-6223(84)90094-0.
[74] N.R. Laine, F.J. Vastola, P.L. Walker, The importance of active surface area in the carbon-oxygen reaction, J. Phys. Chem. 67 (1963) 2030–2034, https://doi.org/10.1021/j100804a016.
[75] C. Vix-Guterl, P. Ehrburger, Role of chemistry in advanced carbon-based composites, in: Fibers and Composites, first ed., CRC Press, Taylor & Francis Group, Boca Raton, FL, USA, 2003, p. 206.
[76] M.E. Spahr, H. Buqa, A. Würsig, D. Goers, L. Hardwick, P. Novák, F. Krumeich, J. Dentzer, C. Vix-Guterl, Surface reactivity of graphite materials and their surface passivation during the first electrochemical lithium insertion, J. Power Sources 153 (2006) 300–311, https://doi.org/10.1016/j.jpowsour.2005.05.032.
[77] D. Cericola, M.E. Spahr, Impedance spectroscopic studies of the porous structure of electrodes containing graphite materials with different particle size and shape, Electrochim. Acta 191 (2016) 558–566, https://doi.org/10.1016/j.electacta.2016.01.121.
[78] J. Landesfeind, M. Ebner, A. Eldiven, V. Wood, H.A. Gasteiger, Tortuosity of battery electrodes: validation of impedance-derived values and critical comparison with 3D tomography, J. Electrochem. Soc. 165 (2018) A469–A476, https://doi.org/10.1149/2.0231803jes.

[79] D. Goers, M.E. Spahr, A. Leone, W. Märkle, P. Novák, The influence of the local current density on the electrochemical exfoliation of graphite in lithium-ion battery negative electrodes, Electrochim. Acta 56 (2011) 3799–3808, https://doi.org/10.1016/j.electacta.2011.02.046.
[80] J.L. Gómez-Cámer, C. Bünzli, M.M. Hantel, T. Poux, P. Novák, On the correlation between electrode expansion and cycling stability of graphite/Si electrodes for Li-ion batteries, Carbon 105 (2016) 42–51, https://doi.org/10.1016/j.carbon.2016.04.022.
[81] M. Winter, G.H. Wrodnigg, J.O. Besenhard, W. Biberacher, P. Novák, Dilatometric investigations of graphite electrodes in nonaqueous lithium battery electrolytes, J. Electrochem. Soc. 147 (2000) 2427–2431, https://doi.org/10.1149/1.1393548.
[82] M. Holzapfel, H. Buqa, L.J. Hardwick, M. Hahn, A. Würsig, W. Scheifele, P. Novák, R. Kötz, C. Veit, F.-M. Petrat, Nano silicon for lithium-ion batteries, Electrochim. Acta 52 (2006) 973–978, https://doi.org/10.1016/j.electacta.2006.06.034.
[83] M.R. Wagner, P.R. Raimann, A. Trifonova, K.-C. Möller, J.O. Besenhard, M. Winter, Dilatometric and mass spectrometric investigations on lithium ion battery anode materials, Anal. Bioanal. Chem. 379 (2004) 272–276, https://doi.org/10.1007/s00216-004-2570-9.
[84] S. Yang, H. Song, X. Chen, Expansion of mesocarbon microbeads, Carbon 44 (2006) 730–733, https://doi.org/10.1016/j.carbon.2005.09.019.
[85] J. Christensen, J. Newman, Stress generation and fracture in lithium insertion materials, J. Solid State Electrochem. 10 (2006) 293–319, https://doi.org/10.1007/s10008-006-0095-1.
[86] F.P. Campana, R. Kötz, J. Vetter, P. Novák, H. Siegenthaler, In situ atomic force microscopy study of dimensional changes during Li+ ion intercalation/de-intercalation in highly oriented pyrolytic graphite, Electrochem. Commun. 7 (2005) 107–112, https://doi.org/10.1016/j.elecom.2004.11.015.
[87] Z.X. Shu, Electrochemical intercalation of lithium into graphite, J. Electrochem. Soc. 140 (1993) 922, https://doi.org/10.1149/1.2056228.
[88] T. Waldmann, B.-I. Hogg, M. Wohlfahrt-Mehrens, Li plating as unwanted side reaction in commercial Li-ion cells – a review, J. Power Sources 384 (2018) 107–124, https://doi.org/10.1016/j.jpowsour.2018.02.063.
[89] S.S. Zhang, in: Identifying Rate Limitation and a Guide to Design of Fast-Charging Li-Ion Battery, InfoMat. n/a, 2019, https://doi.org/10.1002/inf2.12058.
[90] X.L. Yao, S. Xie, C.H. Chen, Q.S. Wang, J.H. Sun, Y.L. Li, S.X. Lu, Comparisons of graphite and spinel Li1.33Ti1.67O4 as anode materials for rechargeable lithium-ion batteries, Electrochim. Acta 50 (2005) 4076–4081, https://doi.org/10.1016/j.electacta.2005.01.034.
[91] C.P. Sandhya, B. John, C. Gouri, Lithium titanate as anode material for lithium-ion cells: a review, Ionics 20 (2014) 601–620, https://doi.org/10.1007/s11581-14-1113-4.
[92] T. Ohzuku, A. Ueda, N. Yamamoto, Zero-strain insertion material of Li[Li[1/3]Ti[5/3]]O[4] for rechargeable lithium cells, J. Electrochem. Soc. 142 (1995) 1431–1435.
[93] P. Reale, S. Panero, B. Scrosati, J. Garche, M. Wohlfahrt-Mehrens, M. Wachtler, A safe, low-cost, and sustainable lithium-ion polymer battery, J. Electrochem. Soc. 151 (2004), A2138, https://doi.org/10.1149/1.1819790.
[94] D. Bresser, E. Paillard, M. Copley, P. Bishop, M. Winter, S. Passerini, The importance of "going nano" for high power battery materials, J. Power Sources 219 (2012) 217–222, https://doi.org/10.1016/j.jpowsour.2012.07.035.
[95] A. Birrozzi, M. Copley, J. von Zamory, M. Pasqualini, S. Calcaterra, F. Nobili, A. Di Cicco, H. Rajantie, M. Briceno, E. Bilbé, L. Cabo-Fernandez, L.J. Hardwick, D. Bresser, S. Passerini, Scaling up "nano" Li4Ti5O12 for high-power lithium-ion anodes using large scale flame spray pyrolysis, J. Electrochem. Soc. 162 (2015) A2331–A2338, https://doi.org/10.1149/2.0711512jes.
[96] D. Li, H. Zhou, Two-phase transition of Li-intercalation compounds in Li-ion batteries, Mater. Today 17 (2014) 451–463, https://doi.org/10.1016/j.mattod.2014.06.002.
[97] Y.-Q. Wang, L. Gu, Y.-G. Guo, H. Li, X.-Q. He, S. Tsukimoto, Y. Ikuhara, L.-J. Wan, Rutile-TiO2 nanocoating for a high-rate Li4Ti5O12 anode of a lithium-ion battery, J. Am. Chem. Soc. 134 (2012) 7874–7879, https://doi.org/10.1021/ja301266w.
[98] Y.-B. He, M. Liu, Z.-D. Huang, B. Zhang, Y. Yu, B. Li, F. Kang, J.-K. Kim, Effect of solid electrolyte interface (SEI) film on cyclic performance of Li4Ti5O12 anodes for Li ion batteries, J. Power Sources 239 (2013) 269–276, https://doi.org/10.1016/j.jpowsour.2013.03.141.
[99] H. Zhao, Y. Li, Z. Zhu, J. Lin, Z. Tian, R. Wang, Structural and electrochemical characteristics of Li4 xAlxTi5O12 as anode material for lithium-ion batteries, Electrochim. Acta 53 (2008) 7079–7083, https://doi.org/10.1016/j.electacta.2008.05.038.
[100] C.H. Chen, J.T. Vaughey, A.N. Jansen, D.W. Dees, A.J. Kahaian, T. Goacher, M. M. Thackeray, Studies of Mg-substituted Li4 xMgxTi5O12 spinel electrodes (0⩽x⩽1) for lithium batteries, J. Electrochem. Soc. 148 (2001) A102–A104, https://doi.org/10.1149/1.1344523.
[101] G.-N. Zhu, H.-J. Liu, J.-H. Zhuang, C.-X. Wang, Y.-G. Wang, Y.-Y. Xia, Carbon-coated nano-sized Li4Ti5O12 nanoporous micro-sphere as anode material for high-rate lithium-ion batteries, Energy Environ. Sci. 4 (2011) 4016–4022, https://doi.org/10.1039/C1EE01680F.
[102] K. Amine, I. Belharouak, Z. Chen, T. Tran, H. Yumoto, N. Ota, S.-T. Myung, Y.-K. Sun, Nanostructured anode material for high-power battery system in electric vehicles, Adv. Mater. 22 (2010) 3052–3057, https://doi.org/10.1002/adma.201000441.
[103] L. Zhao, Y.-S. Hu, H. Li, Z. Wang, L. Chen, Porous Li4Ti5O12 coated with N-doped carbon from ionic liquids for Li-ion batteries, Adv. Mater. 23 (2011) 1385–1388, https://doi.org/10.1002/adma.201003294.
[104] K.-S. Park, A. Benayad, D.-J. Kang, S.-G. Doo, Nitridation-driven conductive Li4Ti5O12 for lithium ion batteries, J. Am. Chem. Soc. 130 (2008) 14930–14931, https://doi.org/10.1021/ja806104n.
[105] P.G. Kitz, P. Novák, E.J. Berg, Influence of water contamination on the SEI formation in Li-ion cells: an operando EQCM-D study, ACS Appl. Mater. Interfaces 12 (2020) 15934–15942, https://doi.org/10.1021/acsami.0c01642.
[106] R. Bernhard, S. Meini, H.A. Gasteiger, On-line electrochemical mass spectrometry investigations on the gassing behavior of Li4Ti5O12 electrodes and its origins, J. Electrochem. Soc. 161 (2014) A497–A505, https://doi.org/10.1149/2.013404jes.
[107] M. He, E. Castel, A. Laumann, G. Nuspl, P. Novák, E.J. Berg, In situ gas analysis of Li4Ti5O12-based electrodes at elevated temperatures, J. Electrochem. Soc. 162 (2015) A870–A876, https://doi.org/10.1149/2.0311506jes.
[108] D. Leanza, C.A.F. Vaz, I. Czekaj, P. Novák, M. El Kazzi, Solving the puzzle of Li4Ti5O12 surface reactivity in aprotic electrolytes in Li-ion batteries by nanoscale XPEEM spectromicroscopy, J. Mater. Chem. A. 6 (2018) 3534–3542, https://doi.org/10.1039/C7TA09673A.
[109] M.N. Obrovac, V.L. Chevrier, Alloy negative electrodes for Li-ion batteries, Chem. Rev. 114 (2014) 11444–11502, https://doi.org/10.1021/cr500207g.
[110] A. Franco Gonzalez, N.-H. Yang, R.-S. Liu, Silicon anode design for lithium-ion batteries: progress and perspectives, J. Phys. Chem. C 121 (2017) 27775–27787, https://doi.org/10.1021/acs.jpcc.7b07793.
[111] X. Zuo, J. Zhu, P. Müller-Buschbaum, Y.-J. Cheng, Silicon based lithium-ion battery anodes: a chronicle perspective review, Nano Energy 31 (2017) 113–143, https://doi.org/10.1016/j.nanoen.2016.11.013.
[112] K. Feng, M. Li, W. Liu, A.G. Kashkooli, X. Xiao, M. Cai, Z. Chen, Silicon-based anodes for lithium-ion batteries: from fundamentals to practical applications, Small 14 (2018), 1702737, https://doi.org/10.1002/smll.201702737.
[113] M.N. Obrovac, Si-alloy negative electrodes for Li-ion batteries, Curr. Opinion in Electrochem. 9 (2018) 8–17, https://doi.org/10.1016/j.coelec.2018.02.002.
[114] S. Chae, M. Ko, K. Kim, K. Ahn, J. Cho, Confronting issues of the practical implementation of Si anode in high-energy lithium-ion batteries, Joule 1 (2017) 47–60, https://doi.org/10.1016/j.joule.2017.07.006.
[115] W.-F. Ren, Y. Zhou, J.-T. Li, L. Huang, S.-G. Sun, Si anode for next-generation lithium-ion battery, Curr. Opinion in Electrochem. 18 (2019) 46–54, https://doi.org/10.1016/j.coelec.2019.09.006.
[116] F. Dou, L. Shi, G. Chen, D. Zhang, Silicon/carbon composite anode materials for lithium-ion batteries, Electrochem. Energy Rev. 2 (2019) 149–198, https://doi.org/10.1007/s41918-018-00028-w.
[117] Y. Zhang, N. Du, D. Yang, Designing superior solid electrolyte interfaces on silicon anodes for high-performance lithium-ion batteries, Nanoscale 11 (2019) 19086–19104, https://doi.org/10.1039/C9NR05748J.
[118] F. Li, J. Xu, Z. Hou, M. Li, R. Yang, Silicon anodes for high-performance storage devices: structural design, material compounding, advances in electrolytes and binders, ChemNanoMat 6 (2020) 720–738, https://doi.org/10.1002/cnma.201900708.
[119] Z. Liu, Q. Yu, Y. Zhao, R. He, M. Xu, S. Feng, S. Li, L. Zhou, L. Mai, Silicon oxides: a promising family of anode materials for lithium-ion batteries, Chem. Soc. Rev. 48 (2019) 285–309, https://doi.org/10.1039/C8CS00441B.
[120] J. Wu, Y. Cao, H. Zhao, J. Mao, Z. Guo, The critical role of carbon in marrying silicon and graphite anodes for high-energy lithium-ion batteries, Carbon Energy 1 (2019) 57–76, https://doi.org/10.1002/cey2.2.
[121] S. Chae, S.-H. Choi, N. Kim, J. Sung, J. Cho, Integration of graphite and silicon anodes for the commercialization of high-energy lithium-ion batteries, Angew. Chem. Int. Ed. 59 (2020) 110–135, https://doi.org/10.1002/anie.201902085.
[122] N. Liu, H. Wu, M.T. McDowell, Y. Yao, C. Wang, Y. Cui, A yolk-shell design for stabilized and scalable Li-ion battery alloy anodes, Nano Lett. 12 (2012) 3315–3321, https://doi.org/10.1021/nl3014814.
[123] N. Liu, Z. Lu, J. Zhao, M.T. McDowell, H.-W. Lee, W. Zhao, Y. Cui, A pomegranate-inspired nanoscale design for large-volume-change lithium battery anodes, Nat. Nanotechnol. 9 (2014) 187–192, https://doi.org/10.1038/nnano.2014.6.
[124] F.-H. Du, B. Li, W. Fu, Y.-J. Xiong, K.-X. Wang, J.-S. Chen, Surface binding of polypyrrole on porous silicon hollow nanospheres for Li-ion battery anodes with high structure stability, Adv. Mater. 26 (2014) 6145–6150, https://doi.org/10.1002/adma.201401937.
[125] Q. Xu, J.-Y. Li, J.-K. Sun, Y.-X. Yin, L.-J. Wan, Y.-G. Guo, Watermelon-Inspired Si/C microspheres with hierarchical buffer structures for densely compacted lithium-ion battery anodes, Adv. Energy Mater. 7 (2017), 1601481, https://doi.org/10.1002/aenm.201601481.
[126] S. Fang, Z. Tong, P. Nie, G. Liu, X. Zhang, Raspberry-like nanostructured silicon composite anode for high-performance lithium-ion batteries, ACS Appl. Mater. Interfaces 9 (2017) 18766–18773, https://doi.org/10.1021/acsami.7b03157.
[127] A. Hirata, S. Kohara, T. Asada, M. Arao, C. Yogi, H. Imai, Y. Tan, T. Fujita, M. Chen, Atomic-scale disproportionation in amorphous silicon monoxide, Nat. Commun. 7 (2016), 11591, https://doi.org/10.1038/ncomms11591.
[128] Y. Reynier, C. Vincens, C. Leys, B. Amestoy, E. Mayousse, B. Chavillon, L. Blanc, E. Gutel, W. Porcher, T. Hirose, C. Matsui, Practical implementation of Li doped SiO in high energy density 21700 cell, J. Power Sources 450 (2020), 227699, https://doi.org/10.1016/j.jpowsour.2020.227699.
[129] K. Kitada, O. Pecher, P.C.M.M. Magusin, M.F. Groh, R.S. Weatherup, C.P. Grey, Unraveling the reaction mechanisms of SiO anodes for Li-ion batteries by

combining in situ 7Li and ex situ 7Li/29Si solid-state NMR spectroscopy, J. Am. Chem. Soc. 141 (2019) 7014–7027, https://doi.org/10.1021/jacs.9b01589.
[130] A.I. Freytag, A.D. Pauric, M. Jiang, G.R. Goward, 7Li and 29Si NMR enabled by high-density cellulose-based electrodes in the lithiation process in silicon and silicon monoxide anodes, J. Phys. Chem. C 123 (2019) 11362–11368, https://doi.org/10.1021/acs.jpcc.8b11963.
[131] D. Mazouzi, Z. Karkar, C. Reale Hernandez, P. Jimenez Manero, D. Guyomard, L. Roué, B. Lestriez, Critical roles of binders and formulation at multiscales of silicon-based composite electrodes, J. Power Sources 280 (2015) 533–549, https://doi.org/10.1016/j.jpowsour.2015.01.140.
[132] T. Kwon, J.W. Choi, A. Coskun, The emerging era of supramolecular polymeric binders in silicon anodes, Chem. Soc. Rev. 47 (2018) 2145–2164, https://doi.org/10.1039/C7CS00858A.
[133] Y. Ma, J. Ma, G. Cui, Small things make big deal: powerful binders of lithium batteries and post-lithium batteries, Energy Storage Mater. 20 (2019) 146–175, https://doi.org/10.1016/j.ensm.2018.11.013.
[134] G.G. Eshetu, E. Figgemeier, Confronting the challenges of next-generation silicon anode-based lithium-ion batteries: role of designer electrolyte additives and polymeric binders, ChemSusChem 12 (2019) 2515–2539, https://doi.org/10.1002/cssc.201900209.
[135] F. Holtstiege, P. Baermann, R. Noelle, M. Winter, T. Placke, Pre-lithiation strategies for rechargeable energy storage technologies: concepts, promises and challenges, Batteries 4 (2018) 4–42.
[136] V. Aravindan, Y.-S. Lee, S. Madhavi, Best practices for mitigating irreversible capacity loss of negative electrodes in Li-ion batteries, Adv. Energy Mater. 7 (2017), 1602607, https://doi.org/10.1002/aenm.201602607.
[137] C.L. Berhaut, D.Z. Dominguez, D. Tomasi, C. Vincens, C. Haon, Y. Reynier, W. Porcher, N. Boudet, N. Blanc, G.A. Chahine, S. Tardif, S. Pouget, S. Lyonnard, Prelithiation of silicon/graphite composite anodes: benefits and mechanisms for long-lasting Li-Ion batteries, Energy Storage Mater. 29 (2020) 190–197, https://doi.org/10.1016/j.ensm.2020.04.008.
[138] J. Sturm, A. Rheinfeld, I. Zilberman, F.B. Spingler, S. Kosch, F. Frie, A. Jossen, Modeling and simulation of inhomogeneities in a 18650 nickel-rich, silicon-graphite lithium-ion cell during fast charging, J. Power Sources 412 (2019) 204–223, https://doi.org/10.1016/j.jpowsour.2018.11.043.
[139] Panasonic, Spec Sheet for NCR18650BF, 2015.
[140] Z. Karkar, T. Jaouhari, A. Tranchot, D. Mazouzi, D. Guyomard, B. Lestriez, L. Roué, How silicon electrodes can be calendered without altering their mechanical strength and cycle life, J. Power Sources 371 (2017) 136–147, https://doi.org/10.1016/j.jpowsour.2017.10.042.
[141] D.J. Pereira, J.W. Weidner, T.R. Garrick, The effect of volume change on the accessible capacities of porous silicon-graphite composite anodes, J. Electrochem. Soc. 166 (2019) A1251–A1256, https://doi.org/10.1149/2.1211906jes.
[142] C. Heubner, U. Langklotz, A. Michaelis, Theoretical optimization of electrode design parameters of Si based anodes for lithium-ion batteries, J. Energy Storage 15 (2018) 181–190, https://doi.org/10.1016/j.est.2017.11.009.
[143] R. Dash, S. Pannala, Retracted ARTICLE: Theoretical limits of energy density in silicon-carbon composite anode based lithium ion batteries, Sci. Rep. 6 (2016), 27449, https://doi.org/10.1038/srep27449.
[144] Y. Jin, S. Li, A. Kushima, X. Zheng, Y. Sun, J. Xie, J. Sun, W. Xue, G. Zhou, J. Wu, F. Shi, R. Zhang, Z. Zhu, K. So, Y. Cui, J. Li, Self-healing SEI enables full-cell cycling of a silicon-majority anode with a coulombic efficiency exceeding 99.9%, Energy Environ. Sci. 10 (2017) 580–592, https://doi.org/10.1039/C6EE02685K.
[145] H. Wang, J. Fu, C. Wang, J. Wang, A. Yang, C. Li, Q. Sun, Y. Cui, H. Li, A binder-free high silicon content flexible anode for Li-ion batteries, Energy Environ. Sci. 13 (2020) 848–858, https://doi.org/10.1039/C9EE02615K.
[146] J. Lopez, D.G. Mackanic, Y. Cui, Z. Bao, Designing polymers for advanced battery chemistries, Nat. Rev. Mater. 4 (2019) 312–330, https://doi.org/10.1038/s41578-019-0103-6.
[147] T. Kwon, J.W. Choi, A. Coskun, Prospect for supramolecular chemistry in high-energy-density rechargeable batteries, Joule 3 (2019) 662–682, https://doi.org/10.1016/j.joule.2019.01.006.
[148] T. Devic, B. Lestriez, L. Roué, Silicon electrodes for Li-ion batteries. Addressing the challenges through coordination chemistry, ACS Energy Lett 4 (2019) 550–557, https://doi.org/10.1021/acsenergylett.8b02433.
[149] R. Kerr, D. Mazouzi, M. Eftekharnia, B. Lestriez, N. Dupré, M. Forsyth, D. Guyomard, P.C. Howlett, High-capacity retention of Si anodes using a mixed lithium/phosphonium bis(fluorosulfonyl)imide ionic liquid electrolyte, ACS Energy Lett 2 (2017) 1804–1809, https://doi.org/10.1021/acsenergylett.7b00403.
[150] M. Tesemma, F.-M. Wang, A.M. Haregewoin, N.L. Hamidah, P. Muhammad Hendra, S.D. Lin, C.-S. Chern, Q.-T. Pham, C.-H. Su, Investigation of the dipole moment effects of fluorofunctionalized electrolyte additives in a lithium ion battery, ACS Sustain. Chem. Eng. 7 (2019) 6640–6653, https://doi.org/10.1021/acssuschemeng.8b05635.
[151] S.N.S. Hapuarachchi, Z. Sun, C. Yan, Advances in in situ techniques for characterization of failure mechanisms of Li-ion battery anodes, Adv. Sustain. Sys. 2 (2018), 1700182, https://doi.org/10.1002/adsu.201700182.
[152] V. Müller, R. Bernhard, J. Wegener, J. Pfeiffer, S. Rössler, R.-G. Scurtu, M. Memm, M.A. Danzer, M. Wohlfahrt-Mehrens, Evaluation of scalable porous Si-rich Si/C composites with low volume expansion in coin cells to prismatic cell formats, Energy Technol. (2020) 2000217, https://doi.org/10.1002/ente.202000217.
[153] O.O. Taiwo, J.M. Paz-García, S.A. Hall, T.M.M. Heenan, D.P. Finegan, R. Mokso, P. Villanueva-Pérez, A. Patera, D.J.L. Brett, P.R. Shearing, Microstructural degradation of silicon electrodes during lithiation observed via operando X-ray tomographic imaging, J. Power Sources 342 (2017) 904–912, https://doi.org/10.1016/j.jpowsour.2016.12.070.
[154] S. Müller, P. Pietsch, B.-E. Brandt, P. Baade, V. De Andrade, F. De Carlo, V. Wood, Quantification and modeling of mechanical degradation in lithium-ion batteries based on nanoscale imaging, Nat. Commun. 9 (2018) 2340, https://doi.org/10.1038/s41467-018-04477-1.
[155] V. Vanpeene, J. Villanova, A. King, B. Lestriez, E. Maire, L. Roué, Dynamics of the morphological degradation of Si-based anodes for Li-ion batteries characterized by in situ synchrotron X-ray tomography, Adv. Energy Mater. 9 (2019), 1803947, https://doi.org/10.1002/aenm.201803947.
[156] K. Dong, H. Markötter, F. Sun, A. Hilger, N. Kardjilov, J. Banhart, I. Manke, Insitu and operando tracking of microstructure and volume evolution of silicon electrodes by using synchrotron X-ray imaging, ChemSusChem 12 (2019) 261–269, https://doi.org/10.1002/cssc.201801969.
[157] H. Chen, M. Ling, L. Hencz, H.Y. Ling, G. Li, Z. Lin, G. Liu, S. Zhang, Exploring chemical, mechanical, and electrical functionalities of binders for advanced energy-storage devices, Chem. Rev. 118 (2018) 8936–8982, https://doi.org/10.1021/acs.chemrev.8b00241.
[158] Z. Karkar, D. Guyomard, L. Roué, B. Lestriez, A comparative study of polyacrylic acid (PAA) and carboxymethyl cellulose (CMC) binders for Si-based electrodes, Electrochim. Acta 258 (2017) 453–466, https://doi.org/10.1016/j.electacta.2017.11.082.
[159] A.K. Padhi, Phospho-olivines as positive-electrode materials for rechargeable lithium batteries, J. Electrochem. Soc. 144 (1997) 1188.
[160] K. Zaghib, A. Guerfi, P. Hovington, A. Vijh, M. Trudeau, A. Mauger, J. B. Goodenough, C.M. Julien, Review and analysis of nanostructured olivine-based lithium recheargeable batteries: status and trends, J. Power Sources 232 (2013) 357–369, https://doi.org/10.1016/j.jpowsour.2012.12.095.
[161] M.Z. Bazant, Theory of chemical kinetics and charge transfer based on nonequilibrium thermodynamics, Acc. Chem. Res. 46 (2013) 1144–1160, https://doi.org/10.1021/ar300145c.
[162] H. Liu, F.C. Strobridge, O.J. Borkiewicz, K.M. Wiaderek, K.W. Chapman, P. J. Chupas, C.P. Grey, Capturing metastable structures during high-rate cycling of $LiFePO_4$ nanoparticle electrodes, Science 344 (2014), 1252817, https://doi.org/10.1126/science.1252817.
[163] N. Nitta, F. Wu, J.T. Lee, G. Yushin, Li-ion battery materials: present and future, Mater. Today 18 (2015) 252–264, https://doi.org/10.1016/j.mattod.2014.10.040.
[164] N. Ravet, J.B. Goodenough, S. Besner, M. Simoneau, P. Hovington, M. Armand, in: The Electrochemical Society and the Electrochemical Society of Japan Meeting Abstracts, Abstract 127, Vol. 99-2, Honolulu, HI, 1999.
[165] N. Ravet, Y. Chouinard, J.F. Magnan, S. Besner, M. Gauthier, M. Armand, Electroactivity of natural and synthetic triphylite, J. Power Sources 97–98 (2001) 503–507, https://doi.org/10.1016/S0378-7753(01)00727-3.
[166] T.V.S.L. Satyavani, A. Srinivas Kumar, P.S.V. Subba Rao, Methods of synthesis and performance improvement of lithium iron phosphate for high rate Li-ion batteries: a review, Engineering Science and Technology, Int. J. 19 (2016) 178–188, https://doi.org/10.1016/j.jestch.2015.06.002.
[167] A.H. Omidi, A. Babaei, A. Ataie, Low temperature synthesis of nanostructured LiFePO4/C cathode material for lithium ion batteries, Mater. Res. Bull. 125 (2020), 110807, https://doi.org/10.1016/j.materresbull.2020.110807.
[168] J. Guo, M. Yu, F. Wu, Preparation of high purity iron phosphate based on the advanced liquid-phase precipitation method and its enhanced properties, J. Solid State Chem. 287 (2020), 121346, https://doi.org/10.1016/j.jssc.2020.121346.
[169] Q. Li, R. Xiao, X. Liao, Z. Ma, Y. Huang, Y. Zhang, X. Ke, Extra Li-ion storage of LiFePO4/C composite materials synthesized with Fe1.5P, J. Alloys Compd. 835 (2020), 155148, https://doi.org/10.1016/j.jallcom.2020.155148.
[170] W. Yang, L. Zhang, Y. Chen, H. Yao, J. Li, Y. Lin, Z. Huang, Improved electrochemical performances and magnetic properties of lithium iron phosphate with in situ Fe2P surface modification by the control of the reductive gas flow rate, Appl. Surf. Sci. 521 (2020), 146389, https://doi.org/10.1016/j.apsusc.2020.146389.
[171] Y. Zhang, J.A. Alarco, J.Y. Nerkar, A.S. Best, G.A. Snook, P.C. Talbot, Nanoscale characteristics of practical LiFePO4 materials - effects on electrical, magnetic and electrochemical properties, Mater. Char. 162 (2020), 110171, https://doi.org/10.1016/j.matchar.2020.110171.
[172] M.G. Rigamonti, M. Chavalle, H. Li, P. Antitomaso, L. Hadidi, M. Stucchi, F. Galli, H. Khan, M. Dollé, D.C. Boffito, G.S. Patience, LiFePO4 spray drying scale-up and carbon-cage for improved cyclability, J. Power Sources 462 (2020), 228103, https://doi.org/10.1016/j.jpowsour.2020.228103.
[173] S. Weng, T. Huo, K. Liu, J. Zhang, W. Li, In-situ polymerization of hydroquinone-formaldehyde resin to construct 3D porous composite LiFePO4/carbon for remarkable performance of lithium-ion batteries, J. Alloys Compd. 818 (2020), 152858, https://doi.org/10.1016/j.jallcom.2019.152858.
[174] C. Busson, M.-A. Blin, P. Guichard, P. Soudan, O. Crosnier, D. Guyomard, B. Lestriez, A primed current collector for high performance carbon-coated LiFePO4 electrodes with no carbon additive, J. Power Sources 406 (2018) 7–17, https://doi.org/10.1016/j.jpowsour.2018.10.018.
[175] H. Guo, C. Wu, L. Liao, J. Xie, S. Zhang, P. Zhu, G. Cao, X. Zhao, Performance improvement of lithium manganese phosphate by controllable morphology tailoring with acid-engaged nano engineering, Inorg. Chem. 54 (2015) 667–674, https://doi.org/10.1021/ic5026075.
[176] A. Örnek, E. Bulut, M. Can, Influence of gradual cobalt substitution on lithium nickel phosphate nano-scale composites for high voltage applications, Mater. Char. 106 (2015) 152–162, https://doi.org/10.1016/j.matchar.2015.05.029.

[177] S. Tan, Y.J. Ji, Z.R. Zhang, Y. Yang, Recent progress in research on high-voltage electrolytes for lithium-ion batteries, ChemPhysChem 15 (2014) 1956–1969, https://doi.org/10.1002/cphc.201402175.

[178] K.J. Kreder, G. Assat, A. Manthiram, Microwave-Assisted solvothermal synthesis of three polymorphs of LiCoPO4 and their electrochemical properties, Chem. Mater. 27 (2015) 5543–5549, https://doi.org/10.1021/acs.chemmater.5b01670.

[179] J. Ludwig, T. Nilges, Recent progress and developments in lithium cobalt phosphate chemistry- Syntheses, polymorphism and properties, J. Power Sources 382 (2018) 101–115, https://doi.org/10.1016/j.jpowsour.2018.02.038.

[180] E.A. Olivetti, G. Ceder, G.G. Gaustad, X. Fu, Lithium-ion battery supply chain considerations: analysis of potential bottlenecks in critical metals, Joule 1 (2017) 229–243, https://doi.org/10.1016/j.joule.2017.08.019.

[181] S. Gong, X. Bai, R. Liu, H. Liu, Y. Gu, Study on discharge voltage and discharge capacity of LiFe1 xMnxPO4 with high Mn content, J. Mater. Sci. Mater. Electron. 31 (2020) 7742–7752, https://doi.org/10.1007/s10854-020-03311-z.

[182] E.B. Fredj, S. Rousselot, L. Danis, T. Bibienne, M. Gauthier, G. Liang, M. Dollé, Synthesis and characterization of LiFe1 xMnxPO4 (x = 0.25, 0.50, 0.75) lithium ion battery cathode synthesized via a melting process, J. Energy Storage 27 (2020), 101116, https://doi.org/10.1016/j.est.2019.101116.

[183] D.A. Bograchev, Y.M. Volfkovisch, V.E. Sosenkin, O.A. Podgornova, N.V. Kosova, The influence of porous structure on the electrochemical properties of LiFe0.5Mn0.5PO4 cathode material prepared by mechanochemically assisted solid-state synthesis, Energies 13 (2020) 542.

[184] H. Zhuang, Y. Bao, Y. Nie, Y. Qian, Y. Deng, G. Chen, Synergistic effect of composite carbon source and simple pre-calcining process on significantly enhanced electrochemical performance of porous LiFe0.5Mn0.5PO4/C agglomerations, Electrochim. Acta 314 (2019) 102–114, https://doi.org/10.1016/j.electacta.2019.05.066.

[185] B. Zhang, H. Wei, J. Zhang, G. Ji, J. Zhang, X. Ou, Porous spherical LiFePO4·LiMnPO4·Li3V2(PO4)3@C@rGO composites as a high-rate and long-cycle cathode for lithium ion batteries, Ceram. Int. 45 (2019) 13607–13613, https://doi.org/10.1016/j.ceramint.2019.03.055.

[186] D. Bresser, K. Hosoi, D. Howell, H. Li, H. Zeisel, K. Amine, S. Passerini, Perspectives of automotive battery R&D in China, Germany, Japan, and the USA, J. Power Sources 382 (2018) 176–178, https://doi.org/10.1016/j.jpowsour.2018.02.039.

[187] K. Mizushima, P.C. Jones, P.J. Wiseman, J.B. Goodenough, LixCoO2 (0<x<1): a new cathode material for batteries of high energy density, Mater. Res. Bull. 15 (1980) 783–789, https://doi.org/10.1016/0025-5408(80)90012-4.

[188] M.M. Thackeray, P.J. Johnson, L.A. de Picciotto, P.G. Bruce, J.B. Goodenough, Electrochemical extraction of lithium from LiMn2O4, Mater. Res. Bull. 19 (1984) 179–187, https://doi.org/10.1016/0025-5408(84)90088-6.

[189] J.M. Tarascon, D. Guyomard, Li metal-free rechargeable batteries based on Li1+ xMn2O4 cathodes (0≤x≤1) and carbon anodes, J. Electrochem. Soc. 138 (1991) 2864–2868, https://doi.org/10.1149/1.2085331.

[190] K.K. Lee, W.S. Yoon, K.B. Kim, K.Y. Lee, S.T. Hong, Characterization of LiNi0.85Co0.10M0.05O2 (M = Al, Fe) as a cathode material for lithium secondary batteries, J. Power Sources (2001) 97–98, https://doi.org/10.1016/S0378-7753(01)00516-X, 308–312.

[191] T. Ohzuku, Y. Makimura, Layered lithium insertion material of LiCo1/3Ni1/3Mn1/3O2 for lithium-ion batteries, Chem. Lett. 30 (2001) 642–643.

[192] Y. Koyama, Y. Makimura, I. Tanaka, H. Adachi, T. Ohzuku, Systematic research on insertion materials based on superlattice models in a phase triangle of LiCoO2 LiNiO2 LiMnO2, J. Electrochem. Soc. 151 (2004), A1499, https://doi.org/10.1149/1.1783908.

[193] N. Yabuuchi, Y. Koyama, N. Nakayama, T. Ohzuku, Solid-state chemistry and electrochemistry of LiCo1/3Ni1/3Mn1/3O2 for advanced lithium-ion batteries, J. Electrochem. Soc. 152 (2005), A1434, https://doi.org/10.1149/1.1924227.

[194] J.R. Dahn, U. von Sacken, C.A. Michal, Structure and electrochemistry of Li1±yNiO2 and a new Li2NiO2 phase with the Ni (OH)2 structure, Solid State Ionics 44 (1990) 87–97, https://doi.org/10.1016/0167-2738(90)90049-W.

[195] T. Ohzuku, Electrochemistry and structural chemistry of LiNiO2 (R3m) for 4 volt secondary lithium cells, J. Electrochem. Soc. 140 (1993) 1862, https://doi.org/10.1149/1.2220730.

[196] T. Ohzuku, A. Ueda, M. Nagayama, Y. Iwakoshi, H. Komori, Comparative study of LiCoO2, LiNi1/2Co1/2O2 and LiNiO2 for 4 volt secondary lithium cells, Electrochim. Acta 38 (1993) 1159–1167, https://doi.org/10.1016/0013-4686(93)80046-3.

[197] J.K. Ngala, N.A. Chernova, M. Ma, M. Mamak, P.Y. Zavalij, M.S. Whittingham, The synthesis, characterization and electrochemical behavior of the layered LiNi0.4Mn0.4Co0.2O2 compound, J. Mater. Chem. 14 (2004) 214–220, https://doi.org/10.1039/B309834F.

[198] E. Rossen, C.D.W. Jones, J.R. Dahn, Structure and electrochemistry of LixMnyNi1 yO2, Solid State Ionics 57 (1992) 311–318, https://doi.org/10.1016/0167-2738(92)90164-K.

[199] T. Ohzuku, Synthesis and characterization of LiAl[sub 1/4]Ni[sub 3/4]O[sub 2] (r3m) for lithium-ion (shuttlecock) batteries, J. Electrochem. Soc. 142 (1995) 4033, https://doi.org/10.1149/1.2048458.

[200] A. Rougier, I. Saadoune, P. Gravereau, P. Willmann, C. Delmasa, Effect of cobalt substitution on cationic distribution in LiNi1 yCoyO2 electrode materials, Solid State Ionics 90 (1996) 83–90, https://doi.org/10.1016/S0167-2738(96)00370-0.

[201] I. Saadoune, C. Delmas, LiNi1–yCoyO2 positive electrode materials: relationships between the structure, physical properties and electrochemical behaviour, J. Mater. Chem. 6 (1996) 193–199, https://doi.org/10.1039/JM9960600193.

[202] H.-J. Noh, S. Youn, C.S. Yoon, Y.-K. Sun, Comparison of the structural and electrochemical properties of layered Li[NixCoyMnz]O2 (x = 1/3, 0.5, 0.6, 0.7, 0.8 and 0.85) cathode material for lithium-ion batteries, J. Power Sources 233 (2013) 121–130, https://doi.org/10.1016/j.jpowsour.2013.01.063.

[203] S.-M. Bak, E. Hu, Y. Zhou, X. Yu, S.D. Senanayake, S.-J. Cho, K.-B. Kim, K. Y. Chung, X.-Q. Yang, K.-W. Nam, Structural changes and thermal stability of charged LiNixMnyCozO2 cathode materials studied by combined in situ time-resolved XRD and mass spectroscopy, ACS Appl. Mater. Interfaces 6 (2014) 22594–22601, https://doi.org/10.1021/am506712c.

[204] E. McCalla, G.H. Carey, J.R. Dahn, Lithium loss mechanisms during synthesis of layered LixNi2 xO2 for lithium ion batteries, Solid State Ionics 219 (2012) 11–19, https://doi.org/10.1016/j.ssi.2012.05.007.

[205] J.P. Peres, C. Delmas, A. Rougier, M. Broussely, F. Perton, P. Biensan, P. Willmann, The relationship between the composition of lithium nickel oxide and the loss of reversibility during the first cycle, J. Phys. Chem. Solid. 57 (1996) 1057–1060, https://doi.org/10.1016/0022-3697(95)00395-9.

[206] C. Delmas, J.P. Pérès, A. Rougier, A. Demourgues, F. Weill, A. Chadwick, M. Broussely, F. Perton, Ph Biensan, P. Willmann, On the behavior of the LixNiO2 system: an electrochemical and structural overview, J. Power Sources 68 (1997) 120–125, https://doi.org/10.1016/S0378-7753(97)02664-5.

[207] I.A. Shkrob, J.A. Gilbert, P.J. Phillips, R. Klie, R.T. Haasch, J. Bareño, D. P. Abraham, Chemical weathering of layered Ni-rich oxide electrode materials: evidence for cation exchange, J. Electrochem. Soc. 164 (2017) A1489–A1498, https://doi.org/10.1149/2.0861707jes.

[208] Y. Chen, S. Song, X. Zhang, Y. Liu, The challenges, solutions and development of high energy Ni-rich NCM/NCA LiB cathode materials, J. Phys. Conf. 1347 (2019), 012012, https://doi.org/10.1088/1742-6596/1347/1/012012.

[209] J. Sicklinger, M. Metzger, H. Beyer, D. Pritzl, H.A. Gasteiger, Ambient storage derived surface contamination of NCM811 and NCM111: performance implications and mitigation strategies, J. Electrochem. Soc. 166 (2019) A2322–A2335, https://doi.org/10.1149/2.0011912jes.

[210] Y. Bi, T. Wang, M. Liu, R. Du, W. Yang, Z. Liu, Z. Peng, Y. Liu, D. Wang, X. Sun, Stability of Li2CO3 in cathode of lithium ion battery and its influence on electrochemical performance, RSC Adv. 6 (2016) 19233–19237, https://doi.org/10.1039/C6RA00648E.

[211] S.E. Renfrew, B.D. McCloskey, Residual lithium carbonate predominantly accounts for first cycle CO2 and CO outgassing of Li-stoichiometric and Li-rich layered transition-metal oxides, J. Am. Chem. Soc. 139 (2017) 17853–17860, https://doi.org/10.1021/jacs.7b08461.

[212] Y. Kim, Investigation of the gas evolution in lithium ion batteries: effect of free lithium compounds in cathode materials, J. Solid State Electrochem. 17 (2013) 1961–1965, https://doi.org/10.1007/s10008-013-2050-2.

[213] R. Moshtev, P. Zlatilova, S. Vasilev, I. Bakalova, A. Kozawa, Synthesis, XRD characterization and electrochemical performance of overlithiated LiNiO2, J. Power Sources 81–82 (1999) 434–441, https://doi.org/10.1016/S0378-7753(99)00247-5.

[214] J. Kim, Y. Hong, K.S. Ryu, M.G. Kim, J. Cho, Washing Effect of a LiNi0.83Co0.15Al0.02O2 Cathode in Water, Electrochem. Solid State Lett. 9 (2006) A19, https://doi.org/10.1149/1.2135427.

[215] D.P. Abraham, R.D. Twesten, M. Balasubramanian, I. Petrov, J. McBreen, K. Amine, Surface changes on LiNi0.8Co0.2O2 particles during testing of high-power lithium-ion cells, Electrochem. Commun. 4 (2002) 620–625, https://doi.org/10.1016/S1388-2481(02)00388-0.

[216] F. Lin, I.M. Markus, D. Nordlund, T.-C. Weng, M.D. Asta, H.L. Xin, M.M. Doeff, Surface reconstruction and chemical evolution of stoichiometric layered cathode materials for lithium-ion batteries, Nat. Commun. 5 (2014) 3529.

[217] C. Delmas, M. Ménétrier, L. Croguennec, S. Levasseur, J.P. Pérès, C. Pouillerie, G. Prado, L. Fournès, F. Weill, Lithium batteries: a new tool in solid state chemistry, Int. J. Inorg. Mater. 1 (1999) 11–19, https://doi.org/10.1016/S1463-0176(99)00003-4.

[218] A.O. Kondrakov, A. Schmidt, J. Xu, H. Geßwein, R. Mönig, P. Hartmann, H. Sommer, T. Brezesinski, J. Janek, Anisotropic lattice strain and mechanical degradation of high- and low-nickel NCM cathode materials for Li-ion batteries, J. Phys. Chem. C 121 (2017) 3286–3294, https://doi.org/10.1021/acs.jpcc.6b12885.

[219] C.S. Yoon, D.-W. Jun, S.-T. Myung, Y.-K. Sun, Structural stability of LiNiO2 cycled above 4.2 V, ACS Energy Lett 2 (2017) 1150–1155, https://doi.org/10.1021/acsenergylett.7b00304.

[220] C.S. Yoon, H.-H. Ryu, G.-T. Park, J.-H. Kim, K.-H. Kim, Y.-K. Sun, Extracting maximum capacity from Ni-rich Li[Ni0.95Co0.025Mn0.025]O2 cathodes for high-energy-density lithium-ion batteries, J. Mater. Chem. A. 6 (2018) 4126–4132, https://doi.org/10.1039/C7TA11346C.

[221] H.-H. Ryu, K.-J. Park, C.S. Yoon, Y.-K. Sun, Capacity fading of Ni-rich Li [NixCoyMn1–x–y]O2 (0.6 ≤ x ≤ 0.95) cathodes for high-energy-density lithium-ion batteries: bulk or surface degradation? Chem. Mater. 30 (2018) 1155–1163, https://doi.org/10.1021/acs.chemmater.7b05269.

[222] C. Pouillerie, L. Croguennec, Ph Biensan, P. Willmann, C. Delmas, Synthesis and characterization of new LiNi1 yMgyO2 positive electrode materials for lithium-ion batteries, J. Electrochem. Soc. 147 (2000) 2061, https://doi.org/10.1149/1.1393486.

[223] M. Bonda, M. Holzapfel, S. de Brion, C. Darie, T. Fehér, P.J. Baker, T. Lancaster, S. J. Blundell, F.L. Pratt, Effect of magnesium doping on the orbital and magnetic order in LiNiO2, Phys. Rev. B 78 (2008) 104409.

[224] S. Albrecht, J. Kümpers, M. Kruft, S. Malcus, C. Vogler, M. Wahl, M. Wohlfahrt-Mehrens, Electrochemical and thermal behavior of aluminum- and magnesium-doped spherical lithium nickel cobalt mixed oxides Li1 x(Ni1 y zCoyMz)O2 (M = Al, Mg), J. Power Sources 119–121 (2003) 178–183, https://doi.org/10.1016/S0378-7753(03)00175-7.

[225] L. Croguennec, E. Suard, P. Willmann, C. Delmas, Structural and electrochemical characterization of the LiNi1-yTiyO2 electrode materials obtained by direct solid-state reactions, Chem. Mater. 14 (2002) 2149–2157, https://doi.org/10.1021/cm011265v.

[226] U.-H. Kim, D.-W. Jun, K.-J. Park, Q. Zhang, P. Kaghazchi, D. Aurbach, D.T. Major, G. Goobes, M. Dixit, N. Leifer, C.M. Wang, P. Yan, D. Ahn, K.-H. Kim, C.S. Yoon, Y.-K. Sun, Pushing the limit of layered transition metal oxide cathodes for high-energy density rechargeable Li ion batteries, Energy Environ. Sci. 11 (2018) 1271–1279, https://doi.org/10.1039/C8EE00227D.

[227] B. Pişkin, C.S. Uygur, M.K. Aydınol, Morphology effect on electrochemical properties of doped (W and Mo) 622NMC, 111NMC, and 226NMC cathode materials, Int. J. Hydrogen Energy 45 (2020) 7874–7880, https://doi.org/10.1016/j.ijhydene.2019.07.249.

[228] C.S. Yoon, U.-H. Kim, G.-T. Park, S.J. Kim, K.-H. Kim, J. Kim, Y.-K. Sun, Self-passivation of a LiNiO2 cathode for a lithium-ion battery through Zr doping, ACS Energy Lett 3 (2018) 1634–1639, https://doi.org/10.1021/acsenergylett.8b00805.

[229] B. Xiao, X. Sun, Surface and subsurface reactions of lithium transition metal oxide cathode materials: an overview of the fundamental origins and remedying approaches, Adv. Energy Mater. 8 (2018), 1802057, https://doi.org/10.1002/aenm.201802057.

[230] Y.-K. Sun, S.-T. Myung, B.-C. Park, K. Amine, Synthesis of spherical nano- to microscale Core Shell particles Li[(Ni0.8Co0.1Mn0.1)1-x(Ni0.5Mn0.5)x]O2 and their applications to lithium batteries, Chem. Mater. 18 (2006) 5159–5163, https://doi.org/10.1021/cm061746k.

[231] Y.-K. Sun, Z. Chen, H.-J. Noh, D.-J. Lee, H.-G. Jung, Y. Ren, S. Wang, C.S. Yoon, S.-T. Myung, K. Amine, Nanostructured high-energy cathode materials for advanced lithium batteries, Nat. Mater. 11 (2012) 942–947, https://doi.org/10.1038/nmat3435.

[232] P. Yan, J. Zheng, J. Liu, B. Wang, X. Cheng, Y. Zhang, X. Sun, C. Wang, J.-G. Zhang, Tailoring grain boundary structures and chemistry of Ni-rich layered cathodes for enhanced cycle stability of lithium-ion batteries, Nat. Energy 3 (2018) 600–605, https://doi.org/10.1038/s41560-018-0191-3.

[233] J. Kim, H. Ma, H. Cha, H. Lee, J. Sung, M. Seo, P. Oh, M. Park, J. Cho, A highly stabilized nickel-rich cathode material by nanoscale epitaxy control for high-energy lithium-ion batteries, Energy Environ. Sci. 11 (2018) 1449–1459, https://doi.org/10.1039/C8EE00155C.

[234] X. Jiang, S. Chu, Y. Chen, Y. Zhong, Y. Liu, Z. Shao, LiNi0.29Co0.33Mn0.38O2 polyhedrons with reduced cation mixing as a high-performance cathode material for Li-ion batteries synthesized via a combined co-precipitation and molten salt heating technique, J. Alloys Compd. 691 (2017) 206–214, https://doi.org/10.1016/j.jallcom.2016.08.139.

[235] Y. Kim, Lithium nickel cobalt manganese oxide synthesized using alkali chloride flux: morphology and performance as a cathode material for lithium ion batteries, ACS Appl. Mater. Interfaces 4 (2012) 2329–2333, https://doi.org/10.1021/am300386j.

[236] J. Li, A.R. Cameron, H. Li, S. Glazier, D. Xiong, M. Chatzidakis, J. Allen, G. A. Botton, J.R. Dahn, Comparison of single crystal and polycrystalline LiNi0.5Mn0.3Co0.2O2Positive electrode materials for high voltage Li-ion cells, J. Electrochem. Soc. 164 (2017) A1534–A1544, https://doi.org/10.1149/2.0991707jes.

[237] T. Kimijima, N. Zettsu, K. Teshima, Growth manner of octahedral-shaped Li(Ni1/3Co1/3Mn1/3)O2 single crystals in molten Na2SO4, Cryst. Growth Des. 16 (2016) 2618–2623, https://doi.org/10.1021/acs.cgd.5b01723.

[238] H. Li, J. Li, X. Ma, J.R. Dahn, Synthesis of single crystal LiNi0.6Mn0.2Co0.2O2with enhanced electrochemical performance for lithium ion batteries, J. Electrochem. Soc. 165 (2018) A1038–A1045, https://doi.org/10.1149/2.0951805jes.

[239] C. Sigala, A. Verbaere, J.L. Mansot, D. Guyomard, Y. Piffard, M. Tournoux, The Cr-substituted spinel Mn oxides LiCryMn2 yO4(0≤y≤1): rietveld analysis of the structure modifications induced by the electrochemical lithium deintercalation, J. Solid State Chem. 132 (1997) 372–381, https://doi.org/10.1006/jssc.1997.7476.

[240] K. Amine, H. Tukamoto, H. Yasuda, Y. Fujita, Preparation and electrochemical investigation of LiMn2 xMexO4 (Me: Ni, Fe, and x = 0.5, 1) cathode materials for secondary lithium batteries, J. Power Sources 68 (1997) 604–608, https://doi.org/10.1016/S0378-7753(96)02590-6.

[241] H. Kawai, M. Nagata, H. Kageyama, H. Tukamoto, A.R. West, 5 V lithium cathodes based on spinel solid solutions Li2Co1+XMn3 XO8: -1≤X≤1, Electrochim. Acta 45 (1999) 315–327, https://doi.org/10.1016/S0013-4686(99)00213-3.

[242] Y. Ein-Eli, LiMn2 xCuxO4 spinels (0.1 ≤ x ≤ 0.5): a new class of 5 V cathode materials for Li batteries, J. Electrochem. Soc. 145 (1998) 1238, https://doi.org/10.1149/1.1838445.

[243] J.-H. Kim, S.-T. Myung, C.S. Yoon, S.G. Kang, Y.-K. Sun, Comparative study of LiNi0.5Mn1.5O4-δ and LiNi0.5Mn1.5O4 cathodes having two crystallographic Structures: Fd3¯m and P4332, Chem. Mater. 16 (2004) 906–914, https://doi.org/10.1021/cm035050s.

[244] Q.M. Zhong, A. Bonakdarpour, M. Zhang, Y. Gao, J.R. Dahn, Synthesis and electrochemistry of LiNi[x]Mn[2-x]O4, J. Electrochem. Soc. 144 (1997) 205–213.

[245] R. Jung, M. Metzger, F. Maglia, C. Stinner, H.A. Gasteiger, Oxygen release and its effect on the cycling stability of LiNixMnyCozO2(NMC) cathode materials for Li-ion batteries, J. Electrochem. Soc. 164 (2017) A1361–A1377, https://doi.org/10.1149/2.0021707jes.

[246] S. Kuppan, Y. Xu, Y. Liu, G. Chen, Phase transformation mechanism in lithium manganese nickel oxide revealed by single-crystal hard X-ray microscopy, Nat. Commun. 8 (2017), 14309, https://doi.org/10.1038/ncomms14309.

[247] S. Kuppan, H. Duncan, G. Chen, Controlling side reactions and self-discharge in high-voltage spinel cathodes: the critical role of surface crystallographic facets, Phys. Chem. Chem. Phys. 17 (2015) 26471–26481, https://doi.org/10.1039/C5CP04899K.

[248] B. Hai, A.K. Shukla, H. Duncan, G. Chen, The effect of particle surface facets on the kinetic properties of LiMn1.5Ni0.5O4 cathode materials, J. Mater. Chem. A. 1 (2013) 759–769, https://doi.org/10.1039/C2TA00212D.

[249] M. Kuenzel, G.-T. Kim, M. Zarrabeitia, S.D. Lin, A.R. Schuer, D. Geiger, U. Kaiser, D. Bresser, S. Passerini, Crystal engineering of TMPOx-coated LiNi0.5Mn1.5O4 cathodes for high-performance lithium-ion batteries, Mater. Today (2020), https://doi.org/10.1016/j.mattod.2020.04.003.

[250] G. Gabrielli, P. Axmann, M. Wohlfahrt-Mehrens, Study of LiNi0.5Mn1.5O4 morphological features for reduced electrolyte decomposition at high potential, J. Electrochem. Soc. 163 (2016) A470–A476, https://doi.org/10.1149/2.0541603jes.

[251] J. Chong, J. Zhang, H. Xie, X. Song, G. Liu, V. Battaglia, S. Xun, R. Wang, High performance LiNi0.5Mn1.5O4 cathode material with a bi-functional coating for lithium ion batteries, RSC Adv. 6 (2016) 19245–19251, https://doi.org/10.1039/C6RA00119J.

[252] Y.-K. Sun, Y.-S. Lee, M. Yoshio, K. Amine, Synthesis and electrochemical properties of ZnO-coated LiNi0.5Mn1.5 O 4 spinel as 5 V cathode material for lithium secondary batteries, Electrochem. Solid State Lett. 5 (2002) A99–A102, https://doi.org/10.1149/1.1465375.

[253] X. Fang, M. Ge, J. Rong, C. Zhou, Graphene-oxide-coated LiNi0.5Mn1.5O4 as high voltage cathode for lithium ion batteries with high energy density and long cycle life, J. Mater. Chem. A. 1 (2013) 4083–4088, https://doi.org/10.1039/C3TA01534C.

[254] H.M. Wu, I. Belharouak, A. Abouimrane, Y.-K. Sun, K. Amine, Surface modification of LiNi0.5Mn1.5O4 by ZrP2O7 and ZrO2 for lithium-ion batteries, J. Power Sources 195 (2010) 2909–2913, https://doi.org/10.1016/j.jpowsour.2009.11.029.

[255] K. Ariyoshi, Y. Iwakoshi, N. Nakayama, T. Ohzuku, Topotactic two-phase reactions of Li[Ni[sub 1/2]Mn[sub 3/2]]O[sub 4] (P4[sub 3]32) in nonaqueous lithium cells, J. Electrochem. Soc. 151 (2004) A296, https://doi.org/10.1149/1.1639162.

[256] S.H. Park, S.-W. Oh, S.H. Kang, I. Belharouak, K. Amine, Y.-K. Sun, Comparative study of different crystallographic structure of LiNi0.5Mn1.5O4 δ cathodes with wide operation voltage (2.0–5.0V), Electrochim. Acta 52 (2007) 7226–7230, https://doi.org/10.1016/j.electacta.2007.05.050.

[257] M. Mancini, P. Axmann, G. Gabrielli, M. Kinyanjui, U. Kaiser, M. Wohlfahrt-Mehrens, A high-voltage and high-capacity Li1+xNi0.5Mn1.5O4 cathode material: from synthesis to full lithium-ion cells, ChemSusChem 9 (2016) 1843–1849, https://doi.org/10.1002/cssc.201600365.

[258] Z. Lu, D.D. MacNeil, J.R. Dahn, Layered cathode materials Li[NixLi(1/3 2x/3)Mn(2/3 x/3)]O2 for lithium-ion batteries, Electrochem. Solid State Lett. 4 (2001) A191–A194, https://doi.org/10.1149/1.1407994.

[259] Z. Lu, L.Y. Beaulieu, R.A. Donaberger, C.L. Thomas, J.R. Dahn, Synthesis, structure, and electrochemical behavior of Li[NixLi1/3-2x/3]Mn[2/3 x/3]O2, J. Electrochem. Soc. 149 (2002) A778, https://doi.org/10.1149/1.1471541.

[260] M.M. Thackeray, S.-H. Kang, C.S. Johnson, J.T. Vaughey, R. Benedek, S. A. Hackney, Li2MnO3-stabilized LiMO2 (M = Mn, Ni, Co) electrodes for lithium-ion batteries, J. Mater. Chem. 17 (2007) 3112–3125, https://doi.org/10.1039/B702425H.

[261] M. Rossouw, M. Thackeray, Lithium manganese oxides from Li2MnO3 for rechargeable lithium battery applications, Mater. Res. Bull. 26 (1991) 463–473, https://doi.org/10.1016/0025-5408(91)90186-.

[262] S. Hy, H. Liu, M. Zhang, D. Qian, B.-J. Hwang, Y.S. Meng, Performance and design considerations for lithium excess layered oxide positive electrode materials for lithium ion batteries, Energy Environ. Sci. 9 (2016) 1931–1954, https://doi.org/10.1039/C5EE03573B.

[263] M. Saubanère, E. McCalla, J.-M. Tarascon, M.-L. Doublet, The intriguing question of anionic redox in high-energy density cathodes for Li-ion batteries, Energy Environ. Sci. 9 (2016) 984–991, https://doi.org/10.1039/C5EE03048J.

[264] D.-H. Seo, J. Lee, A. Urban, R. Malik, S. Kang, G. Ceder, The structural and chemical origin of the oxygen redox activity in layered and cation-disordered Li-excess cathode materials, Nat. Chem. 8 (2016) 692–697, https://doi.org/10.1038/nchem.2524.

[265] D. Qian, B. Xu, M. Chi, Y.S. Meng, Uncovering the roles of oxygen vacancies in cation migration in lithium excess layered oxides, Phys. Chem. Chem. Phys. 16 (2014) 14665–14668, https://doi.org/10.1039/C4CP01799D.

[266] B. Xu, C.R. Fell, M. Chi, Y.S. Meng, Identifying surface structural changes in layered Li-excess nickel manganese oxides in high voltage lithium ion batteries: a joint experimental and theoretical study, Energy Environ. Sci. 4 (2011) 2223–2233, https://doi.org/10.1039/C1EE01131F.

[267] A.R. Armstrong, M. Holzapfel, P. Novák, C.S. Johnson, S.-H. Kang, M. M. Thackeray, P.G. Bruce, Demonstrating oxygen loss and associated structural reorganization in the lithium battery cathode Li[Ni0.2Li0.2Mn0.6]O2, J. Am. Chem. Soc. 128 (2006) 8694–8698, https://doi.org/10.1021/ja062027+.

[268] P. Vanaphuti, S. Bong, L. Ma, S. Ehrlich, Y. Wang, Systematic study of different anion doping on the electrochemical performance of cobalt-free lithium–manganese-rich layered cathode, ACS Appl. Energy Mater. 3 (2020) 4852–4859, https://doi.org/10.1021/acsaem.0c00439.

[269] H. Pan, S. Zhang, J. Chen, M. Gao, Y. Liu, T. Zhu, Y. Jiang, Li- and Mn-rich layered oxide cathode materials for lithium-ion batteries: a review from fundamentals to research progress and applications, Mol. Syst. Des. Eng. 3 (2018) 748–803, https://doi.org/10.1039/C8ME00025E.
[270] X. Lan, Y. Xin, L. Wang, X. Hu, Nanoscale surface modification of Li-rich layered oxides for high-capacity cathodes in Li-ion batteries, J. Nanoparticle Res. 20 (2018) 80, https://doi.org/10.1007/s11051-018-4165-y.
[271] J. Wang, X. He, E. Paillard, N. Laszczynski, J. Li, S. Passerini, Lithium- and manganese-rich oxide cathode materials for high-energy lithium ion batteries, Adv. Energy Mater. 6 (2016), 1600906, https://doi.org/10.1002/aenm.201600906.
[272] M. Schmidt, U. Heider, A. Kuehner, R. Oesten, M. Jungnitz, N. Ignat'ev, P. Sartori, Lithium fluoroalkylphosphates: a new class of conducting salts for electrolytes for high energy lithium-ion batteries, J. Power Sources 97–98 (2001) 557–560, https://doi.org/10.1016/S0378-7753(01)00640-1.
[273] J.M. Tarascon, D. Guyomard, New electrolyte compositions stable over the 0 to 5 V voltage range and compatible with the Li1+xMn2O4/carbon Li-ion cells, Solid State Ionics 69 (1994) 293–305, https://doi.org/10.1016/0167-2738(94)90418-9.
[274] L.J. Krause, W. Lamanna, J. Summerfield, M. Engle, G. Korba, R. Loch, R. Atanasoski, Corrosion of aluminum at high voltages in non-aqueous electrolytes containing perfluoroalkylsulfonyl imides; new lithium salts for lithium-ion cells, J. Power Sources 68 (1997) 320–325, https://doi.org/10.1016/S0378-7753(97)02517-2.
[275] R. Fong, U. von Sacken, J.R. Dahn, Studies of lithium intercalation into carbons using nonaqueous electrochemical cells, J. Electrochem. Soc. 137 (1990) 2009–2013.
[276] H. Yang, G.V. Zhuang, P.N. Ross Jr., Thermal stability of LiPF6 salt and Li-ion battery electrolytes containing LiPF6, J. Power Sources 161 (2006) 573–579, https://doi.org/10.1016/j.jpowsour.2006.03.058.
[277] L. Zheng, H. Zhang, P. Cheng, Q. Ma, J. Liu, J. Nie, W. Feng, Z. Zhou, Li[(FSO2)(n-C4F9SO2)N] versus LiPF6 for graphite/LiCoO2 lithium-ion cells at both room and elevated temperatures: a comprehensive understanding with chemical, electrochemical and XPS analysis, Electrochim. Acta 196 (2016) 169–188, https://doi.org/10.1016/j.electacta.2016.02.152.
[278] J. Kalhoff, G.G. Eshetu, D. Bresser, S. Passerini, Safer electrolytes for lithium-ion batteries: state of the art and perspectives, ChemSusChem 8 (2015) 2154–2175, https://doi.org/10.1002/cssc.201500284.
[279] A. Hammami, N. Raymond, M. Armand, Lithium-ion batteries: runaway risk of forming toxic compounds, Nature 424 (2003) 635–636, https://doi.org/10.1038/424635b.
[280] M. Armand, F.E.K.C. el Moursli, Bisperhaloacyl or Bispersulfonyl Imides of Alkali Metals, Their Solid Solutions with Polymers, and Their Use as Battery Electrolytes, 1983.
[281] R. Hagiwara, K. Tamaki, K. Kubota, T. Goto, T. Nohira, Thermal properties of mixed alkali bis(trifluoromethylsulfonyl)amides, J. Chem. Eng. Data 53 (2008) 355–358, https://doi.org/10.1021/je700368r.
[282] H.-B. Han, S.-S. Zhou, D.-J. Zhang, S.-W. Feng, L.-F. Li, K. Liu, W.-F. Feng, J. Nie, H. Li, X.-J. Huang, M. Armand, Z.-B. Zhou, Lithium bis(fluorosulfonyl)imide (LiFSI) as conducting salt for nonaqueous liquid electrolytes for lithium-ion batteries: physicochemical and electrochemical properties, J. Power Sources 196 (2011) 3623–3632, https://doi.org/10.1016/j.jpowsour.2010.12.040.
[283] J. Kalhoff, D. Bresser, M. Bolloli, F. Alloin, J.-Y. Sanchez, S. Passerini, Enabling LiTFSI-based electrolytes for safer lithium-ion batteries by using linear fluorinated carbonates as (Co)solvent, ChemSusChem 7 (2014) 2939–2946, https://doi.org/10.1002/cssc.201402502.
[284] C. Michot, M. Armand, J.-Y. Sanchez, Y. Choquette, M. Gauthier, Ionic Conducting Material Having Good Anticorrosive Properties, 1995.
[285] H. Zhang, C. Liu, L. Zheng, F. Xu, W. Feng, H. Li, X. Huang, M. Armand, J. Nie, Z. Zhou, Lithium bis(fluorosulfonyl)imide/poly(ethylene oxide) polymer electrolyte, Electrochim. Acta 133 (2014) 529–538, https://doi.org/10.1016/j.electacta.2014.04.099.
[286] H. Zhang, W. Feng, J. Nie, Z. Zhou, Recent progresses on electrolytes of fluorosulfonimide anions for improving the performances of rechargeable Li and Li-ion battery, J. Fluor. Chem. 174 (2015) 49–61, https://doi.org/10.1016/j.jfluchem.2014.07.028.
[287] M. Martinez-Ibañez, E. Sanchez-Diez, L. Qiao, Y. Zhang, X. Judez, A. Santiago, I. Aldalur, J. Carrasco, H. Zhu, M. Forsyth, M. Armand, H. Zhang, Unprecedented improvement of single Li-ion conductive solid polymer electrolyte through salt additive, Adv. Funct. Mater. 30 (2020), 2000455, https://doi.org/10.1002/adfm.202000455.
[288] K. Xu, Electrolytes and interphases in Li-ion batteries and beyond, Chem. Rev. 114 (2014) 11503–11618, https://doi.org/10.1021/cr500003w.
[289] U. Lischka, U. Wietelmann, M. Wegner, Lithium-bisoxalatoborat, Verfahren zu dessen Herstellung und dessen Verwendung, DE19829030C1, n.d.
[290] W. Xu, C.A. Angell, Weakly coordinating anions, and the exceptional conductivity of their nonaqueous solutions, Electrochem. Solid State Lett. 4 (2001) E1–E4, https://doi.org/10.1149/1.1344281.
[291] S. Shui Zhang, An unique lithium salt for the improved electrolyte of Li-ion battery, Electrochem. Commun. 8 (2006) 1423–1428, https://doi.org/10.1016/j.elecom.2006.06.016.
[292] M. Armand, Y. Choquette, M. Gauthier, C. Michot, Salts of Pentacyclic or Tetraazapentalene-Based Anions for Use as Ionic Conductors, 1998.
[293] L. Niedzicki, G.Z. Żukowska, M. Bukowska, P. Szczeciński, S. Grugeon, S. Laruelle, M. Armand, S. Panero, B. Scrosati, M. Marcinek, W. Wieczorek, New type of imidazole based salts designed specifically for lithium ion batteries, Electrochim. Acta 55 (2010) 1450–1454, https://doi.org/10.1016/j.electacta.2009.05.008.
[294] M. Armand, P. Johansson, M. Bukowska, P. Szczeciński, L. Niedzicki, M. Marcinek, M. Dranka, J. Zachara, G. Żukowska, M. Marczewski, G. Schmidt, W. Wieczorek, Review—development of Hückel type Anions: from molecular modeling to industrial commercialization. A success story, J. Electrochem. Soc. 167 (2020), 070562, https://doi.org/10.1149/1945-7111/ab829c.
[295] D.R. MacFarlane, M. Forsyth, P.C. Howlett, M. Kar, S. Passerini, J.M. Pringle, H. Ohno, M. Watanabe, F. Yan, W. Zheng, S. Zhang, J. Zhang, Ionic liquids and their solid-state analogues as materials for energy generation and storage, Nat. Rev. Mater. 1 (2016), 15005.
[296] Z. Zeng, X. Liu, X. Jiang, Z. Liu, Z. Peng, X. Feng, W. Chen, D. Xia, X. Ai, H. Yang, Y. Cao, in: Enabling an Intrinsically Safe and High-Energy-Density 4.5 V-Class Li-Ion Battery with Nonflammable Electrolyte, InfoMat, 2020, https://doi.org/10.1002/inf2.12089.
[297] G. GebresilassieEshetu, M. Armand, B. Scrosati, S. Passerini, Energy storage materials synthesized from ionic liquids, Angew. Chem. Int. Ed. 53 (2014) 13342–13359, https://doi.org/10.1002/anie.201405910.
[298] G.M.A. Girard, M. Hilder, H. Zhu, D. Nucciarone, K. Whitbread, S. Zavorine, M. Moser, M. Forsyth, D.R. MacFarlane, P.C. Howlett, Electrochemical and physicochemical properties of small phosphonium cation ionic liquid electrolytes with high lithium salt content, Phys. Chem. Chem. Phys. 17 (2015) 8706–8713, https://doi.org/10.1039/C5CP00205B.
[299] M. Forsyth, L. Porcarelli, X. Wang, N. Goujon, D. Mecerreyes, Innovative electrolytes based on ionic liquids and polymers for next-generation solid-state batteries, Acc. Chem. Res. 52 (2019) 686–694, https://doi.org/10.1021/acs.accounts.8b00566.
[300] N. von Aspern, M. Leissing, C. Wölke, D. Diddens, T. Kobayashi, M. Börner, O. Stubbmann-Kazakova, V. Kozel, G.-V. Röschenthaler, J. Smiatek, S. Nowak, M. Winter, I. Cekic-Laskovic, Non-flammable fluorinated phosphorus(III)-Based electrolytes for advanced lithium-ion battery performance, ChemElectroChem 7 (2020) 1499–1508, https://doi.org/10.1002/celc.202000386.
[301] X. Cao, Y. Xu, L. Zhang, M.H. Engelhard, L. Zhong, X. Ren, H. Jia, B. Liu, C. Niu, B. E. Matthews, H. Wu, B.W. Arey, C. Wang, J.-G. Zhang, W. Xu, Nonflammable electrolytes for lithium ion batteries enabled by ultraconformal passivation interphases, ACS Energy Lett 4 (2019) 2529–2534, https://doi.org/10.1021/acsenergylett.9b01926.
[302] H.-B. Han, Y.-X. Zhou, K. Liu, J. Nie, X.-J. Huang, M. Armand, Z.-B. Zhou, Efficient preparation of (Fluorosulfonyl)(pentafluoroethanesulfonyl)imide and its alkali salts, Chem. Lett. 39 (2010) 472–474.
[303] H. Han, J. Guo, D. Zhang, S. Feng, W. Feng, J. Nie, Z. Zhou, Lithium (fluorosulfonyl)(nonafluorobutanesulfonyl)imide (LiFNFSI) as conducting salt to improve the high-temperature resilience of lithium-ion cells, Electrochem. Commun. 13 (2011) 265–268, https://doi.org/10.1016/j.elecom.2010.12.030.
[304] S. Zhou, H. Han, J. Nie, M. Armand, Z. Zhou, X. Huang, Improving the high-temperature resilience of LiMn2O4Based batteries: LiFNFSI an effective salt, J. Electrochem. Soc. 159 (2012) A1158–A1164, https://doi.org/10.1149/2.026208jes.
[305] H. Zhang, H. Han, X. Cheng, L. Zheng, P. Cheng, W. Feng, J. Nie, M. Armand, X. Huang, Z. Zhou, Lithium salt with a super-delocalized perfluorinated sulfonimide anion as conducting salt for lithium-ion cells: physicochemical and electrochemical properties, J. Power Sources 296 (2015) 142–149, https://doi.org/10.1016/j.jpowsour.2015.07.026.
[306] H. Zhang, X. Cheng, Q. Ma, W. Feng, L. Zheng, J. Nie, X. Huang, M. Armand, Z. Zhou, New ionic liquids based on a super-delocalized perfluorinated sulfonimide anion: physical and electrochemical properties, Electrochim. Acta 207 (2016) 66–75, https://doi.org/10.1016/j.electacta.2016.03.201.
[307] S.S. Zhang, A review on electrolyte additives for lithium-ion batteries, J. Power Sources 162 (2006) 1379–1394, https://doi.org/10.1016/j.jpowsour.2006.07.074.
[308] A.M. Haregewoin, A.S. Wotango, B.-J. Hwang, Electrolyte additives for lithium ion battery electrodes: progress and perspectives, Energy Environ. Sci. 9 (2016) 1955–1988, https://doi.org/10.1039/C6EE00123H.
[309] B. Yang, H. Zhang, L. Yu, W. Fan, D. Huang, Lithium difluorophosphate as an additive to improve the low temperature performance of LiNi0.5Co0.2Mn0.3O2/graphite cells, Electrochim. Acta 221 (2016) 107–114, https://doi.org/10.1016/j.electacta.2016.10.037.
[310] Q.Q. Liu, L. Ma, C.Y. Du, J.R. Dahn, Effects of the LiPO2F2 additive on unwanted lithium plating in lithium-ion cells, Electrochim. Acta 263 (2018) 237–248, https://doi.org/10.1016/j.electacta.2018.01.058.
[311] L. Ma, L. Ellis, S.L. Glazier, X. Ma, Q. Liu, J. Li, J.R. Dahn, LiPO2F2as an electrolyte additive in Li[Ni0.5Mn0.3Co0.2]O2/graphite pouch cells, J. Electrochem. Soc. 165 (2018) A891–A899, https://doi.org/10.1149/2.0381805jes.
[312] L. Ma, L. Ellis, S.L. Glazier, X. Ma, J.R. Dahn, Combinations of LiPO2F2and other electrolyte additives in Li[Ni0.5Mn0.3Co0.2]O2/graphite pouch cells, J. Electrochem. Soc. 165 (2018) A1718–A1724, https://doi.org/10.1149/2.0661809jes.
[313] G. Park, H. Nakamura, Y. Lee, M. Yoshio, The important role of additives for improved lithium ion battery safety, J. Power Sources 189 (2009) 602–606, https://doi.org/10.1016/j.jpowsour.2008.09.088.
[314] B. Li, M. Xu, T. Li, W. Li, S. Hu, Prop-1-ene-1,3-sultone as SEI formation additive in propylene carbonate-based electrolyte for lithium ion batteries, Electrochem. Commun. 17 (2012) 92–95, https://doi.org/10.1016/j.elecom.2012.02.016.
[315] J.C. Burns, N.N. Sinha, G. Jain, H. Ye, C.M. VanElzen, W.M. Lamanna, A. Xiao, E. Scott, J. Choi, J.R. Dahn, Impedance reducing additives and their effect on cell

performance, J. Electrochem. Soc. 159 (2012) A1095–A1104, https://doi.org/10.1149/2.077207jes.
[316] D.Y. Wang, A. Xiao, L. Wells, J.R. Dahn, Effect of mixtures of lithium hexafluorophosphate (LiPF6) and lithium bis(fluorosulfonyl)imide (LiFSI) as salts in Li[Ni1/3Mn1/3Co1/3]O2/graphite pouch cells, J. Electrochem. Soc. 162 (2014) A169–A175, https://doi.org/10.1149/2.0821501jes.
[317] V. Sharova, A. Moretti, T. Diemant, A. Varzi, R.J. Behm, S. Passerini, Comparative study of imide-based Li salts as electrolyte additives for Li-ion batteries, J. Power Sources 375 (2018) 43–52, https://doi.org/10.1016/j.jpowsour.2017.11.045.
[318] Z. Zhang, L. Hu, H. Wu, W. Weng, M. Koh, P.C. Redfern, L.A. Curtiss, K. Amine, Fluorinated electrolytes for 5 V lithium-ion battery chemistry, Energy Environ. Sci. 6 (2013) 1806–1810, https://doi.org/10.1039/C3EE24414H.
[319] H. Jia, L. Zou, P. Gao, X. Cao, W. Zhao, Y. He, M.H. Engelhard, S.D. Burton, H. Wang, X. Ren, Q. Li, R. Yi, X. Zhang, C. Wang, Z. Xu, X. Li, J.-G. Zhang, W. Xu, High-performance silicon anodes enabled by nonflammable localized high-concentration electrolytes, Adv. Energy Mater. 9 (2019), 1900784, https://doi.org/10.1002/aenm.201900784.
[320] E.R. Logan, J.R. Dahn, Electrolyte design for fast-charging Li-ion batteries, Trends in Chemistry 2 (2020) 354–366, https://doi.org/10.1016/j.trechm.2020.01.011.
[321] D.E. Fenton, J.M. Parker, P.V. Wright, Complexes of alkali metal ions with poly (ethylene oxide), Polymer 14 (1973) 589.
[322] M. Armand, J.M. Chabagno, M. Duclot, Poly-ethers as solid electrolytes, in: St Andrews (Ed.), Scotland, 1978, pp. 651–654.
[323] H. Zhang, C. Li, M. Piszcz, E. Coya, T. Rojo, L.M. Rodriguez-Martinez, M. Armand, Z. Zhou, Single lithium-ion conducting solid polymer electrolytes: advances and perspectives, Chem. Soc. Rev. 46 (2017) 797–815, https://doi.org/10.1039/C6CS00491A.
[324] A.M. Stephan, Review on gel polymer electrolytes for lithium batteries, Eur. Polym. J. 42 (2006) 21–42, https://doi.org/10.1016/j.eurpolymj.2005.09.017.
[325] G. Feuillade, Ph Perche, Ion-conductive macromolecular gels and membranes for solid lithium cells, J. Appl. Electrochem. 5 (1975) 63–69, https://doi.org/10.1007/BF00625960.
[326] J.-M. Tarascon, A.S. Gozdz, C. Schmutz, F. Shokoohi, P.C. Warren, Performance of Bellcore's plastic rechargeable Li-ion batteries, Solid State Ionics 86–88 (1996) 49–54, https://doi.org/10.1016/0167-2738(96)00330-X. Part 1.
[327] A.S. Gozdz, C.N. Schmutz, J.-M. Tarascon, P.C. Warren, Polymeric Electrolytic Cell Separator Membrane, US5418091, n.D.
[328] A.S. Gozdz, C.N. Schmutz, J.-M. Tarascon, P.C. Warren, Method of Making an Electrolyte Activatable Lithium-Ion Rechargeable Battery Cell, US5456000, n.D.
[329] H. Jia, H. Onishi, N. von Aspern, U. Rodehorst, K. Rudolf, B. Billmann, R. Wagner, M. Winter, I. Cekic-Laskovic, A propylene carbonate based gel polymer electrolyte for extended cycle life and improved safety performance of lithium ion batteries, J. Power Sources 397 (2018) 343–351, https://doi.org/10.1016/j.jpowsour.2018.07.039.
[330] B.S. Lalia, T. Fujita, N. Yoshimoto, M. Egashira, M. Morita, Electrochemical performance of nonflammable polymeric gel electrolyte containing triethylphosphate, J. Power Sources 186 (2009) 211–215, https://doi.org/10.1016/j.jpowsour.2008.09.075.
[331] J.-H. Shin, W.A. Henderson, S. Passerini, Ionic liquids to the rescue? Overcoming the ionic conductivity limitations of polymer electrolytes, Electrochem. Commun. 5 (2003) 1016–1020, https://doi.org/10.1016/j.elecom.2003.09.017.
[332] M. Armand, F. Endres, D.R. MacFarlane, H. Ohno, B. Scrosati, Ionic-liquid materials for the electrochemical challenges of the future, Nat. Mater. 8 (2009) 621–629, https://doi.org/10.1038/nmat2448.
[333] I. Osada, H. deVries, B. Scrosati, S. Passerini, Ionic-liquid-based polymer electrolytes for battery applications, Angew. Chem. Int. Ed. 55 (2016) 500–513, https://doi.org/10.1002/anie.201504971.
[334] D. Chen, D. Wang, Y. Yang, Q. Huang, S. Zhu, Z. Zheng, Self-healing materials for next-generation energy harvesting and storage devices, Adv. Energy Mater. 7 (2017), 1700890, https://doi.org/10.1002/aenm.201700890.
[335] Y. Zhao, J. Guo, in: Development of Flexible Li-Ion Batteries for Flexible Electronics, InfoMat, 2020, https://doi.org/10.1002/inf2.12117.
[336] B. Zhou, D. He, J. Hu, Y. Ye, H. Peng, X. Zhou, X. Xie, Z. Xue, A flexible, self-healing and highly stretchable polymer electrolyte via quadruple hydrogen bonding for lithium-ion batteries, J. Mater. Chem. A. 6 (2018) 11725–11733, https://doi.org/10.1039/C8TA01907J.
[337] B.B. Jing, C.M. Evans, Catalyst-free dynamic networks for recyclable, self-healing solid polymer electrolytes, J. Am. Chem. Soc. 141 (2019) 18932–18937, https://doi.org/10.1021/jacs.9b09811.
[338] W.B. Hawley, J. Li, Electrode manufacturing for lithium-ion batteries—analysis of current and next generation processing, J. Energy Storage 25 (2019), 100862, https://doi.org/10.1016/j.est.2019.100862.
[339] A.A. Franco, A. Rucci, D. Brandell, C. Frayret, M. Gaberscek, P. Jankowski, P. Johansson, Boosting rechargeable batteries R&D by multiscale modeling: myth or reality? Chem. Rev. 119 (2019) 4569–4627, https://doi.org/10.1021/acs.chemrev.8b00239.
[340] A.M. Saillenfait, F. Gallissot, I. Langonné, J.P. Sabaté, Developmental toxicity of N-methyl-2-pyrrolidone administered orally to rats, Food Chem. Toxicol. 40 (2002) 1705–1712, https://doi.org/10.1016/S0278-6915(02)00115-1.
[341] J.-T. Li, Z.-Y. Wu, Y.-Q. Lu, Y. Zhou, Q.-S. Huang, L. Huang, S.-G. Sun, Water soluble binder, an electrochemical performance booster for electrode materials with high energy density, Adv. Energy Mater. 7 (2017), 1701185, https://doi.org/10.1002/aenm.201701185.
[342] K.B. Hatzell, M.B. Dixit, S.A. Berlinger, A.Z. Weber, Understanding inks for porous-electrode formation, J. Mater. Chem. 5 (2017) 20527–20533, https://doi.org/10.1039/C7TA07255D.
[343] H. Bockholt, W. Haselrieder, A. Kwade, Intensive powder mixing for dry dispersing of carbon black and its relevance for lithium-ion battery cathodes, Powder Technol. 297 (2016) 266–274, https://doi.org/10.1016/j.powtec.2016.04.011.
[344] A. Giessmann, Coating Substrates and Textiles - A Practical Guide to Coating and Laminating Technologies, first ed., Springer, Berlin, Heidelberg, Germany, 2012.
[345] M. Schmitt, M. Baunach, L. Wengeler, K. Peters, P. Junges, P. Scharfer, W. Schabel, Slot-die processing of lithium-ion battery electrodes—coating window characterization, Chem. Eng. Process: Process Intensification 68 (2013) 32–37, https://doi.org/10.1016/j.cep.2012.10.011.
[346] D.L. Wood, J.D. Quass, J. Li, S. Ahmed, D. Ventola, C. Daniel, Technical and economic analysis of solvent-based lithium-ion electrode drying with water and NMP, Dry. Technol. 36 (2018) 234–244, https://doi.org/10.1080/07373937.2017.1319855.
[347] S. Jaiser, M. Müller, M. Baunach, W. Bauer, P. Scharfer, W. Schabel, Investigation of film solidification and binder migration during drying of Li-Ion battery anodes, J. Power Sources 318 (2016) 210–219, https://doi.org/10.1016/j.jpowsour.2016.04.018.
[348] S. Jaiser, L. Funk, M. Baunach, P. Scharfer, W. Schabel, Experimental investigation into battery electrode surfaces: the distribution of liquid at the surface and the emptying of pores during drying, J. Colloid Interface Sci. 494 (2017) 22–31, https://doi.org/10.1016/j.jcis.2017.01.063.
[349] P. Scharfer, M. Schmitt, W. Schabel, R. Diehm, Method and Device for Intermittent Coating, US2017252773 A1, n.D.
[350] C. Meyer, M. Kosfeld, W. Haselrieder, A. Kwade, Process modeling of the electrode calendering of lithium-ion batteries regarding variation of cathode active materials and mass loadings, J. Energy Storage 18 (2018) 371–379, https://doi.org/10.1016/j.est.2018.05.018.
[351] L.S. Kremer, A. Hoffmann, T. Danner, S. Hein, B. Prifling, D. Westhoff, C. Dreer, A. Latz, V. Schmidt, M. Wohlfahrt-Mehrens, Manufacturing process for improved ultra-thick cathodes in high-energy lithium-ion batteries, Energy Technol. 8 (2020), 1900167, https://doi.org/10.1002/ente.201900167.
[352] B. Ludwig, Z. Zheng, W. Shou, Y. Wang, H. Pan, Solvent-free manufacturing of electrodes for lithium-ion batteries, Sci. Rep. 6 (2016), 23150, https://doi.org/10.1038/srep23150.
[353] M. Al-Shroofy, Q. Zhang, J. Xu, T. Chen, A.P. Kaur, Y.-T. Cheng, Solvent-free dry powder coating process for low-cost manufacturing of LiNi1/3Mn1/3Co1/3O2 cathodes in lithium-ion batteries, J. Power Sources 352 (2017) 187–193, https://doi.org/10.1016/j.jpowsour.2017.03.131.
[354] G. Schälicke, I. Landwehr, A. Dinter, K.-H. Pettinger, W. Haselrieder, A. Kwade, Solvent-free manufacturing of electrodes for lithium-ion batteries via electrostatic coating, Energy Technol. 8 (2020), 1900309, https://doi.org/10.1002/ente.201900309.
[355] S. El Khakani, N. Verdier, D. Lepage, A. Prébé, D. Aymé-Perrot, D. Rochefort, M. Dollé, Melt-processed electrode for lithium ion battery, J. Power Sources 454 (2020), 227884, https://doi.org/10.1016/j.jpowsour.2020.227884.
[356] K. Astafyeva, C. Dousset, Y. Bureau, S.-L. Stalmach, B. Dufour, High energy Li-ion electrodes prepared via a solventless melt process, Batteries & Supercaps 3 (2020) 341–343, https://doi.org/10.1002/batt.201900187.
[357] Y. Yang, W. Yuan, X. Zhang, Y. Yuan, C. Wang, Y. Ye, Y. Huang, Z. Qiu, Y. Tang, Overview on the applications of three-dimensional printing for rechargeable lithium-ion batteries, Appl. Energy 257 (2020), 114002, https://doi.org/10.1016/j.apenergy.2019.114002.
[358] J.B. Habedank, L. Kraft, A. Rheinfeld, C. Krezdorn, A. Jossen, M.F. Zaeh, Increasing the discharge rate capability of lithium-ion cells with laser-structured graphite anodes: modeling and simulation, J. Electrochem. Soc. 165 (2018) A1563–A1573, https://doi.org/10.1149/2.1181807jes.
[359] W. Pfleging, P. Gotcu, Femtosecond laser processing of thick film cathodes and its impact on lithium-ion diffusion kinetics, Appl. Sci. 9 (2019) 3588.
[360] D.L. Wood III, J. Li, C. Daniel, Prospects for reducing the processing cost of lithium ion batteries, J. Power Sources 275 (2015) 234–242, https://doi.org/10.1016/j.jpowsour.2014.11.019.
[361] X. Zhang, W.J. Jiang, X.P. Zhu, A. Mauger, Qilu, C.M. Julien, Aging of LiNi1/3Mn1/3Co1/3O2 cathode material upon exposure to H2O, J. Power Sources 196 (2011) 5102–5108, https://doi.org/10.1016/j.jpowsour.2011.02.009.
[362] N.V. Faenza, L. Bruce, Z.W. Lebens-Higgins, I. Plitz, N. Pereira, L.F.J. Piper, G. G. Amatucci, Growth of ambient induced surface impurity species on layered positive electrode materials and impact on electrochemical performance, J. Electrochem. Soc. 164 (2017) A3727–A3741, https://doi.org/10.1149/2.0921714jes.
[363] M. Bichon, D. Sotta, N. Dupré, E. De Vito, A. Boulineau, W. Porcher, B. Lestriez, Study of immersion of LiNi0.5Mn0.3Co0.2O2 material in water for aqueous processing of positive electrode for Li-ion batteries, ACS Appl. Mater. Interfaces 11 (2019) 18331–18341, https://doi.org/10.1021/acsami.9b00999.
[364] H. Liu, Y. Yang, J. Zhang, Investigation and improvement on the storage property of LiNi0.8Co0.2O2 as a cathode material for lithium-ion batteries, J. Power Sources 162 (2006) 644–650, https://doi.org/10.1016/j.jpowsour.2006.07.028.
[365] B.C. Church, D.T. Kaminski, J. Jiang, Corrosion of aluminum electrodes in aqueous slurries for lithium-ion batteries, J. Mater. Sci. 49 (2014) 3234–3241, https://doi.org/10.1007/s10853-014-8028-3.
[366] M. Kuenzel, D. Bresser, T. Diemant, D. Vieira Carvalho, G.-T. Kim, R.J. Behm, S. Passerini, Complementary strategies toward the aqueous processing of high-voltage LiNi0.5Mn1.5O4 lithium-ion cathodes, ChemSusChem 11 (2018) 562–573, https://doi.org/10.1002/cssc.201702021.
[367] I. Doberdò, N. Löffler, N. Laszczynski, D. Cericola, N. Penazzi, S. Bodoardo, G.-T. Kim, S. Passerini, Enabling aqueous binders for lithium battery cathodes –

carbon coating of aluminum current collector, J. Power Sources 248 (2014) 1000–1006, https://doi.org/10.1016/j.jpowsour.2013.10.039.
[368] N. Loeffler, G.-T. Kim, F. Mueller, T. Diemant, J.-K. Kim, R.J. Behm, S. Passerini, InSitu coating of Li[Ni0.33Mn0.33Co0.33]O2 particles to enable aqueous electrode processing, ChemSusChem 9 (2016) 1112–1117, https://doi.org/10.1002/cssc.201600353.
[369] W. Bauer, F.A. Çetinel, M. Müller, U. Kaufmann, Effects of pH control by acid addition at the aqueous processing of cathodes for lithium ion batteries, Electrochim. Acta 317 (2019) 112–119, https://doi.org/10.1016/j.electacta.2019.05.141.
[370] M. Bichon, D. Sotta, E. De Vito, W. Porcher, B. Lestriez, Performance and Ageing Behavior of Water-Processed NMC532/Graphite Lithium-Ion Cells, J. Power Sources. (n.d.) Submitted Manuscript.
[371] A. Kazzazi, D. Bresser, A. Birrozzi, J. von Zamory, M. Hekmatfar, S. Passerini, Comparative analysis of aqueous binders for high-energy Li-rich NMC as a lithium-ion cathode and the impact of adding phosphoric acid, ACS Appl. Mater. Interfaces 10 (2018) 17214–17222, https://doi.org/10.1021/acsami.8b03657.
[372] N. Laszczynski, A. Birrozzi, K. Maranski, M. Copley, M.E. Schuster, S. Passerini, Effect of coatings on the green electrode processing and cycling behaviour of LiCoPO4, J. Mater. Chem. A. 4 (2016) 17121–17128, https://doi.org/10.1039/C6TA05262B.
[373] M. Wood, J. Li, R.E. Ruther, Z. Du, E.C. Self, H.M. Meyer, C. Daniel, I. Belharouak, D.L. Wood, Chemical stability and long-term cell performance of low-cobalt, Ni-Rich cathodes prepared by aqueous processing for high-energy Li-Ion batteries, Energy Storage Mater. 24 (2020) 188–197, https://doi.org/10.1016/j.ensm.2019.08.020.
[374] N. Loeffler, Guk-T. Kim, S. Passerini, C. Gutierrez, I. Cendoya, I. DeMeatza, F. Alessandrini, G.B. Appetecchi, Performance and ageing robustness of graphite/NMC pouch prototypes manufactured through eco-friendly materials and processes, ChemSusChem 10 (2017) 3581–3587, https://doi.org/10.1002/cssc.201701087.
[375] Z. Du, K.M. Rollag, J. Li, S.J. An, M. Wood, Y. Sheng, P.P. Mukherjee, C. Daniel, D. L. Wood, Enabling aqueous processing for crack-free thick electrodes, J. Power Sources 354 (2017) 200–206, https://doi.org/10.1016/j.jpowsour.2017.04.030.
[376] R. Sahore, D.L. Wood, A. Kukay, K.M. Grady, J. Li, I. Belharouak, Towards understanding of cracking during drying of thick aqueous-processed LiNi0.8Mn0.1Co0.1O2 cathodes, ACS Sustain. Chem. Eng. 8 (2020) 3162–3169, https://doi.org/10.1021/acssuschemeng.9b06363.
[377] D. Beneventi, D. Chaussy, D. Curtil, L. Zolin, E. Bruno, R. Bongiovanni, M. Destro, C. Gerbaldi, N. Penazzi, S. Tapin-Lingua, Pilot-scale elaboration of graphite/microfibrillated cellulose anodes for Li-ion batteries by spray deposition on a forming paper sheet, Chem. Eng. J. 243 (2014) 372–379, https://doi.org/10.1016/j.cej.2013.12.034.
[378] D. Burchart-Korol, S. Jursova, P. Folęga, P. Pustejovska, Life cycle impact assessment of electric vehicle battery charging in European Union countries, J. Clean. Prod. 257 (2020), https://doi.org/10.1016/j.jclepro.2020.120476, 120476.
[379] T. Träger, B. Friedrich, R. Weyhe, Recovery concept of value metals from automotive lithium-ion batteries, Chem. Ing. Tech. 87 (2015) 1550–1557, https://doi.org/10.1002/cite.201500066.
[380] C. Ekberg, M. Petranikova, Chapter 7 - lithium batteries recycling, in lithium process chemistry, in: Lithium Process Chemistry, first ed., Elsevier, Amsterdam, Netherlands, 2015, pp. 233–267.
[381] G. Lombardo, B. Ebin, M.R. St, J. Foreman, B.-M. Steenari, M. Petranikova, Chemical transformations in Li-ion battery electrode materials by carbothermic reduction, ACS Sustain. Chem. Eng. 7 (2019) 13668–13679, https://doi.org/10.1021/acssuschemeng.8b06540.
[382] E. Mossali, N. Picone, L. Gentilini, O. Rodrìguez, J.M. Pérez, M. Colledani, Lithium-ion batteries towards circular economy: a literature review of opportunities and issues of recycling treatments, J. Environ. Manag. 264 (2020), 110500, https://doi.org/10.1016/j.jenvman.2020.110500.
[383] K. Richa, C.W. Babbitt, G. Gaustad, X. Wang, A future perspective on lithium-ion battery waste flows from electric vehicles, Resour. Conserv. Recycl. 83 (2014) 63–76, https://doi.org/10.1016/j.resconrec.2013.11.008.
[384] B. Ruffino, M.C. Zanetti, P. Marini, A mechanical pre-treatment process for the valorization of useful fractions from spent batteries, Resour. Conserv. Recycl. 55 (2011) 309–315, https://doi.org/10.1016/j.resconrec.2010.10.002.
[385] G. Lombardo, B. Ebin, M.R. St, J. Foreman, B.-M. Steenari, M. Petranikova, Incineration of EV Lithium-ion batteries as a pretreatment for recycling – determination of the potential formation of hazardous by-products and effects on metal compounds, J. Hazard Mater. 393 (2020), 122372, https://doi.org/10.1016/j.jhazmat.2020.122372.
[386] S.M. Shin, N.H. Kim, J.S. Sohn, D.H. Yang, Y.H. Kim, Development of a metal recovery process from Li-ion battery wastes, Hydrometallurgy 79 (2005) 172–181, https://doi.org/10.1016/j.hydromet.2005.06.004.
[387] D. Steward, A. Mayyas, M. Mann, Economics and challenges of Li-ion battery recycling from end-of-life vehicles, Procedia Manufact. 33 (2019) 272–279, https://doi.org/10.1016/j.promfg.2019.04.033.
[388] S. Virolainen, M. Fallah Fini, A. Laitinen, T. Sainio, Solvent extraction fractionation of Li-ion battery leachate containing Li, Ni, and Co, Separ. Purif. Technol. 179 (2017) 274–282, https://doi.org/10.1016/j.seppur.2017.02.010.
[389] C. Tunsu, T. Retegan, Chapter 6 - hydrometallurgical processes for the recovery of metals from WEEE, in: WEEE Recycling, first ed., Elsevier, 2016, pp. 139–175.
[390] T. Georgi-Maschler, B. Friedrich, R. Weyhe, H. Heegn, M. Rutz, Development of a recycling process for Li-ion batteries, J. Power Sources 207 (2012) 173–182, https://doi.org/10.1016/j.jpowsour.2012.01.152.
[391] Y. Tang, H. Xie, B. Zhang, X. Chen, Z. Zhao, J. Qu, P. Xing, H. Yin, Recovery and regeneration of LiCoO2-based spent lithium-ion batteries by a carbothermic reduction vacuum pyrolysis approach: controlling the recovery of CoO or Co, Waste Manag. 97 (2019) 140–148, https://doi.org/10.1016/j.wasman.2019.08.004.
[392] L. Sun, K. Qiu, Vacuum pyrolysis and hydrometallurgical process for the recovery of valuable metals from spent lithium-ion batteries, J. Hazard Mater. 194 (2011) 378–384, https://doi.org/10.1016/j.jhazmat.2011.07.114.
[393] X. Zhong, W. Liu, J. Han, F. Jiao, W. Qin, T. Liu, C. Zhao, Pyrolysis and physical separation for the recovery of spent LiFePO4 batteries, Waste Manag. 89 (2019) 83–93, https://doi.org/10.1016/j.wasman.2019.03.068.
[394] C. Peng, K. Lahtinen, E. Medina, P. Kauranen, M. Karppinen, T. Kallio, B. P. Wilson, M. Lundström, Role of impurity copper in Li-ion battery recycling to LiCoO2 cathode materials, J. Power Sources 450 (2020), 227630, https://doi.org/10.1016/j.jpowsour.2019.227630.
[395] J. Ordoñez, E.J. Gago, A. Girard, Processes and technologies for the recycling and recovery of spent lithium-ion batteries, Renew. Sustain. Energy Rev. 60 (2016) 195–205, https://doi.org/10.1016/j.rser.2015.12.363.
[396] Y. Guo, F. Li, H. Zhu, G. Li, J. Huang, W. He, Leaching lithium from the anode electrode materials of spent lithium-ion batteries by hydrochloric acid (HCl), Waste Manag. 51 (2016) 227–233, https://doi.org/10.1016/j.wasman.2015.11.036.
[397] P. Zhang, T. Yokoyama, O. Itabashi, T.M. Suzuki, K. Inoue, Hydrometallurgical process for recovery of metal values from spent lithium-ion secondary batteries, Hydrometallurgy 47 (1998) 259–271, https://doi.org/10.1016/S0304-386X(97)00050-9.
[398] J. Nan, D. Han, X. Zuo, Recovery of metal values from spent lithium-ion batteries with chemical deposition and solvent extraction, J. Power Sources 152 (2005) 278–284, https://doi.org/10.1016/j.jpowsour.2005.03.134.
[399] D. Chen, S. Rao, D. Wang, H. Cao, W. Xie, Z. Liu, Synergistic leaching of valuable metals from spent Li-ion batteries using sulfuric acid- l-ascorbic acid system, Chem. Eng. J. 388 (2020), 124321, https://doi.org/10.1016/j.cej.2020.124321.
[400] C. Peng, J. Hamuyuni, B.P. Wilson, M. Lundström, Selective reductive leaching of cobalt and lithium from industrially crushed waste Li-ion batteries in sulfuric acid system, Waste Manag. 76 (2018) 582–590, https://doi.org/10.1016/j.wasman.2018.02.052.
[401] A. Porvali, A. Chernyaev, S. Shukla, M. Lundström, Lithium ion battery active material dissolution kinetics in Fe(II)/Fe(III) catalyzed Cu-H2SO4 leaching system, Separ. Purif. Technol. 236 (2020), 116305, https://doi.org/10.1016/j.seppur.2019.116305.
[402] C.K. Lee, K.-I. Rhee, Reductive leaching of cathodic active materials from lithium ion battery wastes, Hydrometallurgy 68 (2003) 5–10, https://doi.org/10.1016/S0304-386X(02)00167-6.
[403] J. de Oliveira Demarco, J. Stefanello Cadore, F. da Silveira de Oliveira, E. Hiromitsu Tanabe, D. Assumpção Bertuol, Recovery of metals from spent lithium-ion batteries using organic acids, Hydrometallurgy 190 (2019), 105169, https://doi.org/10.1016/j.hydromet.2019.105169.
[404] R. Golmohammadzadeh, F. Rashchi, E. Vahidi, Recovery of lithium and cobalt from spent lithium-ion batteries using organic acids: process optimization and kinetic aspects, Waste Manag. 64 (2017) 244–254, https://doi.org/10.1016/j.wasman.2017.03.037.
[405] W. Gao, J. Song, H. Cao, X. Lin, X. Zhang, X. Zheng, Y. Zhang, Z. Sun, Selective recovery of valuable metals from spent lithium-ion batteries – process development and kinetics evaluation, J. Clean. Prod. 178 (2018) 833–845, https://doi.org/10.1016/j.jclepro.2018.01.040.
[406] M. Yu, Z. Zhang, F. Xue, B. Yang, G. Guo, J. Qiu, A more simple and efficient process for recovery of cobalt and lithium from spent lithium-ion batteries with citric acid, Separ. Purif. Technol. 215 (2019) 398–402, https://doi.org/10.1016/j.seppur.2019.01.027.
[407] Y. Pranolo, W. Zhang, C.Y. Cheng, Recovery of metals from spent lithium-ion battery leach solutions with a mixed solvent extractant system, Hydrometallurgy 102 (2010) 37–42, https://doi.org/10.1016/j.hydromet.2010.01.007.
[408] D. Dutta, A. Kumari, R. Panda, S. Jha, D. Gupta, S. Goel, M.K. Jha, Close loop separation process for the recovery of Co, Cu, Mn, Fe and Li from spent lithium-ion batteries, Separ. Purif. Technol. 200 (2018) 327–334, https://doi.org/10.1016/j.seppur.2018.02.022.
[409] S. Dhiman, B. Gupta, Partition studies on cobalt and recycling of valuable metals from waste Li-ion batteries via solvent extraction and chemical precipitation, J. Clean. Prod. 225 (2019) 820–832, https://doi.org/10.1016/j.jclepro.2019.04.004.
[410] X. Chen, Y. Chen, T. Zhou, D. Liu, H. Hu, S. Fan, Hydrometallurgical recovery of metal values from sulfuric acid leaching liquor of spent lithium-ion batteries, Waste Manag. 38 (2015) 349–356, https://doi.org/10.1016/j.wasman.2014.12.023.
[411] F. Vasilyev, S. Virolainen, T. Sainio, Numerical simulation of counter-current liquid–liquid extraction for recovering Co, Ni and Li from lithium-ion battery leachates of varying composition, Separ. Purif. Technol. 210 (2019) 530–540, https://doi.org/10.1016/j.seppur.2018.08.036.
[412] T.A. Atia, G. Elia, R. Hahn, P. Altimari, F. Pagnanelli, Closed-loop hydrometallurgical treatment of end-of-life lithium ion batteries: towards zero-waste process and metal recycling in advanced batteries, J. Energy Chem. 35 (2019) 220–227, https://doi.org/10.1016/j.jechem.2019.03.022.
[413] V.C.I. Takahashi, A.B. Botelho Junior, D.C.R. Espinosa, J.A.S. Tenório, Enhancing cobalt recovery from Li-ion batteries using grinding treatment prior to the leaching and solvent extraction process, J. Environ. Chemical Eng. 8 (2020), 103801, https://doi.org/10.1016/j.jece.2020.103801.

[414] D.P. Mantuano, G. Dorella, R.C.A. Elias, M.B. Mansur, Analysis of a hydrometallurgical route to recover base metals from spent rechargeable batteries by liquid–liquid extraction with Cyanex 272, J. Power Sources 159 (2006) 1510–1518, https://doi.org/10.1016/j.jpowsour.2005.12.056.
[415] R. Schröder, M. Aydemir, G. Seliger, Comparatively assessing different shapes of lithium-ion battery cells, Procedia Manufact. 8 (2017) 104–111, https://doi.org/10.1016/j.promfg.2017.02.013.
[416] R.E. Ciez, J.F. Whitacre, Comparison between cylindrical and prismatic lithium-ion cell costs using a process based cost model, J. Power Sources 340 (2017) 273–281, https://doi.org/10.1016/j.jpowsour.2016.11.054.
[417] W. Li, Y. Xia, G. Chen, E. Sahraei, Comparative study of mechanical-electrical-thermal responses of pouch, cylindrical, and prismatic lithium-ion cells under mechanical abuse, Sci. China Technol. Sci. 61 (2018) 1472–1482, https://doi.org/10.1007/s11431-017-9296-0.
[418] J.B. Quinn, T. Waldmann, K. Richter, M. Kasper, M. Wohlfahrt-Mehrens, Energy density of cylindrical Li-ion cells: a comparison of commercial 18650 to the 21700 cells, J. Electrochem. Soc. 165 (2018) A3284–A3291, https://doi.org/10.1149/2.0281814jes.
[419] J. Li, C. Arbizzani, S. Kjelstrup, J. Xiao, Y. Xia, Y. Yu, Y. Yang, I. Belharouak, T. Zawodzinski, S.-T. Myung, R. Raccichini, S. Passerini, Good practice guide for papers on batteries for the Journal of Power Sources, J. Power Sources 452 (2020) 227824, https://doi.org/10.1016/j.jpowsour.2020.227824.
[420] Y. Ding, Z.P. Cano, A. Yu, J. Lu, Z. Chen, Automotive Li-ion batteries: current status and future perspectives, Electrochem. Energy Rev. 2 (2019) 1–28, https://doi.org/10.1007/s41918-018-0022-z.
[421] C.-X. Zu, H. Li, Thermodynamic analysis on energy densities of batteries, Energy Environ. Sci. 4 (2011) 2614–2624, https://doi.org/10.1039/C0EE00777C.
[422] E.J. Berg, C. Villevieille, D. Streich, S. Trabesinger, P. Novák, Rechargeable batteries: grasping for the limits of chemistry, J. Electrochem. Soc. 162 (2015) A2468–A2475, https://doi.org/10.1149/2.0081514jes.
[423] G. Patry, A. Romagny, S. Martinet, D. Froelich, Cost modeling of lithium-ion battery cells for automotive applications, Energy Sci. Eng. 3 (2015) 71–82, https://doi.org/10.1002/ese3.47.
[424] K.G. Gallagher, S.E. Trask, C. Bauer, T. Woehrle, S.F. Lux, M. Tschech, P. Lamp, B. J. Polzin, S. Ha, B. Long, Q. Wu, W. Lu, D.W. Dees, A.N. Jansen, Optimizing areal capacities through understanding the limitations of lithium-ion electrodes, J. Electrochem. Soc. 163 (2016) A138–A149, https://doi.org/10.1149/2.0321602jes.
[425] M. Doyle, J. Newman, The use of mathematical modeling in the design of lithium/polymer battery systems, Electrochim. Acta 40 (1995) 2191–2196, https://doi.org/10.1016/0013-4686(95)00162-8.
[426] M. Doyle, Modeling of galvanostatic charge and discharge of the lithium/polymer/insertion cell, J. Electrochem. Soc. 140 (1993) 1526, https://doi.org/10.1149/1.2221597.
[427] M. Ender, An extended homogenized porous electrode model for lithium-ion cell electrodes, J. Power Sources 282 (2015) 572–580, https://doi.org/10.1016/j.jpowsour.2015.02.098.
[428] D. Westhoff, I. Manke, V. Schmidt, Generation of virtual lithium-ion battery electrode microstructures based on spatial stochastic modeling, Comput. Mater. Sci. 151 (2018) 53–64, https://doi.org/10.1016/j.commatsci.2018.04.060.
[429] C.-H. Chen, F. Brosa Planella, K. O'Regan, D. Gastol, W.D. Widanage, E. Kendrick, Development of experimental techniques for parameterization of multi-scale lithium-ion battery models, J. Electrochem. Soc. 167 (2020), 080534, https://doi.org/10.1149/1945-7111/ab9050.
[430] A.J. Louli, J. Li, S. Trussler, C.R. Fell, J.R. Dahn, Volume, pressure and thickness evolution of Li-ion pouch cells with silicon-composite negative electrodes, J. Electrochem. Soc. 164 (2017) A2689–A2696, https://doi.org/10.1149/2.1691712jes.
[431] J. Seeba, S. Reuber, C. Heubner, A. Müller-Köhn, M. Wolter, A. Michaelis, Extrusion-based fabrication of electrodes for high-energy Li-ion batteries, Chem. Eng. J. (2020), 125551, https://doi.org/10.1016/j.cej.2020.125551.
[432] I.L. Sauer, J.F. Escobar, M.F.P. da Silva, C.G. Meza, C. Centurion, J. Goldemberg, Bolivia and Paraguay: a beacon for sustainable electric mobility? Renew. Sustain. Energy Rev. 51 (2015) 910–925, https://doi.org/10.1016/j.rser.2015.06.038.
[433] R.J. Brodd, Comments on the history of lithium-ion batteries, in: Meeting Abstracts, the Electrochemical Society, ECS), 2002. https://www.electrochem.org/dl/ma/201/pdfs/0259.pdf.
[434] D. Andre, S.-J. Kim, P. Lamp, S.F. Lux, F. Maglia, O. Paschos, B. Stiaszny, Future generations of cathode materials: an automotive industry perspective, J. Mater. Chem. A. 3 (2015) 6709–6732, https://doi.org/10.1039/C5TA00361J.
[435] W. Josefowitz, W. Kranz, D. Macerata, T. Soczka-Guth, H. Mettlach, D. Porcellato, F. Orsini, J. Hansson, Assessment and testing of advanced energy storage systems for propulsion – European testing report, in: Proceedings of the 21st Worldwide Battery, Hybrid and Fuel Cell Electric Vehicle Symposium & Exhibition, Moncao, 2005.
[436] Sae International, Electric and Hybrid Electric Vehicle Rachargeable Energy Storage System (RESS) Safety and Abuse Testing J2464, Surface Vehicle Recommended Practice SAE, 2009.